SIK2: A KEY PLAYER IN FGF2-INDUCED PROLIFERATION AND INSULIN-INDUCED SURVIVAL/HYPERGLYCEMIA-DEPENDENT APOPTOSIS IN MÜLLER CELLS

by

Gamze Küser

B.S., Molecular Biology and Genetics, Boğaziçi University, 2003

M.S., Molecular Biology and Genetics, Boğaziçi University, 2006

Submitted to the Institute for Graduate Studies in
Science and Engineering in partial fulfillment of
the requirements for the degree of
Doctor of Philosophy

Graduate Program in Molecular Biology and Genetics

Boğaziçi University

2011

To my mother

ACKNOWLEDGEMENTS

First and foremost, I would like to thank my thesis supervisor Prof. Kuyaş Buğra for her valuable criticism, and extensive help throughout the study. I am also grateful to her for teaching me critical thinking.

I also like to thank my thesis committee members, Assist. Prof. Arzu Çelik, Prof. Ayşe Özer, Assoc. Prof. Esra Battaloğlu, and İbrahim Yaman, Ph.D. for their valuable criticism.

I would like to express my special thanks to the RECEP lab members and my best friends, Neslihan Zöhrap, Yeliz Yılmaz Sert, Funda Ejder, Aslı Uğurlu, Burçak Özeş, Duygu Dağlıkoca, Alperen Erdoğan, Merve Kılınç, Serli Canseven, Mahmut Can Hız, Özden Akay, Yıldız Koca and Balkan Canher for their endless support, help and warm friendship inside and outside the laboratory. I would like to thank Elif Eren, Yetiş Gültekin, Ulaş Özkurede, Tuncay Şeker, İzzet Akiva, Ece Terzioğlu Kara, Bahar Şahin and Zeynep Özcan for their help, support and kindness. I am grateful to G. Astrid Limb, Ph.D. for providing MIO-M1 cells and Metin Özçelik for his animal handling.

I would also like to thank the former lab members Ferruh Özcan, Ayça Çınaroğu, Yeşim Özmen, Avni Uysal, Demet Candaş, Cihan Erkut, Emin Vural, İbrahim Barış, Birdal Bilir, Rezan Fahrioğlu Yamacı for creating such a warm lab environment which always motivated me during this study.

The last but not the least, I have special thanks to my family and Ali Özgür Abalı for their encouragement throughout my life.

This thesis has been supported by Boğaziçi University Scientific Research Fund, BAP08B104, BAP09B106P, BAP09HB103D and Turkish Scientific and Research Council Fund, TÜBİTAK106T115, TÜBİTAK108T646, TÜBİTAK109T200.

ABSTRACT

SIK2: A KEY PLAYER IN FGF2-INDUCED PROLIFERATION AND INSULIN-INDUCED SURVIVAL/HYPERGLYCEMIA-DEPENDENT APOPTOSIS IN MÜLLER CELLS

Salt inducible kinase 2 (SIK2), a serine/threonine kinase, is primarily expressed in insulin-responsive tissues. It was suggested that SIK2 might be involved in type 2 diabetes by phosphorylating S789 residue of IRS1. In the initial experiments we observed rapid and transient increase of SIK2 activity upon FGF2 stimulation, confirming that the kinase is part of this pathway. Subsequently it was demonstrated that FGF2 dependent ERK and Akt activation was reduced significantly by SIK2 overexpression. SIK2 silencing, on the other hand, enhanced the intensity and the duration of active ERK and Akt levels, and led to a dramatic increase in FGF2-dependent Müller cell proliferation. Gab1 phosphorylation by SIK2 was verified *in vitro*, their interaction was revealed by coimmunoprecipitation. pSer of Gab1 was diminished significantly by SIK2 silencing. In the same time frame, pTyr levels and binding partner associations (p85/Gab1, Shp2/Gab1, Grb2/Gab1) were increased. Based on this data we propose that SIK2 involved in the negative feedback mechanisms acting on FGF/Ras/ERK and FGF/PI3K/Akt pathways and Müller cell proliferation at the level of Gab1 serine phosphorylation. In the context of insulin pathway we established enhanced tyrosine phosphorylation of IRS1, followed by Akt activation resulting in increased Müller cell survival. SIK2 knockdown leads to considerably earlier FGF2-dependent Akt activation. Its overexpression, hampers Akt activation and cell survival. Coimmunoprecipitation studies indicated IRS1 as an *in vivo* SIK2 substrate. We observed lower IRS1 expression and tyrosine phosphorylation, enhanced SIK2 activity/expression and downregulation of both basal and insulin-induced Akt activation in MIO-M1 cells under hyperglycemia. SIK2 gene silencing under hyperglycemia restored pAkt level, under normoglycemia in cells overexpressing SIK2, Akt phosphorylation was decreased and apoptosis increased. Based on these observations, we suggest that SIK2 is a negative modulator of insulin-induced IRS1/Akt mediated Müller glial survival pathway, which may contribute to the glial death observed in diabetes.

ÖZET

SIK2: MÜLLER HÜCRELERİNDE FGF2 İLE İNDÜKLENEN ÇOĞALMA VE İNSÜLİNLE İNDÜKLENEN SAĞKALIM/HİPERGLİSEMİYE BAĞLI HÜCRE ÖLÜMÜNDE YENİ BİR OYUNCU

Tuz indüklenebilir kinaz (SIK2), bir serin/treonin kinaz olup insüline cevap veren dokularda ifade edilmektedir. SIK2'nin tip 2 diyabetle olan ilişkisinin IRS1'i S789 rezidüsünden fosforlamasıyla mümkün olacabileceği önerilmektedir. Yapılan ilk deneylerde FGF2 uyarımı sonucunda SIK2 aktivitesinde hızlı ve geçici bir artış görülmüştür, bu da kinazın bu yolağın bir elemanı olabileceğini doğrulamaktadır. Daha sonra, SIK2 çokça anlatımı ile FGF2'ye bağlı ERK ve Akt aktivasyonlarında azalma gösterilmiştir. SIK2'nin baskılanması ise aktif ERK ve Akt düzeylerinin intensite ve süresini azaltmakta olup FGF2'ye bağlı Müller hücre çoğalmasında çarpıcı bir artışa yol açmaktadır. Gab1'in SIK2 tarafından forforlanması *in vitro*'da doğrulanmış ve etkileşimleri ko-immünçökeltme ile belilenmiştir. Gab1'in serin fosforlanması SIK2 baskılanması ile kayda değer oranda azamaktadır. Aynı sürede tirozin fosforlanması ve bağlanma partnerlerinin etkileşimi (p85/Gab1, Shp2/Gab1, Grb2/Gab1) ise artmaktadır. Bu verilere dayanarak SIK2'nin Gab1'i serininden fosforlayarak FGF/Ras/ERK ve FGF/PI3K/Akt yolaklarının ve buna bağlı Müller hücre çoğalmasının negatif geri bildirim mekanizmasında yer aldığını önermekteyiz. Insülin yolağı çalışmalarında ise artan IRS1 tirozin fosforlanmasını takiben Akt aktivasyonunun Müller hücre sağkalımına yol açtığı saptanmıştır. SIK2'nin baskılanması oldukça erken evrede FGF2'ye bağlı Akt aktivasyonuna neden olmaktadır, çokça anlatımı ise Akt aktivasyonunu ve hücre sağkalımını engellemektedir. Hiperglisemi koşullarında MIO-M1 hücrelerinde IRS1 protein düzeyinde ve tirozin fosforlanmasında azalma, SIK2 aktivite ve ifadesinde artma, aynı zamanda bazal ve insuline bağlı Akt aktivasyonunda düşüş gözlenmiştir. SIK2'nin baskılanması hiperglisemide görülen pAkt düzeyini normal düzeye getirmekte olup fizyolojik glukoz koşullarında SIK2'nin çokça anlatımı ise Akt fosforlanmasını azaltmış ve apoptozu arttırmıştır. Bu gözlemlere dayanarak SIK2'nin insüline bağlı IRS1/Akt aracılığı ile görülen Müller hücre sağkalımının negatif modülatörü olduğunu, bunun da diyabette görülen glia ölümüne katkıda bulunabileceğini önermekteyiz.

TABLE OF CONTENTS

LIST OF FIGURES

LIST OF TABLES

LIST OF ACRONYMS/ABBREVIATIONS

AMPK	AMP-activated Kinase
APS	Amonium Persulfate
ATP	Adenosine Triphosphate
BAD	Bcl-2-associated Death
BAT	Brown Adipose Tissue
BCA	Bicinchoninic Acid
BDNF	Brain-Derived Neurotrophic Factor
bp	Base Pair
BrdU	Bromodeoxyuridine
BSA	Bovine Serum Albumine
$CaCl_2$	Calcium Chloride
cAMP	Cyclic Adenosine 5'-Monophosphate
CBP	CREB Binding Protein
Cbl	Casitas B-lineage Lymphoma
cDNA	Complementary DNA
chREBP	Carbohydrate Responsive Element-Binding Protein
Ci	Curie
c-Nap1	chromosome condensation-related SMC-associated protein 1
CNTF	Ciliary Neurotrophic Factor
RALBP	Cellular Retinaldehyde-Binding Protein
CREB	CRE Binding Protein
Co-IP	Co-Immunoprecipitation
CO_2	Carbondioxide
CRKL	CRK like protein
DAG	Diacylglycerol
DAPI	Diaminophenylindolamine
DMEM	Dulbecco's Modified Eagle Medium
DMSO	Dimethyl Sulfoxide
DNA	Deoxyribonucleic Acid
dNTP	Deoxyribonucleotide Triphosphate

DEPC	Diethylpyrocarbonate
DTT	Dithiothreitol
EBC	Extraction Buffer C
EDTA	Ethylenediaminetetraacetic Acid
EGF	Epithelial Growth Factor
EGFR	Epithelial Growth Factor Receptor
EGTA	Ethylene Glycol Tetraacetic Acid
ERK	Extracellular Regulated Kinase
FBS	Fetal Bovine Serum
FGF	Fibroblast Growth Factor
FGFR	Fibroblast Growth Factor Receptor
FITC	Fluorescein Isothiocyanate
FL	Full Length
FRS2	Fibroblast Growth Factor Receptor Substrate
GAB1	Grb2-Associated Binder 1
GABA	Gamma-Aminobutyric Acid
GAP	Gtpase Activating Protein
GFAP	Glial Fibrillary Acidic Protein
GFP	Green Fluorescent Protein
Grb2	Growth Factor Receptor-Bound Protein 2
GS	Glutamine Synthase
GSK	Glycogen Synthase Kinase
GST	Glutathione S Transferase
GTP	Guanosine-Triphosphate
H_2O	Water
HGF	Hepatocyte Growth Factor
HRP	Horse Radish Peroxidase
HSPG	Heparan Sulfate Proteoglycans
IGF	Insulin-Like Growth Factor
IgG	Immunoglobulin G
IP	Immunoprecipitation
IPTG	Isopropyl-B-D-Thio-Galactoside
IR	Insulin Receptor

IRS	Insulin Receptor Substrate
IVK	*In Vitro* Kinase
JNK	C-Jun N-Terminal Kinase
kb	Kilobase
KCl	Potassium Chloride
KD	Kinase Domain
kDa	Kilodalton
KI	Kinase Inactive
LB	Luria Bertani Broth
LIF	Leukemia İnhibitory Factor
LKB1	Liver Kinase B 1
MAPK	Mitogen-Activated Protein Kinase
MBD	Met Receptor Binding Domain
MIO-M1	Moorfields/Institute of Opthalmology-Müller 1
MITF	Microphthalmia-Associated Transcription Factor
mg	Miligram
$MgCl_2$	Magnesium Chloride
min.	Minutes
MKP	Map Kinase Phosphatase
ml	Mililiter
mm	Milimeter
mM	Milimolar
$MnCl_2$	Manganese Chloride
mRNA	Messenger Ribonucleic Acid
NaCl	Sodium Chloride
Na_3VO_4	Sodium Orthovanadate
NGF	Nerve Growth Factor
NLS	Nuclear Localization Signal
nm	Nanometer
NMDA	N-Methyl-D-Aspartate
ng	Nanogram
NP-40	Nonidet P-40
NT-3	Neurotrophin-3

OD	Optical Density
PAGE	PolyAcylamide Gel Electrophoresis
pAkt	Phospho-Akt
PBS	Phosphate Buffered Saline
PCR	Polymerase Chain Reaction
PC12	Pheochromocytoma
pERK	Phospho-Extracellular Regulated Kinase
pg	Picogram
PH	Plekstrin Homology
PHLPP	Ph-Domain Leucine-Rich Repeat Protein Phosphatase
PI3K	Phosphoinositide 3-Kinase
PIP2	Phosphatidylinositol 4,5-Bisphosphate
PIP3	Phosphatidylinositol (3,4,5)-Triphosphate
PKA	Protein Kinase A
PKC	Protein Kinase C
PLCγ	Phospholipase C-gamma
pM	Picomolar
PMSF	Phenylmethanesulfonylfluoride
PP2A	Protein Phosphatase 2A
pSer	Phophoserine
PTB	Phosphotyrosine Binding
pThr	Phosphothreonine
pTyr	Phosphotyrosine
PVDF	Polyvinylidene Fluoride
qRT-PCR	Quantitative Real-Time Polymerase Chain Reaction
RGC	Retina Ganglion Cells
RK-rich	Arginine-Lysine-rich
RNA	Ribonucleic Acid
RPE	Retina Pigmented Epithelium
rpm	Rotations Per Minute
RTK	Receptor Tyrosine Kinase
RT-PCR	Reverse Transcriptase-Polymerase Chain Reaction
SAPK	Stress-Activated Protein Kinase

SDS	Sodium Dedocyl Sulfate
SDS-PAGE	SDS- Polyacrylamide Gel Electrophoresis
Sef	Similar Expression To Fgf Genes
Ser	Serine
SH	Src Homology Domain
SHP2	Sh2-Domain Containing Phosphatase 2
shRNA	Small Hairpin RNA
SIK2	Salt Inducible Kinase 2
siRNA	Small Interfering RNA
Sos	Son of Sevenless
Spry	Sprouty
Srebp	Sterol Regulatory Element Binding Proteins
STZ	Streptozotocin
TAE	Tris-Acetate-EDTA
TBS	Tris Buffered Saline
TBST	Tris Buffered Saline Tween
TEMED	Tetramethylethylenediamine
TGF	Transforming Growth Factor
Thr	Threonine
TORC2	Transducer of Regulated CREB Activity
TRB-3	Tribbles-3
TSC	Tuberous Sclerosis Complex
TUNEL	Terminal Deoxynucleotidyl Transferase Dutp Nick End Labeling
UBA	Ubiquitin-Associated
UTR	Untranslated Region
UV	Ultraviolet
VEGF	Vascular Endothelial Growth Factor
WB	Western Blot
WT	Wild-Type
xg	Times Gravity

1. INTRODUCTION

1.1. The Retina

The retina is a complex neural circuit involved in transducing light into a pattern of electrical impulses to the brain. This tissue at the back of the eye (Figure 1.1) is a multi-layered structure, has a common architecture, evolutionary conserved across species with six classes of neurons, including two types of light sensitive photoreceptor cells; cones (daytime color vision) and rods (low light sensors) in mammalian species. Photoreceptor signals are processed through three types of interneurons; horizontal cells, bipolar cells and amacrine cells. The mammalian retina contains three types of glial cells. In addition to microglial cells, there are two forms of neuron-supporting macroglial cells, astrocytes and Müller (radial glial) cells (Bringmann *et al.*, 2006).

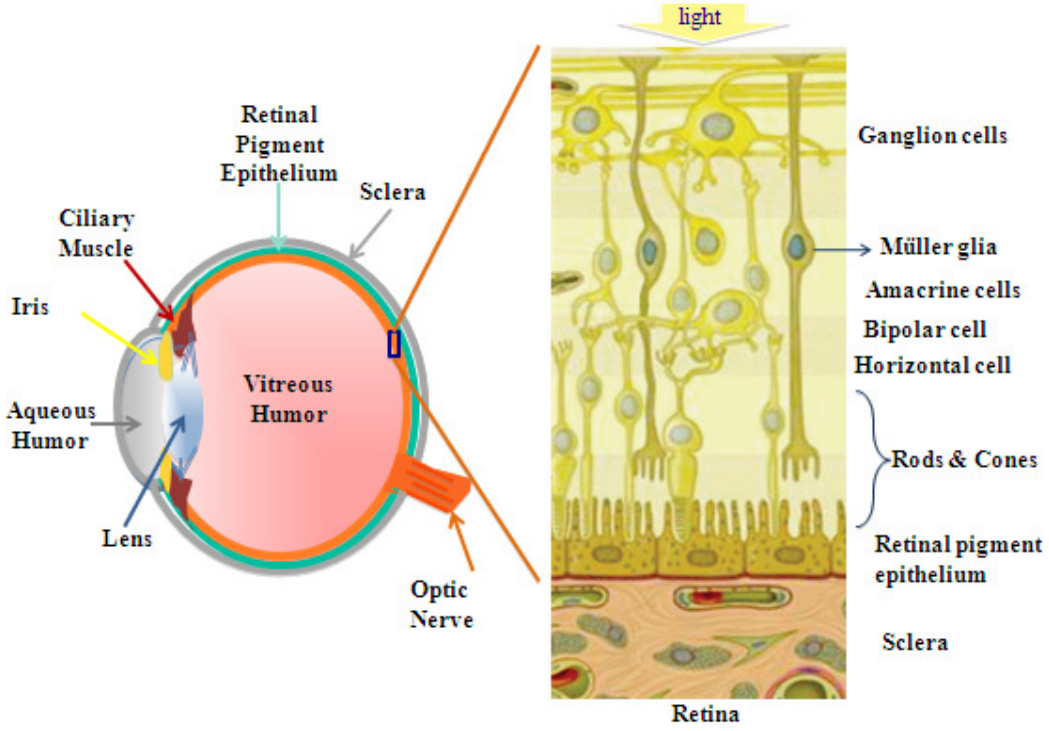

Figure 1.1. The vertebrate eye and magnified layered structure of the retina (Modified from Bringmann *et al.*, 2006).

1.2. Müller Cells of The Retina

Müller cells are the main glial cells of the retina. Although their cell bodies are located within the inner nuclear layer, their processes span the entire thickness of the tissue and contacting with both retinal neurons and blood vessels (Bringmann *et al*., 2006) (Figure 1.2). During retinal development at the PN8-10 precursors are differentiated into mature Müller cells. In the adult, they are mainly involved in maintenance of homeostasis of the retinal extracellular space by balancing K^+ ions, pH by the activity of carbonic anhydrase and by removing neurotransmitters GABA, glycine and glutamate. Glutamine synthetase (GS) localized to the Müller cells, converts internalized glutamate to glutamine which is recycled back to neurons. The clearance of synaptic glutamate is required for the normal functioning of excitatory synapses and for the prevention of neurotoxicity (Barnett and Pow, 2000).

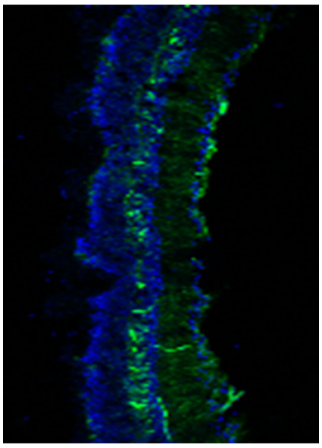

Figure 1.2. Retinal section from rats with GFP expressed in their Müller cells. Retinal cell nuclei were stained with DAPI.

Müller cells are also thought to provide trophic factors for neuronal survival. Trophic factors secreted from Müller cells have been reported to support retinal ganglion cell survival and neuritogenesis (Garcia *et al*., 2002). Müller glia within the retina or in culture express mRNA and protein for the neurotrophin, nerve growth factor (NGF; Chakrabarti et al., 1990), brain-derived neurotrophic factor (BDNF; Seki *et al*., 2005), neurotrophin-3 (NT3, Taylor *et al*., 2003) and their high-affinity Trk (Wahlin *et al*., 2000 and Oku *et al*., 2002) or low-affinity p75 (Garcia and Vecino, 2003) receptors. In addition, FGF2 (Bugra *et al*. 1997, Gao and Hollyfield, 1992), ciliary neurotrophic factor (CNTF; Cao *et al*.,

1997) and leukemia inhibitory factor (LIF; Neophytou *et al*., 1997) are expressed in these cells. These molecules may contribute to different aspects of differentiation, proliferation, neuroprotection and survival of RGCs, interneurons and photopeceptors in the retina (Meyer-Franke *et al*., 1995, Harada *et al*., 2000, Peterson *et al*., 2000 and Kawasaki *et al*., 2000). Müller cells contribute to the regulation of blood flow and angiogenesis by the synthesis of vascular endothelial growth factor (VEGF) and transforming growth factor β (TGFβ; Bringmann *et al.*, 2006).

An important neuroprotective effect may be exerted by Müller cells because of their involvement in the retinal defense against free radicals by synthesizing the tripeptide glutathione from glutamate, cysteine, and glycine (Pow and Crook, 1995; Reichelt *et al*., 1997; Schütte and Werner, 1998). Reduced glutathione is provided to neurons (Schütte and Werner, 1998; Francke *et al*., 2003) which acts as a scavenger of free radicals and reactive oxygen compounds. Another way of neuroprotection is the uptake followed by detoxification of potentially harmful substances and even particles by Müller cells. This involves the phagocytosis of debris from dead neurons or pigment epithelial cells (Francke *et al*., 2001) and foreign bodies such as copper particles (Rosenthal and Appleton, 1975). Multidrug-resistance transporters expressed in the Müller cell membrane (Francke *et al*., 2003) are thought to remove large molecules from the extracellular space. The glutamine synthetase of Müller cells which is the only enzyme available for ammonia detoxification in the retina.

Another remarkable feature of Müller cells is their high rate of glucose utilization and glycogen storage and lactate formation in the presence of oxygen. In cultured human Müller cells, aerobic glycolysis is the major pathway of glucose metabolism (Winkler *et al*., 2000). In the presence of glucose and oxygen, cultured Müller cells obtain their ATP principally from glycolysis and have a low rate of oxygen consumption (Winkler *et al*., 2000). Aerobically, 99% of the total lactic acid production is accounted for glucose used in glycolysis. This metabolic pattern may spare oxygen for retinal neurons, particularly in the inner nuclear and ganglion cell layers under normal physiological conditions. High glycogen level, as well as the presence of glycogen synthase (GS) and glycogen phosphorylase proteins in Müller glia indicates that glycogen can be used as energy reserve for Müller cells themselves and for the neural retina. Müller cells convert glucose into

pyruvate and then lactate that is transported into neurons and utilized as energy source in photoreceptors (Poitry-Yamata *et al*., 1995).

Investigations of Müller cell functions *in vitro* have been challenging, because of the difficulty in obtaining pure cell populations and the tendency of these cells to differentiate rapidly in culture (Sarthy *et al*., 1998). Moorfiels Institute of Ophthalmology - Müller 1 (MIO-M1) cell line is a spontaneously immortalized human Müller cell line that was a small proportion of the cells isolated from human cadaveric retinae (Limb *et al*., 2002). They could continue proliferation for 120 passages in culture (Limb *et al*., 2002; Lawrence *et al*., 2007) retain all the differentiated Müller cell characteristics, and express well-characterized markers of Müller glial cells, including CRALBP, EGFR, vimentin and gluthamine synthase (Lawrence *et al*., 2007). They also express retinal stem cell markers, Sox2, Pax6, Chx10 and Notch1 *in vitro* (Lawrence *et al*., 2007). When MIO-M1 cells were incubated for 7 days in culture with FGF2, they were differentiated into almost all types of neurons (Lawrence *et al*., 2007).

Müller cell dysfunction or degeneration has been suggested as a primary cause for visual loss in Müller cell sheen dystrophy (Kellner *et al*., 1998), retinoschisis (Condon *et al*., 1986; De Jong *et al*., 1991; Kirsch *et al*., 1996), macular hole formation (Gass, 1999; Sugiyama *et al*., 2006), and at least one type of retinitis pigmentosa (Maw *et al*., 1997).

1.2.1. Müller Cell Gliosis

Müller cells, as the glia of the central nervous system, undergo an abnormal proliferation called gliosis as a result of retinal injury and diseases such as experimental retinal detachment, retinal ischemia-reperfusion, and endotoxin-induced uveitis, glaucoma, proliferative retinopathies and diabetic retinopathy. The upregulation of the intermediate filament protein, glial fibrillary acidic protein (GFAP) in the response of Müller cells to retinal diseases and injuries is established as stress indicator (Bignami and Dahl, 1979; Eisenfeld *et al*., 1984; Bringmann and Reichenbach, 2001). Another Müller cell response is the activation of ERK1/2 which is observed in animal models of various retinopathies such as retinal detachment, ischemia-reperfusion, uveitis, and glaucoma (Geller *et al*., 2001; Akiyama *et al*., 2002; Takeda *et al*., 2002; Tezel *et al*., 2003). ERK activation in response

to these retinopathies is suggested to upregulate GFAP expression via CREB in Müller cells and downregulate cyclin kinase inhibitor, $p27^{kip1}$ that mediates entry of Müller cells into the cell cycle (Bringmann *et al*., 2009).

Gliosis is two-faced, contributing to both damage and protection of neurons (Bringmann and Reichenbach, 2001). Early after injury it is thought that gliosis is neuroprotective, representing a cellular attempt to protect the tissue from further damage by the release of neurotrophic factors and antioxidants (Schütte and Werner, 1998; Frasson *et al*., 1999; Honjo *et al*., 2000; Oku *et al*., 2002). Some of the factors released by activated Müller cells such as the VEGF, may have both neuroprotective (Yasuhara *et al*., 2004) and detrimental effects, as VEGF may exacerbate disease progression by inducing vascular leakage and neovascularization. Likewise, Müller cells increase the expression of nitric oxide synthase in response to ischemia and early in diabetic retinopathy (Goureau *et al*., 1994; Abu-El-Asrar *et al*., 2001). Enzymatically formed nitric oxide exerts beneficial effects by counteracting ischemia through dilating retinal vessels, and low nitric oxide protects neurons from glutamate toxicity via closing of N-methyl-D-aspartate (NMDA) receptor channels (Kashii *et al*., 1996). However, higher concentrations of nitric oxide and subsequent formation of free nitrogen radicals are cytotoxic for neurons, and are implicated in the development of diabetic retinopathy (Roth, 1997; Goureau *et al*., 1999; Koeberle and Ball, 1999).

It has been postulated that at later stages of gliosis the de-differentiation of the Müller cells contributes to neuronal cell death via impairment of neurotransmitter removal and dysregulation of the ion and water homeostasis after down-regulation of K+ channels causing edema. Generally, an impairment of supportive functions of Müller cells may have an additive effect on dysfunction and loss of neurons, by increasing the susceptibility of neurons to stressful stimuli in the diseased retina. Finally, Müller cells may re-enter the proliferation cycle to establish a glial scar (Burke and Smith, 1981). During retinal detachment, for example, Müller cell processes grow through the outer limiting membrane and fill the spaces left by dying photoreceptors (Lewis and Fisher, 2000). Within the subretinal space, the Müller cell processes then form a fibrotic layer that completely inhibits the regeneration of outer photoreceptor segments (Anderson *et al*., 1986). Glial scars involve the expression of inhibitory molecules on the surface of reactive glial cells

which additionally inhibit regular tissue repair and neuroregeneration (Fawcett and Asher, 1999).

The molecular mechanisms underlying this gliotic response in retina as a result of disease states are still not well understood. *In vitro* studies indicate that FGF2-evoked signaling is crucial for the proliferation of an immortalized Müller cell line, MIO-M1 and primary Müller cell cultures (Hollborn *et al.,* 2004, Hicks and Courtois, 1992, Cinaroglu, 2005). Our recent studies have shown that FGF9 also induces Müller cell proliferation in primary cell cultures (Cinaroglu, 2005). ERK1/2, p38 and Akt activations are involved in mediating the mitogenic effect of FGF2 seen in MIO-M1 cells (Hollborn *et al*., 2004). The stimulating effect of FGF2 on the MAPK activation may have important consequences with regard to induction of retinal proliferation and survival of retinal neurons (Kinkl *et al*., 2001). During experimental detachment, FGF2 is released within minutes from Müller cells, RPE and neurons in the retina, as indicated by the phosphorylation of the FGF receptors, and by activation of ERK1/2 in Müller cells (Geller *et al*., 2001); this observation may imply FGF2 as one of the signaling molecules that cause the detachment-induced retinal gliosis. In diabetic rat models, the mRNA and the protein levels of FGF2 are increased in retina, but its expression does not change in Müller cells (Layton *et al.,* 2006).

An alternate glial cell response to retinal damages is the transdifferentiation of Müller cells into neurons. A small subpopulation of Müller cells undergo this proliferation and de-differentiation process to compensate for the neural loss after retinal damages. Fish and to a limited extent birds (posthatch chicks) have regenerative responses to injuries where Müller cells transdifferentiate into all types of neurons and completely restore the vision. However, in the mammalian retina the regenerative response of the Müller glia to injury is even more limited than that of birds both in quantity and types of neurons generated (Karl and Reh, 2010).

1.2.2. Müller Cells in Diabetic Retinopathy

A major complication of diabetes in the retina is the development of diabetic retinopathy. Retinal neuron and glial cell degenerations are evident early on in the course of diabetes and especially glial degeneration/dysfunction could contribute to microangiopathy and neuronal loss (Barber *et al*., 2005; Barber *et al*., 1998). Diabetes depresses retinal insulin signaling with decreased IR, Akt1 and Akt3 activities (Rajala *et al*., 2009; Reiter *et al*., 2003; Reiter *et al*., 2006). Apoptosis of retinal vascular and neuronal cells is suggested to be associated with increased release of extracellular glutamate, loss of trophic factor/ survival signaling (insulin-induced PI3K/Akt), increased oxidative stress and neuro-inflammation (Barber *et al*., 2011). Given the Müller cells importance in maintaining neuronal and vascular function in the retina, it is of particularly important to explore Müller glia dysfunction/death within the context of diabetic retinopathy. In diabetic animals, several functions of Müller cells were dysregulated, including alterations in their capacity to regulate potassium and glutamate in the extracellular space, accumulation of GABA, upregulation of pro-inflammatory cytokines, and increased expression of angiogenic growth factors, such as VEGF and insulin-like growth factor (IGF)-1 (Lieth *et al*., 1998; Li and Puro, 2002; Pannicke *et al*., 2006; Gerhardinger *et al*., 2005; Amin *et al*., 1997; Inokuchi *et al*., 2001). Diabetes has been reported to accelerate Müller glia apoptosis *in vivo* (Hammes *et al*., 1995). Later in another study Müller glial cells were reported to undergo apoptosis by downregulation of Akt under hyperglycemic conditions although the mechanism leading to this is not fully understood. Consistent with this *in vitro* result, a significant decrease in Akt activity was observed in Müller cells in the retina of longterm diabetic animals (Xi *et al*., 2005).

Both the hyperglycemia and insulin-deficiency in diabetes contribute equally to diabetic retinopathy by inducing retinal cell death (Fort *et al*., 2011). Hyperglycemia causes neuronal apoptosis via both altering the neuroprotective effect on insulin-mediated Akt signaling and glycosylation of proteins involved in cell survival (Nakamura *et al*., 2001). Later, it has been proposed that hyperglycemia induces insulin resistance in the retina (Fort *et al*., 2011).

1.3. Fibroblast Growth Factors

The FGF family comprises 23 polypeptide growth factors that are evolutionarily conserved among different species from nematodes to humans (Ornitz *et al*., 2001). The members vary in size from 17 to 34 kDa in vertebrates and share an internal core domain of 120 amino acids, with 28 highly conserved and six identical amino acid residues. They are known to bind heparin and interact with high affinity receptors (FGFRs) on target cell membranes (Eriksson *et al*., 1991, Zhu X *et al*., 1991, Plotnikov *et al*., 1999).

Most FGF family members have an amino-terminal signal peptide and are secreted by a classical pathway. FGF1, 2, 9, 16, and 20 lack this peptide, they are secreted by an alternative pathway (Miyake *et al*., 1998). FGF11-14 lack signal sequences and are intracellular (Smallwood *et al*., 1996). FGF2 and FGF3 contain nuclear localization signals, therefore these proteins can be found in the nucleus (Powell and Klagsbrun, 1991).

FGF family members are differentially expressed in many tissues with different spatiotemporal patterns. FGF3, 4, 8, 15, 17, and 19 are expressed exclusively during embryonic development, whereas others are expressed both in embryonic and adult tissues (Ornitz *et al*., 2001).

The first member of the FGF family, FGF1, was identified by its ability to stimulate proliferation of fibroblasts. Other than cell proliferation, family members are implicated in gastrulation, embryonic axis formation, cellular differentiation and migration during development of vertebrates (Slack, 1994). In the adult organism, they mediate several cellular responses such as tissue repair, wound healing, and angiogenesis (Ornitz *et al*., 2001).

Several FGF family members are expressed during vertebrate eye development and also in the mature retina. FGF3, FGF8, and FGF17 have been identified during development in the optic stalk of several vertebrate models (Crossley and Martin, 1995; Reifers *et al*., 1998; Vogel-Hopker *et al*., 2000; Walshe and Mason, 2003). FGF2 mediates neural, but not RPE differentiation in chick embryonic retina (Pittack *et al*., 1997). FGF1 is expressed at high levels in the peripheral retina during the initial stage of chick

retinogenesis (McCabe *et al.*, 1999). FGF19 has been detected in embryonic human retina (Xie *et al.*, 1999). At neuronal cells of postnatal retina were shown to express FGF1, FGF2 and FGF9, highest levels in the adult (Buğra *et al.*, 1993; Buğra and Hicks, 1997; Çınaroğlu *et al.*, 2005). In the mature chick retina, Müller glia are plastic and can respond to FGF2 by proliferation and subsequent transdifferentiation into neurons via sustained MAPK activation (Fischer *et al.*, 2002; Fischer *et al.*, 2009). FGF1, FGF2 and FGF9 are mitogenic for Müller cells *in vitro.* FGF1, FGF2 proposed to be important for photoreceptor survival (Cinaroglu *et al.*, 2005; Hicks and Courtois, 1992).

1.4. FGF/FGFR Signal Transduction Pathways

FGF's mediate their effects by binding to and activating FGFR's that are a subfamily of cell surface receptor tyrosine kinases (RTK's) with the help of heparan sulfate proteoglycans (HSPG) (Ornitz, 2000). The FGFR family is composed of four members, FGFR1-4, which share between 55% to 72% homology at the protein level (Johnson and Williams, 1993).

Once FGF ligand binds FGFR with the help of HSPG, receptor dimerization sets stage for autophosphorylation of different tyrosine residues in the cytoplasmic portion. This creates docking sites for downstream proteins containing src homology 2 (SH2), src homology 3 (SH3) and phosphotyrosine binding (PTB) domains such as FRS2, Shp2, and PLCγ (Pawson, 1995). Specific signals can be transduced in a cell context-dependent manner and through recruitment of different signaling elements; the three main pathways activated downstream of FGFRs are the phospholipase C-gamma (PLCγ)/Ca^{2+} pathway, the Ras/Mitogen-activated protein kinase (Ras/MAPK) pathway and the phosphoinositide 3-kinase (PI3 kinase)/Akt pathway (Mason, 2007) (Figure 1.3).

1.4.1. PLCγ/Ca^{2+} Pathway

PLCγ is known to be a substrate of all FGFRs. Autophosphorylation at Tyr-766 of FGFR1 creates a docking site for the SH2 domain of PLCγ (Maffucci *et al.*, 2009; Mohammadi *et al.*, 1991). After receptor interaction PLCγ is activated by tyrosine phosphorylation. Active PLCγ hydrolyzes phosphotidylinositol-4,5-diphosphate (PIP2) to

form inositol-1,4,5-triphosphate and diacylglycerol (DAG). In turn, DAG activates protein kinase C (PKC), whereas inositol-1,4,5-triphosphate stimulates Ca^{2+} release from intracellular compartments (Burgess *et al*., 1990; Mohammadi *et al*., 1991). PLCγ modifies the phosphorylation status of Raf via PKC and thereby the Ras/MAPK pathway activation (Huang *et. al.*, 1995).

1.4.2. Ras/ MAPK Pathway

FGF dependent proliferation and differentiation events are mainly transduced via Ras/ERK pathway. The main modulator of the pathway is FRS2, which upon interaction with the juxtamembrane region of FGFRs is phosphorylated on several tyrosine residues, four of which create docking sites for the Grb2-Sos complex and two for Shp2 binding. Sos, a guanine nucleotide exchange factor, recruitment to membrane into close proximity of the small G-protein Ras activates this protein, which in turn activates effector protein Raf. Raf, a serine-threonine kinase, stimulates MEK, MEK phosphorylates ERK on its threonine and tyrosine residues. Activated ERK phosphorylates transcription factors, such as Elk1, Ets1, c-Myc in the nucleus that upregulate gene expressions involved in cell cycle progression (Yang *et al*., 2004). Gab1 also contributes to FGF-mediated ERK signaling through Shp association that diminishes RasGAP/Gab1 binding inducing Ras activation. The sustained activation of ERK by FGF stimulation is considered to induce differentiation, whereas transient activation induces proliferation of PC12 cells (Marshall, 1994; Yamada and Yoshimura, 2002). ERK signal attenuation depends on negative-feedback mechanisms in this pathway. FGF2 induces MIO-M1 cell proliferation via transient ERK activation (Hollborn *et al*., 2004; Çınaroğlu *et al*., 2005).

p38 and c-Jun N-terminal kinase/stress-activated protein kinase (JNK/SAPK) also belongs to the MAPK family. These MAPKs are mainly involved in transmitting cytokine production and cytokine stimulated cellular proliferation and survival (Allen *et al*., 2000, Crawley *et al*., 1997).

1.4.3. PI3K/ AKT Pathway

This is the main pathway that blocks apoptosis and mediates growth factor-dependent cell survival (Hawkins *et al*., 1997). PI3K can be activated by FGFRs either by binding of PI3K-regulatory subunit p85 to phosphorylated tyrosines, Tyr724 of FGFR3 for example, or by the recruitment of PI3K catalytic subunit p110 to the membrane by activated Ras (Rodriguez *et al*., 1994). In the third mechanism, Grb2-associated binder 1 (Gab1)-FRS2-Grb2 complex brings PI3K-p85 subunit to the membrane. The active PI3K can activate Akt directly or indirectly via phosphorylation by PDK1/PRK-2 complex at Thr308 and Ser473 residues (Hadari *et al*., 2001). Activated Akt phosphorylates Bad and Caspase 9 rendering these apoptotic proteins inactive, and forkhead transcription factors such as FKHRL1, FKHR, and AFX, so that they are sequestered in the cytoplasm due to binding of 14-3-3 protein to the phosphoserine residues. This leads to cell survival.

Reduced FGF2-dependent proliferation of MIO-M1 cells observed in the presence of PI3K inhibitor, LY294002 implicates Akt pathway in the mitogenic response (Hollborn *et al*., 2004; Çınaroğlu, 2005).

1.5. Negative Regulation of FGF Signaling Pathways

FGF induced Ras/ERK pathway is negatively regulated at multiple sites (Figure 1.3). Sprouty (Spry), Sef, map kinase phosphatase 1 (MKP1) and Mkp3 proteins are negative feedback inhibitors and their expressions are positively regulated by ERK signaling (Tsang and Dawid, 2004). Spry is tyrosine phosphorylated upon FGF stimulation and binds to Grb2 that prevents Sos1 from activating Ras. Another mechanism involves Spry and Raf1 interaction that prevents Raf1 binding to MEK. Sef, a transmembrane protein, is another antagonist of FGF signaling acting on FGF/FGFR binding or sef-b (sef isoform that lacks signal peptide) downregulates FGF signaling downstream of MEK (Kovalenko *et al*., 2003; Preger et al., 2004). MKP's represent a family of dual-specificity phosphatases that specifically inactivates pERK (Farooq *et al*., 2001). MKP1 dephosphoshorylates pERK in the nucleus and MKP3 in the cytoplasm (Pouyssegur *et al*., 2003). Another negative feedback mechanism involves serine/threonine phosphorylations of Frs2 by ERK that inhibits recruitment of Grb2 through Frs2 (Lax *et al*., 2002; Gotoh, 2008). Another

mechanism for FGF signal attenuation is FGFR degradation that is mediated by binding of ubiquitin ligase Cbl to activated Frs2 and ubiquitination of the receptor that acts as a signal for receptor degradation (Wong *et al*., 2002).

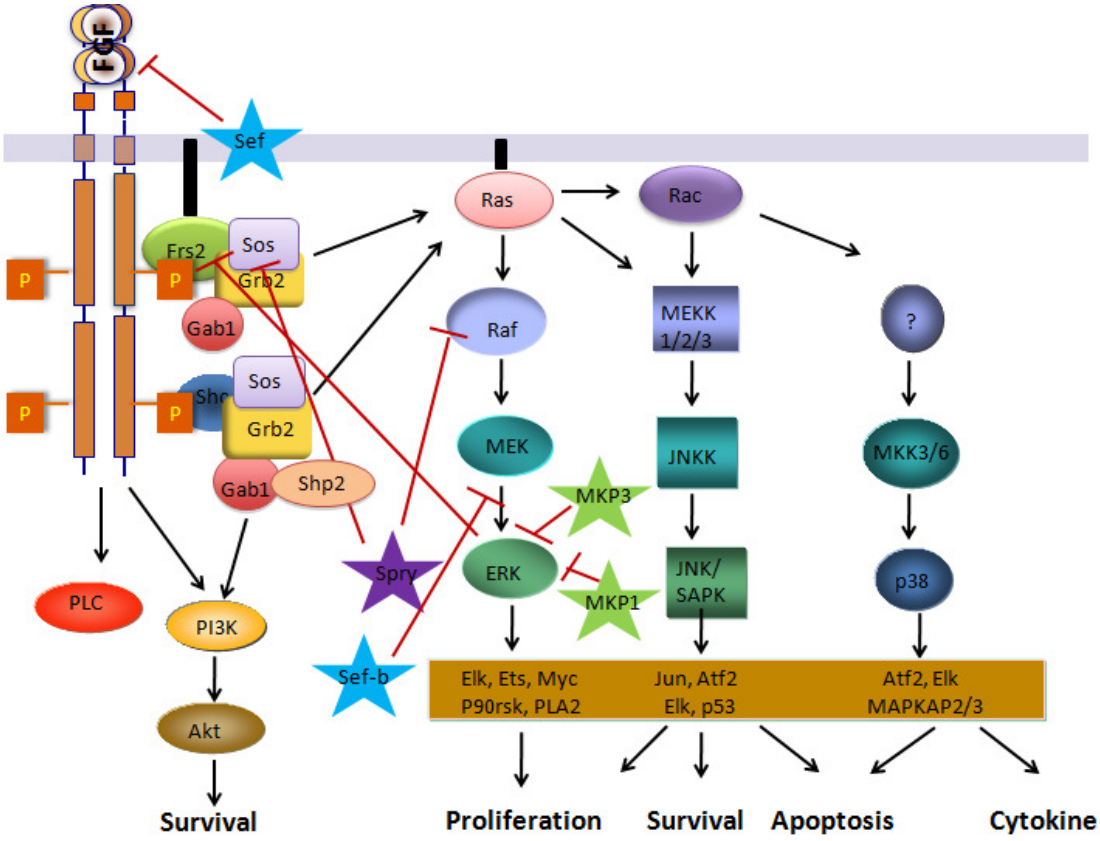

Figure 1.3. Three main pathways downstream of FGFR in response to FGFs. PLCγ/Ca2+ pathway elements, Ras/MAPK pathway elements, and PI3K/Akt pathway elements. Stars: Negative regulators of FGF pathway, red bars: Negative feedback regulations (Modified from Mason *et al*., 2007).

1.6. Gab1

Gab1 is a member of an adaptor/scaffolding protein family that includes Gab2, Gab3, IRS1, IRS2, IRS3, FRS2 and Dok (Schlessinger *et al*., 2000). Gab proteins range in size from 586 to 695 amino acids (Gu *et al*., 1998). Gab1 was originally cloned as a Grb2-associated protein that is tyrosine phosphorylated in cells upon stimulation with various growth factors including EGF, insulin, NGF, HGF, PDGF and FGF2 (Holgado Madruga *et al*., 1996; Rakhit *et al*. 2000; Ong *et al*., 2001). It contains an N-terminal plekstrin-

homology (PH) domain, proline-rich motifs and 16 potential tyrosine-phosphorylation sites and 47 potential serine/threonine phosphorylation sites (Figure 1.4) (Holgado-Madruga *et al*., 1996; Lock *et al*., 2000; Schaeper *et al*., 2000). Gab1 associates with hepatocyte growth factor receptor (Met receptor), but does not associate with the insulin receptor (IR), epidermal growth factor receptor (EGFR) or FGFR. With the amino-terminal PH domain Gab1 is anchored to the membrane and it interacts constitutively with SH3 domain of Grb2 through its proline rich region. Gab1/Grb2 association is essential for Gab1 recruitment to the inner membrane surface of cells. Grb2/Gab1 complex is recruited to the tyrosine phosphorylated Frs2 protein and because of its proximity to FGFR. Gab1 becomes tyrosine phosphorylated on sites that bind to the p85 of PI3 kinase and consequently leads to the activation of cell survival pathways in FGF stimulated cells (Ong *et al*., 2001). Association between the pTyr627 and pTyr659 of Gab proteins and the SH2 domains of Shp2 is an essential part of the mechanism that upregulates its tyrosine phosphorylation of 542/580 residues and the phosphatase activity of Shp2, leading to activation of the MAPK cascade and subsequent biological responses (Cunnick *et al.,* 2001; Araki *et al*., 2003). Gab1 involvement in FGF2-induced ERK signaling has been shown in chondrocytes in that inhibition of the Shp2 association to Gab1 and Frs2 decreases FGF2 induced ERK activation (Krejci *et al*., 2007). It was recently demonstrated that upon EGFR activation, Shp2 dephosphorylates Gab1 on its Ras-GAP interaction motif. Therefore, Ras-GAP disengages from the complex; consequently, increases Ras activity (Montagner *et al.,* 2005). Gab family proteins acting via Shp2 are required for full ERK activation in many signaling pathways. In most of them Gab1/Shp2 complex formation is not absolutely necessary for Ras/ERK activation, but sustained activity is defective in Gab1−/− cells. Thus, binding of Gab1 to Shp2 has been suggested to act as a signal amplifier (Gu *et al*., 2003). Shp2 mediated dephosphorylation of different motifs on Gab proteins also functions in signal termination. Shp2 was reported to dephosphorylate the PI3K binding site on Gab1, thus negatively regulating PI3K/Akt upon EGF stimulation (Zhang *et al*., 2002). Recent studies have proposed that Shp2 mediates a basal level of Ras/MAPK signaling in Müller glial cells during postnatal development and in the adult retina (Cai *et al*., 2011). It has been suggested that, Gab1 hyperphosphorylation on serine/threonine residues attenuates tyrosine phosphorylation. This in turn, prevents interaction with its partners, possibly due to a conformational change that renders the kinase domain of growth factor receptors inaccessible (Gual *et al.,* 2001). Besides Shp2, upon EGF stimulation, ERK

phosphorylates several serine residues in the vicinity of PI3K binding tyrosine residues on Gab1, that blocks PI3K binding to Gab1 and inhibits PI3K/Akt pathway (Lehr *et al*., 2004) (Figure1.4). PKC is another identified Gab1 serine kinase that negatively regulates PI3K/Akt signaling in HGF stimulated cells (Gual *et al*., 2001). Binding of Gab1 to Crk, CrkL and PLCγ have also been reported (Schaeper *et al.,* 2000). Knock-out of the *gab1* gene results in developmental defects in heart, placenta and skin leading to embryonic lethality in mice and its overexpression is implicated in breast cancer (Sachs *et al*., 2000; Yamasaki *et al*., 2003). The intensity and duration of ERK signaling determines the cell fate. For example, EGF activates ERK only transiently, whereas NGF induces sustained ERK activity in PC12 cells (Kaplan, 1998). Underlying mechanism of this differential cell responses is that prolonged Gab1 tyrosine phosphorylation by NGF enhanced p85 and Shp2 association to Gab1. On the other hand, transient tyrosine phosphorylation of Gab1 is observed in EGF stimulated PC12 cells causing transient ERK activation, therefore proliferation of these cells, instead of differentiation due to the limited p85 and Shp2 association to Gab1 (Maroun *et al*., 1999, and Yu *et al*., 2002).

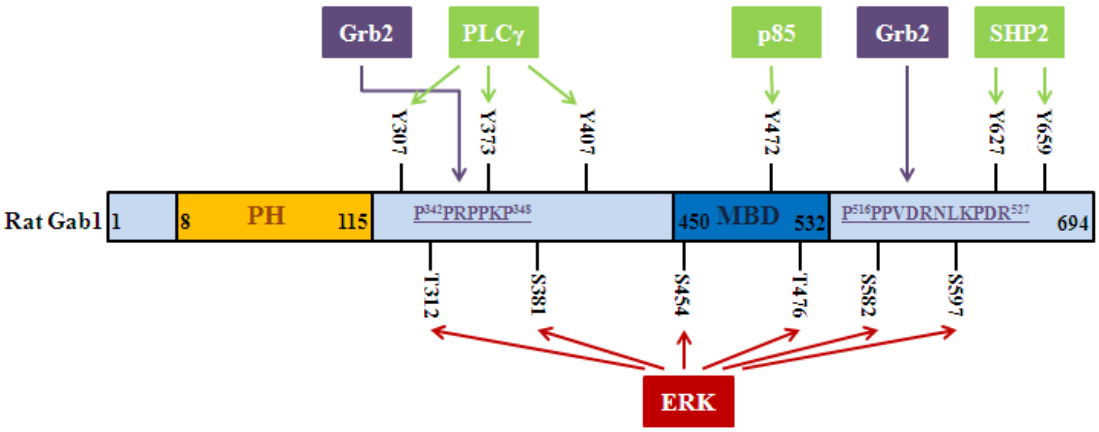

Figure 1.4. Domain structure and multiple tyrosine and serine phosphorylation sites of Gab1. Gab1/Grb2 association sites are shown in purple. Gab1 associates with several binding partners upon growth factor stimulation (green). Gab1 is phosphorylated by ser/thr kinases (red) that attenuate or predetermine the its tyrosine phosphorylations (Modifid from Holgado-Madruga *et al*., 1996).

1.7. Insulin Signal Transduction Pathways

Insulin is one of the anabolic hormones that is secreted from pancreatic β-cells after feeding to control glucose metabolism, cell survival and differentiation (Kanzaki *et al*., 2001). In the presence of insulin, IR is activated by cross-phosphorylation creating binding sites for insulin receptor substrate (IRS) proteins. Other than IRS proteins (IRS1-6), Gab (Gab1-3), Shc and Cbl are also IR substrates (Lehr *et al*., 2000, Baumann *et al*., 2000, Gustafson *et al*., 1995, Sun *et al*., 1991). IRS proteins are phosphorylated by IR that creates docking sites for SH2 domain containing protein p85 and Grb2-Sos complex, which in turn activates PI3K/Akt and Ras/ERK pathway, respectively (Saltiel *et al*., 2001). PI3K/Akt pathway is responsible for most of the metabolic actions of insulin such as glucose uptake, glycogen synthesis, gluconeogenesis and lipogenesis, whereas Ras/MAPK pathway in cooperation with Akt pathway controls cell growth and differentiation (Ueki *et al*., 2002).

Both insulin mRNA and protein was shown in Müller glial cells (Das *et al*., 1987) that suggests these cells may secrete the insulin for neurons as a paracrine hormone. The retina responds to insulin *in vitro* with significant elevations in Akt phosphorylation, while the Ras/ERK pathway is relatively insensitive to insulin stimulation (Diaz *et al*., 2000). Tonically active insulin signaling plays a role in mitogenesis and differentiation during embryonic stages and provide trophic support for retinal cell survival in the adulthood (Hernandez-Sanchez *et al*., 1995). Retinal cells expresses all IR and IRS1/2 proteins and they are all activated by insulin. Although the retina express all three Akt isoforms, Akt-1 was shown to be activated by insulin (Reiter *et al*., 2003). The phosphorylation of caspase-9 by Akt inhibits its activation that promotes cellular survival (Cardone *et al*., 1998). The Bcl family member protein, Bad, has also been implicated in regulating apoptosis in an Akt-dependent manner (Datta *et al*., 1997). Müller cells was shown to express IR and IRS1/2. However, the downstream pathway elements and cellular responses to insulin in these cells remain largely unkown (Folli *et al*., 1994).

1.7.1. Insulin-Induced PI3K/Akt Pathway

Akt family consists of three isoforms that are encoded by different genes. All share a similar structure that posseses an N-terminal PH domain and a C-terminal catalytic domain. Knockout and siRNA studies indicated that the isoforms are involved in the regulation of different biological processes. Akt1, which is ubiquituously expressed, controls cell growth and the lifespan of animals, but not metabolic pathways (Chen *et al*., 2001). By contrast, Akt2, which is particularly enriched in core insulin-sensitive tissues, such as liver and adipocytes, regulates insulin responsiveness, such as glucose uptake and gluconeogenesis (Cho *et al*., 2001). Akt3 is predominantly expressed in the nervous system and testis. It does not have a role in glucose homeostasis, but has significant effects on neural development (Tschopp *et al*., 2005).

In response to insulin stimulation, the SH2 domains of the p85 subunit bind to pYMPM and pYMNM sequences in IRS1 (Sun *et al*., 1993). When p85, the regulatory subunit of PI3K, is recruited to the cell membrane via IRS1 it binds to the p110 subunit forming active PI3K. PIP2 is converted to PIP3 by this enzyme in the vicinity of the membrane. PIP3 recruits PDK1 and Akt to the membrane. PDK1 and mTOR/Rictor complex then phosphorylate Akt on its activation loop Thr308 and Ser473 residues for its full activation, respectively (Dummler and Hemmings, 2007). Akt mediates most of the metabolic actions of insulin through phosphorylation of several downstream substrates. GSK3 is the first identified Akt target that mediates glycogen synthesis via glycogen synthase when it is inactivated by Akt phosphorylation (Frame and Cohen, 2001). Akt also induces glucose uptake by phosphorylating and inhibiting Rab-GTPase-activating protein (AS160), an important gene/protein for the translocation of glucose transporter GLUT4 to the plasma membrane (Sano *et al*., 2003). By phosphorylating TSC1/2, Akt activates the mTOR pathway. By association with Raptor and Rheb, the mTOR complex regulates protein synthesis. Akt also regulates expression of gluconeogenic and lipogenic enzymes by phosphorylating FOXO family transcription factors (Tran *et al*., 2003). Activated Akt phosphorylates Bad and Caspase 9 rendering these proapoptotic proteins inactive leading to cell survival (Figure 1.5).

1.7.2. Insulin-Induced Ras/ MAPK Pathway

Ras/MAPK pathway is activated by insulin following binding of Grb2-Sos complex to the pYVNI motif in IRS proteins, Shc and Gab1, so that Sos comes into the proximity of Ras, triggering the activation of the small GTPase Ras and subsequent activation of Raf, MEK1/2 and at the end ERK1/2 (Sun *et al*., 1993). Activated ERK1/2 is mainly involved in cell growth, survival and differentiation by phosphorylating p90RSK and ELK1 (Pouyssegur *et al*., 2002). Insulin has not been implicated in ERK1/2 activation in the retina (Reiter *et al*., 2003).

1.8. Negative Regulation of Insulin Signaling Pathways

Insulin-induced PI3K/Akt and Ras/MAPK pathways can be negatively regulated at multiple levels (Figure 1.5). The IR can be downregulated at the protein level by ligand-stimulated internalization and degradation or pTyr residues can be dephosphorylated by protein tyrosine phosphatases (PTPs; Friedman *et al*., 1997). Akt activity is downregulated by protein phosphatase 2A (PP2A) and the PH-domain leucine-rich repeat protein phosphatase (PHLPP; Gao *et al*., 2005). Tribbles-3 (TRB3) binds to unphosphorylated Akt and inhibits its phosphorylation and activation (Du *et al*., 2003). The most well known negative-feedback mechanism for the insulin signaling pathway is serine phosphorylation of IRS1 proteins (Zick, 2005). Many of the insulin-induced serine/threonine kinases that are downstream effectors of IRS proteins serve as negative modulators of IRS protein function (Zick, 2005).

1.9. IRS1

IRS1 was first identified by anti-pTyr immunoprecipitation as a 185-kDa pY protein (pp185) in insulin stimulated cells (White *et al*., 1985). It contains N-terminal PH and PTB domains that mediate its membrane and IR association, respectively (Luttrell *et al*., 1995; O'Neill *et al*., 1994). Because it contains 20 potential pY sites, it recruits various SH2 domain containing proteins to the membrane, such as p85 and Grb2-Sos that activates PI3K/Akt and Ras/MAPK pathways. SHP2 can also bind to IRS1 pY sites and dephosphorylate PI3K and Grb2 bound pY residues (Myers *et al*., 1998) (Figure 1.6).

Other than potential pY sites, IRS1 has 50 potential pSer sites that in general, seem to negatively regulate IRS signaling. Even in the basal state, IRS1 proteins are heavily phosphorylated on Ser/Thr residues. Upon insulin stimulation additional Ser/Thr residue phosphorylations are observed (Sun *et al.*, 1992) (Figure 1.6).

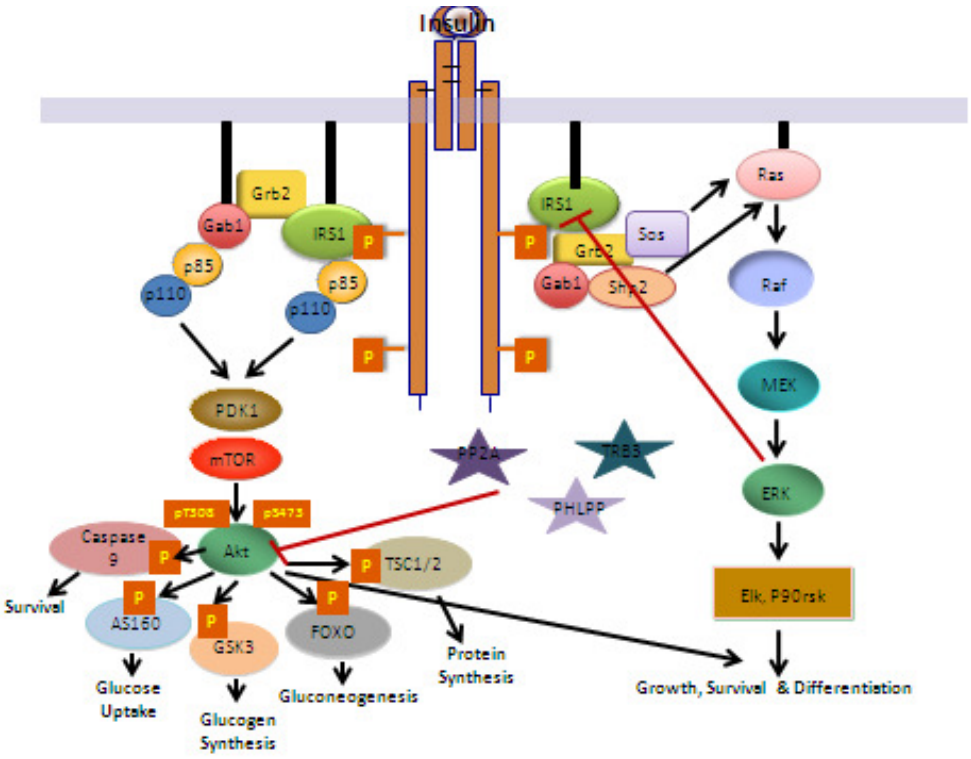

Figure 1.5. Two main pathways downstream of IR in response to insulin. PI3K/Akt pathway elements and Ras/MAPK pathway elements. Stars: Negative regulators of insulin pathway, red bars: Negative feedback regulations (Zick, 2005).

Under physiological conditions, negative feedback regulation is common to insulin signaling to attenuate it. This is accomplished by serine phosphorylation of IRS1 by IKKβ, PKC, ERK, JNK, and mTOR. Generally, serine phosphorylation of IRS1 protein results in its insulin receptor interaction loss, its tyrosine phosphorylation ablation, or its degradation enhanced. These processes eventually lead to downregulation of downstream effectors of IRS1, such as PI3K and subsequently retardation of Akt phosphorylation. Recent studies in cultured cells have shown that IRS-1 becomes serine phosphorylated by these serine/threonine kinases after prolonged exposure to many factors, including insulin (Ricort *et al.*, 1995; Li *et al.*, 1999), TNF-α (Kanety *et al.*, 1995; Hotamisligil *et al.*,1996; Feinstein *et al.*, 1993), free fatty acids (Tanti *et al.*, 1991; Haystead *et al.*, 1990), or glucose (Khan *et al.*, 1989; Kroder *et al.*, 1996), and consequently the IRS1 adaptor protein fails to

become tyrosyl-phosphorylated, which results in attenuation of insuling signaling, known as “insulin resistance”. Cellular stress, chronic insulin exposure and proinflammatory cytokines can induce the degradation of IRS1 through proteasome-dependent or -independent processes in adipocytes (Gual *et al*., 2005).

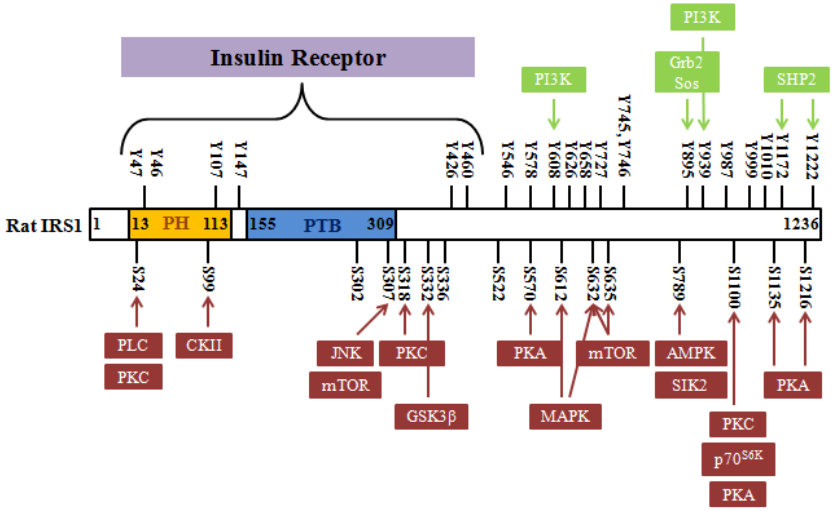

Figure 1.6. Tyrosine and serine phosphorylation of IRS1 upon insulin stimulation. IRS1 associates with several binding partners upon insulin stimulation (green). IRS1 is phosphorylated by many Ser/Thr kinases (red) that attenuate or predetermine its tyrosine phosphorylations.

1.10. Salt-Inducible Kinase Family

Salt-inducible kinase (SIK) proteins are members of the AMP-dependent protein kinases (AMPK)-related family of 14 serine/threonine kinases (Bright *et al*., 2009). In contrast to AMPK, they function as single subunit enzymes and lack the AMP and glycogen sensitivity (Hardie *et al*., 2004). The SIK family comprises three members, (SIK1-3). SIK1 was first identified in the myocardium (Ruiz *et al*., 1994) and cloned from adrenal glands of rats fed with high salt diet (Wang *et al*., 1999). Later, SIK2 and SIK3 proteins were identified by sequence homology (Katoh *et al*., 2004). All isoforms were conserved from *D. melanogaster* and *C. elegans* to humans (Lanjuin and Sengupta, 2002). In mammals, SIK1 is highly expressed in adrenal glands, brain, testes and skeletal muscles and in small amounts adipose tissue, liver and heart (Horike *et al*., 2003). On the other hand, SIK2 is mainly expressed in metabolic tissues such as adipose tissue, liver and brain. SIK3 is ubiquitously expressed (Okamoto *et al*., 2004). Both *Salt inducible kinase 2* and *Salt inducible kinase 3* genes are localized on chromosome 11, while *Salt inducible kinase*

1 gene is on chromosome 21 (Katoh *et al*., 2004). SIKs contain an N-terminal kinase domain with flexible activation loops, A-loops, near their substrate binding pocket. When phosphorylated by LKB1, there is a structural change in the catalytic site that leads to increased kinase activity (Lizcano *et al*., 2004). Adjacent to the kinase domain it contains a ubiquitin-associated (UBA) domain that is important for phosphorylation by LKB1 (Jaleel *et al*., 2006). All the SIKs have C-terminal PKA phosphorylation sites adjacent to an arginine-lysine-rich (RK-rich) region that functions as a non-canonical nuclear localization signal (Katoh *et al*., 2004). Phosphorylation by PKA causes nuclear export of the protein (Katoh *et al*., 2004).

1.10.1. SIK2

SIK2 was first identified in mouse adipose tissue. Its expression was induced in 3T3-L1 preadipoctes at the onset of differentiation, suggesting that the protein is important in the early phase of adipocyte differentiation (Horike *et al*., 2003; Yeh *et al*., 1995). The first substrate of SIK2 that has been identified is rat IRS1, an important regulator of the insulin pathway (Horike *et al*., 2003). Insulin dependent tyrosine phosphorylation of IRS1 by the insulin receptor, a member of the receptor tyrosine kinase family, initiates the activation of downstream elements of the pathway. But phosphorylation of S789 of IRS is known to attenuate insulin signaling either by interfering its association with the insulin receptor at the plasma membrane, preventing docking of downstream effectors or enhancing IRS degradation (Gual *et al*., 2005). As in insulin resistant rats, S789 phosphorylation of IRS is found to be elevated (Qiao *et al*., 2002) and SIK2 expression and activity were induced markedly in the white adipose tissue of diabetic mice (Horike *et al*., 2003), it was suggested that SIK2 might be involved in development of type 2 diabetes (Horike *et al*., 2003) (Figure 1.7). Recent work revealed that SIK2 activity is upregulated in adipocytes by nutrient deprivation and blockage of ATP synthesis that in turn inhibits lipogenic gene expression in white adipocytes (Du *et al*., 2008). It has been suggested that SIK2 inhibits thermogenesis in brown adipose tissue (BAT; Muraoka *et al*., 2009). Before insulin stimulation, SIK2 was proposed to phosphorylate TORC2 at S171, thus it is sequestered in the cytoplasm through interaction with 14-3-3 proteins and inhibits CREB dependent thermogenic gene transcription. In response to insulin signaling, SIK2 becomes phosphorylated on the inhibitory serine 587, most probably via PKA. Concomitant with

SIK2 inhibition, TORC2 becomes dephosphorylated and associated with the promoters of thermogenic genes, *Pgc1α* and *Ucp1* in BAT (Muraoka *et al*., 2009).

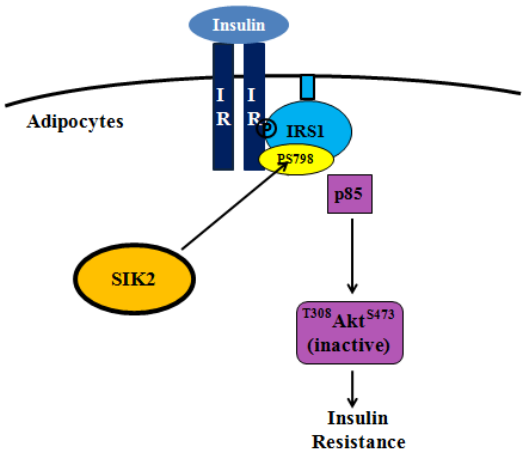

Figure 1.7. The proposed role of SIK2 in adipose insulin resistance (Modified from Horike *et al*., 2003).

SIK2 was shown to target TORC2 in pancreatic islet cells (Screaton *et al*., 2004). In this context elevation of plasma glucose and gut hormone levels are thought to activate PKA that inhibits SIK2 by its S587 phosphorylation leading to hypophosphorylation of TORC2 and its translocation to the nucleus, where it interacts with CREB to upregulate CREB-dependent transcription, insulin being one of the target genes (Screaton *et al*., 2004) (Figure 1.8).

In addition to its role in the pancreas, SIK2 is involved in liver gluconeogenesis by phosphorylating TORC2 (Dentin *et al*., 2007). During fasting, glucagon induces cAMP accumulation that activates PKA. Phosphorylation of SIK2 by PKA inhibits its activity on TORC2 phosphorylation. Dephosphorylated TORC2 in turn translocates to the nucleus and forms a ternary complex with CREB/CBP that turns on the genes involved in gluconeogenesis, *Pepck, G6Pase, Pgc1*. During re-feeding insulin activates Akt2 in liver that in turn activates SIK2 by phosphorylating its Ser358 residue. Activated SIK2 phosphorylates TORC2 at S171 that sequesters it in the cytoplasm and this inhibits gluconeogenic gene expression in the liver (Dentin *et al*., 2007) (Figure 1.9). Other than liver gluconeogenesis SIK2 controls liver lipogenesis (Bricambert *et al*., 2010). In response to glucose, p300 acetylates and activates ChREBP. SIK2 phosphorylates p300 on inhibitory S89 residues that in turn reduces lipogenic gene expression downstream of

carbohydrate responsive element-binding protein (ChREBP) in liver (Bricambert *et al.*, 2010) (Figure 1.10).

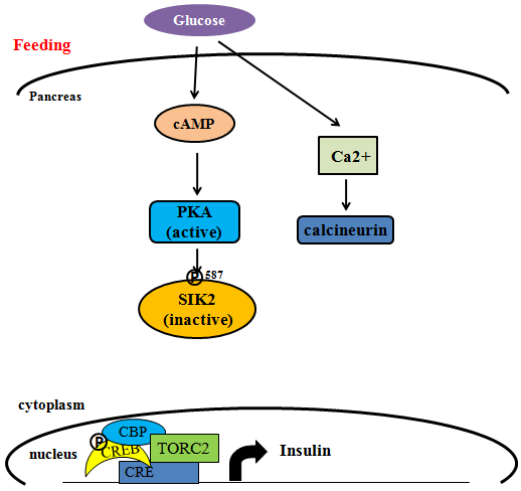

Figure 1.8. The role of SIK2 in CREB-TORC2 dependent insulin secretion from pancreas (Modified from Screaton *et al.,* 2004).

In addition to metabolic functions, SIK2 is also involved in melanogenesis in skin, neuronal survival after ischemia in brain and centrosome separation in ovarian cancer (Horike *et al.*, 2010; Sasaki *et al.*, 2011; Ahmed *et al.*, 2010). SIK2 may repress melanogenesis by repressing TORCs in unstimulated melanocytes. However, after UV irradiation, downregulation of SIK2 expression and PKA-mediated inhibition enhanced a CREB-TORC2-dependent MITF-induced melanogenic programs in the skin (Horike *et al.*, 2010). The second study provided evidence for SIK2 to be a key regulator of a novel survival pathway in primary cortical neurons, potentiated through the CREB-TORC1 axis, in response to ischemic injury. In line with this observation, SIK2 knock-out mice showed reduced neuronal loss following *in vivo* ischemia (Sasaki *et al.*, 2011). The third of these studies localized SIK2 to centrosomes in ovarian cancer cell lines and suggested that the protein might be instrumental in centrosome separation through phosphorylation of c-Nap1 (Ahmed *et al.*, 2010). In the same study, abrogation of SIK2 activity was shown to delay G1/S transition and reduce Akt phosphorylation.

Mouse SIK2 is predicted to be a 103 kDa protein (Horike *et al.*, 2003). The kinase domain spans amino acid residues from 26 to 268 at the N-terminal. The K49 residue, in

the ATP-binding loop, is essential for SIK2's catalytic activity, its replacement with methionine results in a kinase-inactive enzyme (Figure 1.11). SIK2 autophosphorylation activity was shown in transfected COS7 cells and the critical residue is S182 (Horike *et al*., 2003). The second upstream kinase of SIK2 is LKB1, which phosphorylates the T172 residue in the activation loop, thereby increasing its activity 30 fold *in vitro*. Replacement of this residue with glutamic acid (T172E) renders SIK2 constitutively active and the basal activity of this mutant protein is similar to that of wild-type enzyme phosphorylated at this residue (Lizcano *et al*., 2004). The UBA domain of SIK2, spanning amino acid residues 294 and 335, was proposed to directly interact with the kinase domain of SIK2, permitting it to assume a conformation that can be readily phosphorylated and activated by the LKB1:STRAD:MO25 complex (Jaleel *et al*., 2006). The PKA-phosphorylation domain resides between amino acid residues 577-623 adjacent to a RK-rich region containing nuclear localization signal (NLS). S587 phosphorylation by PKA therefore marks SIK2 for nuclear export (Horike *et al*., 2003).

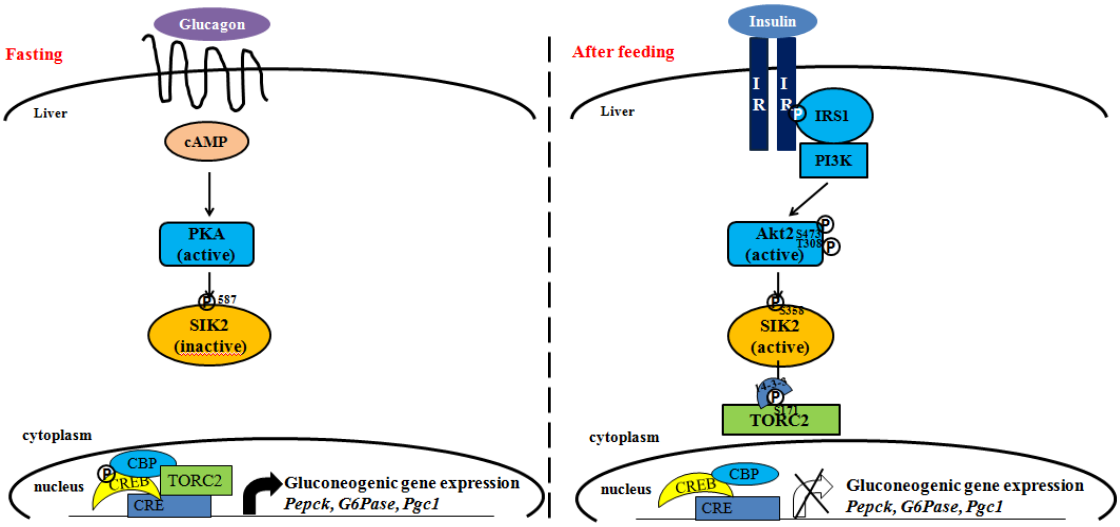

Figure 1.9. The role of SIK2 in CREB-TORC2-dependent hepatic gluconeogenesis under fasting and feeding conditions (Modified from Dentin *et al.,* 2007).

A C-terminal fragment of SIK2 was obtained in a yeast two-hybrid screen of a retinal cDNA library using the cytoplasmic domain of FGFR2 as bait in our laboratory (Özcan, 2003). The full length cDNA of SIK2 was cloned later from retinal tissue (Uysal, 2005; Özcan, 2003) and indicated the existence of three isoforms in this tissue (Uysal, 2005). The

open reading frame of isoform A that is 36 bp longer than that of isoform B and C, consists of 2799 bp. Isoforms B and C differ only in their 3'-UTR. Although there are three alternatively spliced transcripts, they are two cognitive peptides, with a little difference at their carboxyl-terminal. Northern blot analysis revealed the presence of two transcript species, 7.5-8 kb, in the retina, and RT-PCR experiments showed that SIK2 is expressed in all retinal cell layers (Özcan, 2003; Özmen, 2006). Rat SIK2 shows 94% overall identity to mouse and 89.3% to human SIK2. The highest conservation is in their kinase domains, where the amino acid identity is over 98% between the three orthologues. The highest divergence is observed in the C terminal region (Uysal, 2005).

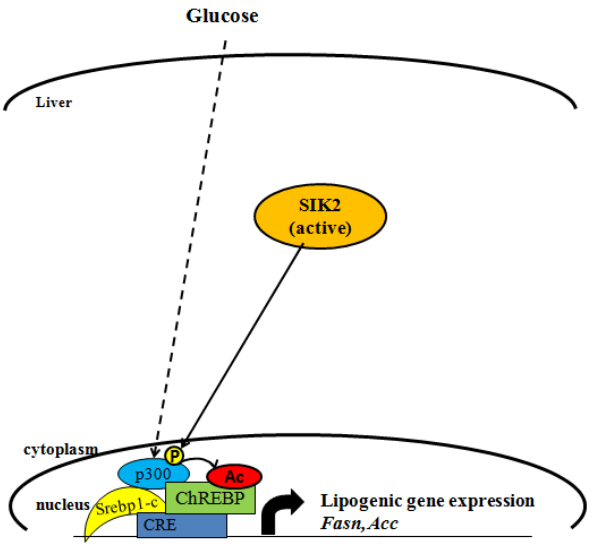

Figure 1.10. The role of SIK2 in p300-Srebp1-c-regulated hepatic lipogenesis.

Our recent work suggested that FGF signaling pathway elements Gab1 and A-Raf as novel SIK2 substrates based on their phosphorylations by SIK2 *in vitro* (Küser, 2006). A consensus SIK2 phosphorylation motif was, based on sequence similarity of the substrates, identified as (I/L)[(B)X or X(B)](S/T)X(S/T)XXX(I/L), where B represents basic residues (Screaton *et al*., 2004; Küser, 2006) (Table1.1).

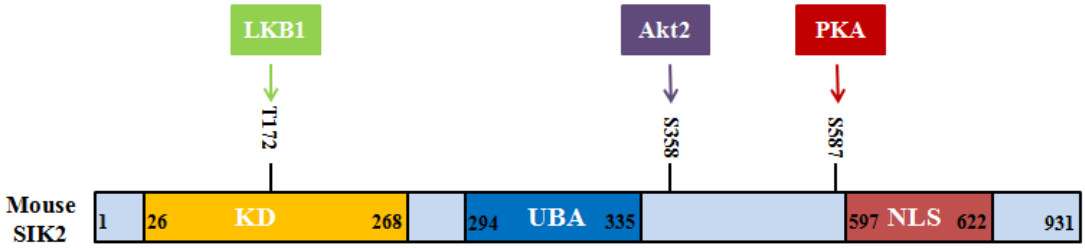

Figure 1.11. Domain structure and phosphorylation sites of mouse SIK2 protein.

Table 1.1. Identified SIK2 substrates containing the SIK2 phosphorylation motif. Red: phosphorylated residue.

Canonical SIK2 Phosphorylation Motif			
(L/I)[(B)X or X(B)](S/T)X(S/T)XXX(L/I)			
Protein Name	**Motif**	**Position**	**SwissProt No.**
Gab1	LPRSYS^{266}HDVL	261-270	NP_002030.2
TORC2	LNRTSS^{171}DSAL	166-175	NP_859066
IRS1	LRLSSS^{794}SGRL	789-798	NP_037101
CNAP1	LHHSLS^{2392}HSLL	2387-2396	NP_055680.3
P300	LLRSGS^{89}SPNL	84-93	NP_001420.2

2. PURPOSE

The aim of this work is to identify the potential role of SIK2 in the FGF2 signal transduction pathway and to investigate if it is involved in the modulation of insulin-dependent Müller cell survival and in chronic hyperglycemia-induced Akt inactivation and apoptosis in MIO-M1 cells. FGF2 was chosen because SIK2 was obtained in a yeast two-hybrid screen of a retinal cDNA library using the cytoplasmic domain of FGFR2 as bait in our laboratory (Özcan, 2003). We focused on insulin, since SIK2 is implicated in the downregulation of insulin signaling (Horike *et al*., 2003) and little is known about the downstream elements of insulin signaling in Müller cells.

FGF2 induces Müller cell proliferation by initiating cascade of events that lead to rapid and transient ERK1/2 phosphorylation (Çınaroğlu, 2005). Reduced FGF2-dependent proliferation of MIO-M1 cells observed in the presence of a PI3K inhibitor, LY294002, implicates the Akt pathway in this mitogenic response (Hollborn *et al*., 2004; Çınaroğlu, 2005). We postulated SIK2 to be a potential negative regulator of FGF signal transduction and thereby Müller cell proliferation. This postulate is based on Gab1 phosphorylation, a main signaling mediator involved in FGF signaling, by SIK2 *in vitro* (Küser, 2006) and it is widely accepted that serine phosphorylation of Gab1 that negatively regulates RTK signaling (Gual *et al*., 2001; Lehr *et al*., 2004). Therefore, in the first part of the study the primary aim was to confirm SIK2 involvement in the negative feedback mechanisms acting on FGF/Ras/ERK and FGF/PI3K/Akt pathways and Müller cell proliferation at the level of Gab1 serine phosphorylation.

Insulin acts as a survival factor for retinal neurons through PI3K/Akt pathway (Barber *et al*., 2001). However, its role in Müller cell survival is not known. Hyperglycemia-induced apoptosis in cultured Müller glia via inactivation of Akt has been observed (Xi *et al*., 2005). SIK2 was shown to phosphorylate IRS1 at S794 and as such implicated in downregulation of insulin signaling in adipocytes (Horike *et al*., 2003). We hypothesized that SIK2 is the potential negative regulator of insulin signal transduction (PI3K/Akt pathway) and thereby Müller cell survival and also links hyperglycemia and Akt inactivation and Müller cell apoptosis. In the second part of the study our aim is to

confirm SIK2 involvement in the negative modulation of insulin-induced Akt activation/ insulin-dependent Müller cell survival and in chronic hyperglycemia-induced Akt inactivation and apoptosis in MIO-M1 cells.

In this context in the first part of this study we investigated;

(i) FGF2-dependent changes in the serine/threonine phosphorylation status and activation of SIK2,
(ii) FGF2-dependent ERK and Akt activation profiles,
(iii) the potential modulatory role of SIK2 in Müller cell proliferation through FGF2/ERK and FGF2/Akt signaling via over-expression and sh-RNA approaches,
(iv) Gab1 phosphorylation by SIK2 and FGF2-dependent Gab1/SIK2 interaction,
(v) FGF2-dependent tyrosine phophorylation and Grb2 and p85 binding partner association profiles of Gab1 and effect of SIK2 silencing on these interactions.

In the second part of the study we explored;

(vi) insulin-dependent ERK and Akt activation profiles,
(vii) insulin-dependent changes in SIK2 phosphorylation and activity profiles and protein levels,
(viii) insulin-dependent tyrosine phophorylation and SIK2 interaction profiles of IRS1,
(ix) insulin-dependent Müller cell death and proliferation,
(x) potential role of SIK2 in insulin-induced Müller cell survival through over-expression and sh-RNA approaches,
(xi) Akt and SIK2 activity/ expression levels upon chronic hyperglycemia,
(xii) potential role of SIK2 in chronic hyperglycemia induced Akt inactivation and Müller cell apoptosis through over-expression and sh-RNA approaches,
(xiii) tyrosine and serine phosphorylation levels of IRS1 upon chronic hyperglycemia,
(xiv) phosphorylation and activity levels of SIK2 in type 1 diabetic rats.

3. MATERIALS

3.1. Cell Lines

MIO-M1 cells were kindly provided by Prof. Astrid Limb from the UCL, Institute of Ophthalmology, London.

3.2. Chemicals, Plastic and Glassware

All chemicals used in this study were purchased from Sigma Aldrich (USA) or Merck (Germany) unless otherwise stated in the text. All solutions, plastic and glassware were sterilized by autoclaving at 121^0C for 20 minutes when possible. Solutions used in RNA work were treated with 0.1% diethylpyrocarbonate (DEPC) for 1 hour before sterilization, glassware were baked at 150^0C for 4 hours.

3.3. Plasmids

The following plasmids were used throughout this study.

Table 3.1. Plasmids used.

pEGFP-C3	Clontech, USA
pcDNA3/HisMax	Invitrogen, USA
pGEX-2TK-P	Amersham, USA

3.4. Kits

The following kits were used throughout this study.

Table 3.2. Kits used.

Kit	Supplier
QuikChange XL Site-Directed Mutagenesis Kit	Stratagene, USA
QIAprep Spin Miniprep kit	Qiagen, Germany
Bicinchoninic acid (BCA) assay kit	Thermo, USA
Purelink HiPure Plasmid Filter Maxiprep Kit	Invitrogen, Germany
RNeasy Mini kit	Qiagen, Germany
In situ cell death detection kit, fluorescent	Roche, Germany
Cell proliferation ELISA kit, BrdU	Roche, Germany

3.5. Equipment

The following equipments were used throughout this study.

Table 3.3. Equipment used.

Equipments	Models
Autoclave	Model MAC-601, Eyela, Japan Model ASB260T, Astell, UK
Balances	Electronic Balance VA 124, Gec Avery,USA DTBH 210, Sartorius, GERMANY
Carbon dioxide tank	2091, Habaş, TURKEY
CCD camera	CCD Camera, JAI Corporation, JAPAN
Centrifuges	ProFuge, 10K, Strategene, USA Mini Centrifuge 17307-05, Cole Parmer, USA Genofuge 16M, Techne, UK Centurion K40R, UK Centrifuge B5,B.Braun B. Int. (GERMANY) Centrifuge 5415R, Microfuge tube, USA J2-MC Centrifuge, Beckman Coulter, USA J2-21 Centrifuge, Beckman Coulter, USA
Cold room	Birikim Elektrik Soğutma, Turkey

Table 3.3. Equipment used. (cont.)

Deep Freezers	2021D (-20^{0}C), Arçelik, Turkey -70^{0}C Freezer, Harris, UK -86^{0}C ULT Freezer, ThermoForma, USA
Documentation System	Gel Doc XR System, Bio Doc, ITALY Stella, Raytest, Germany
Electrophoretic Equipments	Mini-PROTEAN 3 Cell, BIO-RAD, USA Easy-cast system, Hybaid, UK
Heat blocks	DRI-Block DB-2A, Techne, UK StableTemp Dry Bath Incubator, Cole Parmer, USA
Homogenizer	Pellet Pestles Tissue Grinder, Kimble Kontes, USA
Hybridization Oven	Shake'n'Stack, Hybaid, UK
Ice Machine	Scotsman Inc., AF20, ITALY
Incubator	Hepa Class II Forma Series, Thermo Electron
Laminar flow cabinet	Class II A Tezsan, TURKEY Class II B Tezsan, TURKEY
Magnetic Stirrer	M221 Elekro-mag, TURKEY Clifton Hotplate Magnetic Stirrer, HS31, UK
Micropipettes	Gilson, FRANCE
Microscopes	CM110 Inverted Microscope, Prior, UK Zeiss, Axio Observer Z1 Inverted Mic., USA

Table 3.3. Equipment used. (cont.)

pH meter	WTW, GERMANY
Pipettor	Pipetus-akku, Hirscmann Labogerate, GERMANY
Power Supplies	EC135-90, Thermo Electron Corporation Power Pac Universal, BIO-RAD, USA
Protein Visualization	Stella, Raytest, Germany
Pipettor	Pipetus-akku, Hirscmann Labogerate, GERMANY
Power Supplies	EC135-90, Thermo Electron Corporation Power Pac Universal, BIO-RAD, USA
Protein Visualization	Stella, Raytest, Germany
Refrigerators	2082C, Arçelik, TURKEY 4030T, Arçelik, TURKEY
Sealer	Vacuplus FS400A, Electric Petra, GERMANY
Shakers	VIB Orbital Shaker, InterMed, DENMARK Lab-Line Universal Oscillating Shaker, USA Adjustable Rocker, Cole Parmer, USA
Software	Metasystems, GERMANY Quantity One, Bio-Rad, ITALY
Spectrophotometer	CE5502, Cecil, UK NanoDrop ND-1000, Thermo, USA

Table 3.3. Equipment used. (cont.)

Vortex	Vortexmixer VM20,Chiltern Scientific, UK
Water Bath	TE-10A, Techne, UK
Water Purification	UTES, TURKEY
X-Ray Film Cassettes	24X30 IMS, ITALY 24X 30 DIA-X, GERMANY

4. METHODS

4.1. Animals and Tissue Preparation

Albino Wistar rats bred at Boğaziçi University vivarium were used in this study and were treated in accordance with the university guidelines. Adult animals were anesthetized by ether inhalation and sacrificed by cervical dislocation. Dissected retinas were rapidly frozen in liquid nitrogen and stored at -80^{0}C until use.

4.2. Generation of Diabetic Rats with Streptozotocin Injection

Eight experimental and six control male albino Wistar rats, weighing 190-250 g, were injected with 60 mg/kg streptozotocin (STZ) solubilized in 10 mM citrate buffer (1.8 mM citric acid and 8 mM sodium citrate, pH 4.5), or 10 mM citrate buffer alone intravenously, respectively. Animals were sacrified after 2 weeks. Fasting blood glucose levels of the animals were between 75 to 100 mg/dl before the injection. At the day of the sacrifice animals with fasting blood glucose levels higher than 200 considered as diabetic. Dissected retinas were rapidly frozen in liquid nitrogen and stored at -80^{0}C until use.

4.3. MIO-M1 Culture Maintenance

Spontaneously immortalized MIO-M1 Müller glia cells were maintained in dulbecco's modified eagle medium (DMEM) with glutamine supplemented with 10% fetal bovine serum (FBS; Invitrogen, USA) and 0.1% penicillin/streptomycin (Invitrogen, USA). Cells near confluence were washed with phosphate-buffered saline (PBS: 137 mM NaCl, 2.7 mM KCl, 10 mM Na_2HPO_4, 1.8 mM KH_2PO_4), treated with 0.05% trypsin solution (0.05% trypsin in PBS) for 5 minutes and scraped. The cells were pelleted by centrifugation at 2000 xg for 5 minutes and after resuspension in complete medium they were divided into three plates once a week.

4.4. Hyperglycemia Model in MIO-M1 Cells

For *in vitro* hyperglycemia model, subconfluent cells were grown in DMEM contained either 5.5 (physiological conditions, normoglycemia) or 25 mM glucose (hyperglycemia conditions), the media was supplemented with 1 g/l transferrin, 96.6 µg/ml putresceine, 300 nM sodium selenate for 48 hours. When insulin stimulation required 100 pM insulin was added to the medium. Media were changed every 24 hours to maintain constant glucose concentration.

4.5. Treatment of MIO-M1 Cells with Growth Factors

Cells were seeded on 10 cm tissue culture dishes (Greiner, USA) and were allowed to grow to sub-confluency. The cells were washed with PBS and starved in DMEM and 0.1% penicillin/streptomycin overnight. Subsequently, they were treated with 1 ng/ml FGF2 (R&D Systems, USA) and 10 µg/ml heparin for 0 minutes (negative control), 5, 10, 30 minutes and 1 hour. In the studies involving insulin, the cells were incubated with 100 pM insulin for 0 minutes (negative control), 5, 10, 30, 60 minutes and 2 hours. At the end of the treatment periods, cells were immediately washed with ice-cold PBS supplemented with protease and phosphatase inhibitor cocktail (Roche, Germany). The cells were then scraped, pelleted with centrifugation and stored at -80^0C until used. Prior to proliferation and apoptosis assays, cells were treated either with 1 ng/ml FGF2, 100 ng/ml FGF2 or 10 nM insulin for 24 hours.

4.6. Cloning of IRS1, SIK2-(KD-UBA) and full length SIK2 Fragments

4.6.1. RNA Isolation

Total RNA was isolated from MIO-M1 cells or adult rat retina with RNeasy Mini Kit. Briefly, 10^7 cells or 2 retinae were homogenized using 350 µl of the lysis buffer provided in the kit and vortexed/homogenized by pestle. After the addition of equal volume of 70 % ethanol, the samples were applied to the RNeasy mini spin columns. Columns were washed with high salt buffer included in the kit before the RNA elution from columns using 60 µl of RNAse free, DEPC-treated water. The concentrations of RNA

samples were measured using Nanodrop spectrophotometer. The integrity of RNAs was determined by formaldehyde agarose gel electrophoresis.

4.6.2. Formaldehyde Agarose Gel Electrophoresis

Approximately 1.5 µg total RNA was mixed with sample buffer (250 µl 100% deionized formamide, 83 µl 37% formaldehyde, 50 µl 10X MOPS (200 mM Morpholinopropane sulfonic acid (pH7.0), 80 mM sodium acetate, 10 mM EDTA), 50 µl Rnase-free glycerol, 10 µl 2.5% bromophenol blue, 57 µl DEPC-treated water), heated to 65°C for 3 minutes and immediately chilled on ice. Then 0.1 µg ethidium bromide was added to the samples and fractionated on a 1% formaldehyde agarose gel. The gel was prepared by melting of 1.5 g agarose in 127 ml H_2O and 14.19 ml 10X MOPS buffer and addition of 8.1 ml 37% formaldehyde upon cooling to about 55^0C. The gel was run at 50 V. The bands were visualized under UV light and images were captured using GelDoc imaging system and analyzed by Quantity One software (BioRad, Hercules, USA).

4.6.3. cDNA Synthesis

cDNA was synthesized using 2 µg of total RNA and 500 ng of random hexanucleotide primers (Promega, USA), 120 nmol of each dNTP (Fermentas, Lithuania), 12 units of RNasin (Promega, USA) in reverse transcription buffer containing 50 mM Tris-HCl (pH 8.3), 75 mM KCl, 3 mM $MgCl_2$, 10 mM DTT. The mixture was heated at 95^0C for 1 minute to denature RNA and immediately transferred on ice. The sample volume was brought to 30 µl with DEPC-treated water, subsequently 200 units of MMuLV-RTase (Promega, USA) and 30 units of RNasin were added. After 2 hours of incubation at 42^0C, the reaction was stopped by heating the reaction mix to 95^0C for 10 minutes. The reaction volume was brought to 360 µl with water and stored at -20^0C until used.

4.6.4. RT-PCR

Amplifications were carried out using one fiftieth of cDNA (2µl), 0.2 mM dNTP mixture, 3 mM $MgCl_2$, 0.25 µM primer sets, 25 mM N-Tris(hydroxymethyl)methyl-3-aminopropanesulfonic acid (pH 9.3), 50 mM KCl, 1 mM β-mercapthoethanol and 0.5 units

of TaKaRa Ex Taq (Takara Bio. Inc., Japan) in a total volume of 25 µl. The amplification reactions were started with initial denaturation at 95^0C for 5 minutes followed by 40 cycles of denaturation at 95^0C for 45 seconds, annealing at the indicated temperature in table 4.1 for 45 seconds and extension at 72°C for 90 to 120 seconds depending on the product length.

Table 4.1. Cloning primers used.

Cloned Fragments (Positions in nucleotide)	Name	Primer sequence (5'-3')	Tm (^{0}C)	Target size (bp)
FL-SIK2 (1-2781)	SIK2-FL-XhoI-Fw SIK2-FL-Apa-Rw	AGATCTCGAGATGGTCATGGCGGATGGCCCGAG AGAGGGCCCTAATTCACCAGGACATACCCGT	61	2800
SIK2(KD-UBA) (1-1008)	SIK2-(KD-UBA)-BamH1-Fw SIK2-(KD-UBA)-EcoR1-Rw	AGA GGATCCTTCATGGTCATGGC GAT AGAGAATTCTATTCCACCAACAAGAAATAAAT	50	1028
IRS1 (2740-3139)	IRS1-BamHI-Fw IRS1-EcoRI-Rw	AGAGGATCCGGTGGTAAGCTCTTGCCTTGC AGAGAATTCCTAGTTGGTCTGTGCAGCTGTGT	59	399

4.6.5. Agarose Gel Electrophoresis

DNA samples were mixed with 1/6 volume of 6x loading buffer (250 mg bromophenol blue, 550 mg xylene cyanol in 33 ml 150 M Tris, pH 7.6, 60 ml glycerol and 7 ml H_2O) and loaded onto 1 or 2% agarose gels prepared in Tris-Acetate-EDTA (TAE) buffer (40 mM Tris, 1 mM EDTA, 20 mM acetic acid) and addition of 0.5 µg/ml ethidium bromide. The gels were run in the same buffer at 120 V. DNA size marker, Gene Ruler 100 bp DNA ladder, was purchased from Fermentas (Lithuania). The DNA bands were visualized under UV light and the images were documented with GelDoc imaging system (BioRad, USA) and analyzed by Quantity One software (BioRad, USA).

4.6.6. Preparation of the Vectors and the Amplification Products for Cloning

PGEX-2TK-P vector (Amersham, USA) (Figure 4.1) and the RT-PCR fragments of IRS1 and SIK2(KD-UBA) were incubated with 1 unit BamH1 (Promega, USA) and 1 unit EcoR1 (Promega, USA) restriction enzymes per 1 µg of DNA in buffer containing 50 mM Tris-HCl (pH 8.0), 10 mM $MgCl_2$, 50 mM NaCl at 37^0C overnight to generate ends for directional cloning. Samples were fractionated on 1% agarose gels and appropriate DNA fragments, excised under UV light and extracted using QIAQuick Gel Extraction Kit

(Qiagen, Germany) according to manufacturer's instructions. Briefly, excised gel was solubilized in QG buffer containing pH indicator, loaded on a spin column, centrifuged at 10000 xg for 1 minute. Then the column was washed with buffer PE containing ethanol, subsequently DNA was eluted with TE (pH 8.0) buffer containing 10 mM Tris-Cl (pH 8.0), and 1 mM EDTA. Finally, DNA concentrations were obtained by measuring optical density at 260 nm.

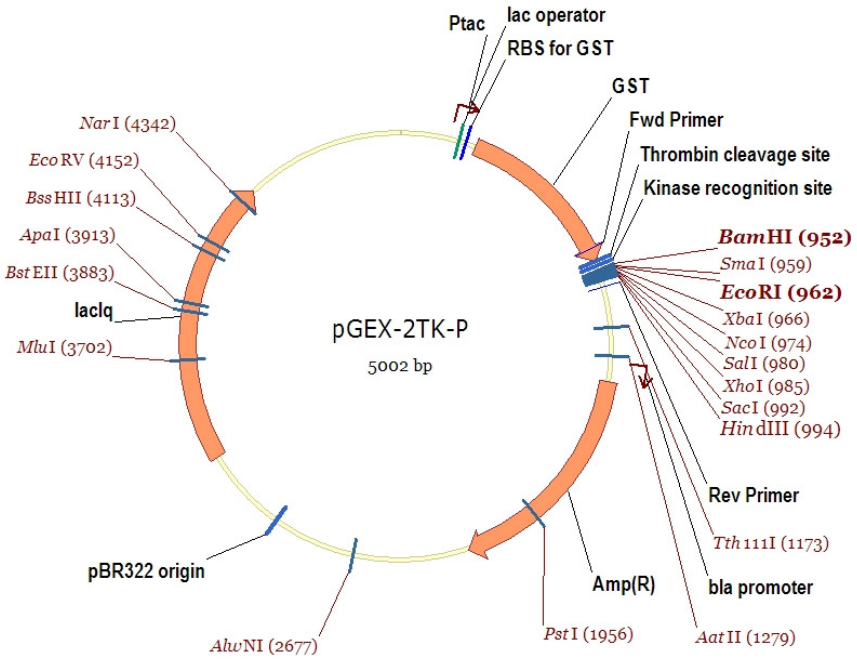

Figure 4.1. Map of pGEX-2TKP vector.

pEGFP-C3 (Clontech, USA) and pcDNA3/HisMax (Invitrogen, USA) vectors (Figure 4.2 and Figure 4.3) and the RT-PCR fragment of FL-SIK2 were incubated with 1 unit XhoI (Promega, USA) and 1 unit ApaI (Promega, USA) restriction enzymes per 1 µg of DNA in buffer containing 50 mM Tris-HCl (pH 8.0), 10 mM $MgCl_2$, 50 mM NaCl at 37^0C overnight to generate ends for directional cloning. Samples were fractionated on 1% agarose gel and XhoI/ApaI cut fragments were excised from of the gel under UV light and extracted using QIAQuick Gel Extraction Kit (Qiagen, Germany) according to manufacturer's instructions.

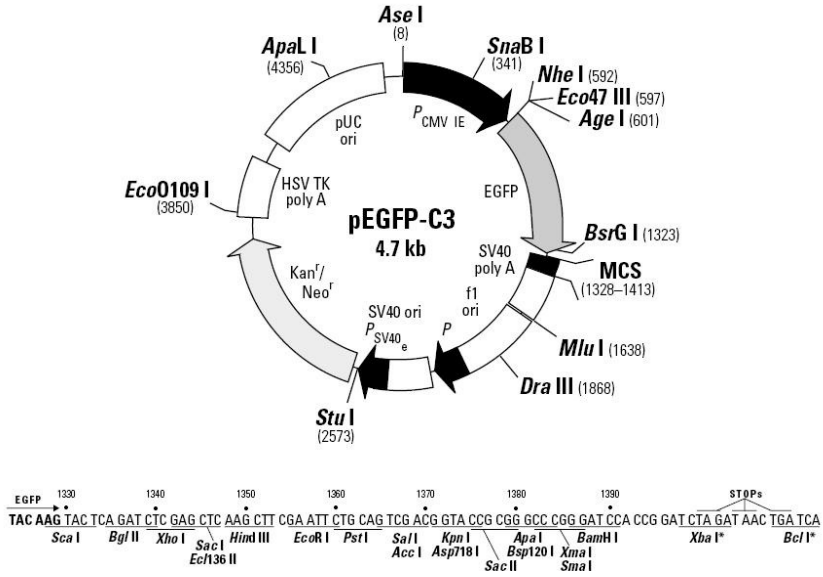

Figure 4.2. Map of pEGFP-C3 vector.

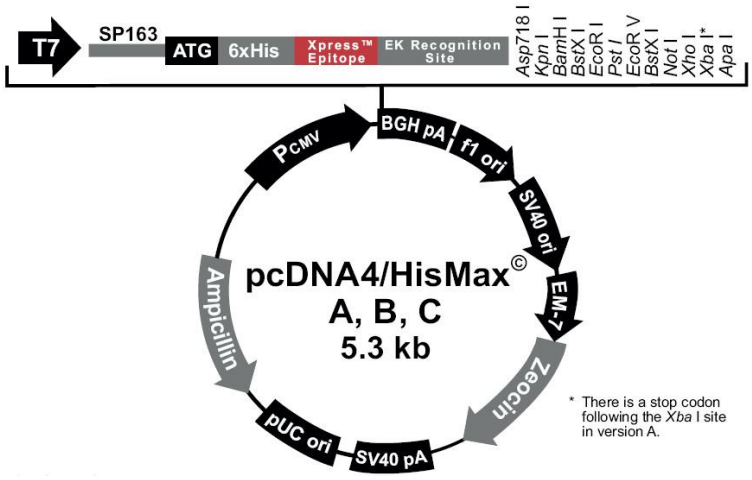

Figure 4.3. Map of pcDNA4/HisMax vector.

4.6.7. Ligation

BamHI/EcoRI cut pGEX-2TKP vector and IRS1 and SIK2-(KD-UBA) cDNA fragments were ligated in 1:5 end ratio. XhoI/ApaI cut pEGFP-C3 and pcDNA/HisMax vectors were ligated with FL-SIK2 fragment in 1:3 end ratio. The reactions were carried out using 50 ng vector in DNA ligase buffer (400 mM Tris-Cl, pH7.8, 100 mM $MgCl_2$, 100

mM DTT, 5 mM ATP), 1 unit of T4 DNA ligase (Promega, USA) and the appropriate amount of amplification fragments at 4^0C overnight.

4.6.8. Competent Cell Preparation

Stock of frozen BL21 bacterial cells were streaked on Luria Bertani broth (LB) agar plates (10 g/l tryptone, 5 g/l yeast extract, 10 g/l NaCl and 18 g/l agar) and incubated overnight at 37^0C. A well isolated individual colony was transferred and grown in 5 ml of liquid LB medium (10 g/l tryptone, 5 g/l yeast extract, 10 g/l NaCl) overnight at 37^0C. This overnight culture was used to inoculate into 50 ml LB medium with 1:100 ratio and grown at 37^0C until OD_{600} reached 0.3-0.4. Then, the cultures were chilled on ice for 30 minutes and centrifuged at 4^0C for 5 minutes at 5000 xg. The bacterial pellet was resuspended in 12.5 ml of ice-cold 50 mM $CaCl_2$, incubated on ice for 15 minutes. The bacteria were collected as before, resuspended in 2 ml of ice-cold 50 mM $CaCl_2$ containing 15% glycerol. The samples were aliquoted, 200 µl each, stored at -80^0C until used.

4.6.9. Transformation

For efficient BL21 transformation, 100 µl of frozen BL21 competent cells were mixed with 12.5 ng of ligation mixture, and another 100 µl were mixed with uncut vector as a control of transformation efficiency. They were kept on ice for 30 minutes, heat-shocked at 42^0C for 90 seconds and cold-shocked on ice for 2 minutes. Subsequently 900 µl of SOC medium (2 g tryptone, 0.5 g yeast extract, 1 ml 1 M NaCl, 0.25 ml 1 M KCl, 1 ml 1 M $MgCl_2$, 1 ml 2 M glucose in 1 l dH_2O) was added and cells were allowed to grow at 37^0C for an hour with shaking at 250 rpm. Subsequently, 100 µl and also the residual bacterial suspensions were plated on LB plates containing 100 µg/ml ampicillin (for pcDNA3/HisMax and pGEX-2TK-P vectors) or 30 µg/ml kanamycin (for pEGFP-C3 vector) and grown overnight at 37^0C.

4.6.10. Colony PCR

To verify that the colonies grown upon transformation contain the desired gene fragments, individual colonies were transferred using sterilized toothpicks into PCR tubes

with 10 µl dH_2O, boiled for 10 minutes to lyse the cells and the amplifications were carried out in the presence of 0.2 mM dNTP mixture, 3 mM $MgCl_2$, 0.25 µM primer pairs (Table 4.1), Taq polymerase buffer (100 mM Tris-HCl, pH 8.8, 500 mM KCl, 0.8 % Nonidet P40) and 0.5 units of Taq polymerase (Fermentas, Lithuania) in a total volume of 20 µl. The amplification reactions were started with initial denaturation at 95^0C for 5 minutes followed by 40 cycles of denaturation at 95^0C for 45 seconds, annealing at 63^0C for 45 seconds and extension at 72^0C for 90 to 120 seconds depending on the expected product length.

4.6.11. Plasmid DNA Isolation and Sequencing

Selected colonies were grown overnight in LB medium containing appropriate antibiotic at 37^0C with shaking at 225 rpm and plasmids were isolated with MiniPrep kit (Qiagen, USA). Briefly bacterial cells were lysed and chromosomal DNA was denatured under strong alkaline conditions (pH 13.0), cell debris and chromosomal DNA were removed by centrifugation at 10000 xg for 10 minutes. Supernatant was applied to the QIAprep spin columns where DNA binds to the silica gel membrane in the presence of high salt. Impurities were removed by washing with wash buffer containing ethanol and plasmid DNA was eluted with TE buffer (10 mM Tris-Cl, pH 8.0, 1 mM EDTA). Plasmids were analyzed in 1% agarose gels, and their identity were confirmed by sequencing at Iontek (Turkey).

Stocks of bacteria carrying plasmids with the desired fragments were prepared by mixing overnight bacterial cultures with 15% glycerol and stored -80^0C until used.

4.7. Generation of Kinase Inactive SIK2

To create kinase inactive mutant of SIK2, SIK2-KD-UBA peptide lysine 49 residue was converted to methionine using the following primers (Table 4.2).

For the site-directed mutagenesis reactions QuickSiteXL Mutagenesis kit (Stratagene, USA) was used and the instructions of the manufacturer were followed strictly. The basic procedure utilizes a supercoiled double-stranded DNA (dsDNA) vector

with an insert of interest (SIK2-(KD-UBA) fragment in pGEX-2TK-P vector) and two synthetic oligonucleotide primers containing the desired mutation. The oligonucleotide primers, each complementary to opposite strands of the vector, are extended during temperature cycling by PfuTurbo DNA polymerase. Incorporation of the oligonucleotide primers generates a mutated plasmid containing staggered nicks. Following temperature cycling, the product is treated with Dpn I endonuclease (target sequence: 5´-Gm6ATC-3´) that is specific for methylated and hemimethylated DNA and is used to digest the parental DNA template and to select for mutation-containing synthesized DNA. DNA isolated from E.coli DH5α strain is dam methylated and therefore susceptible to Dpn I digestion. The nicked vector DNA containing the desired mutations is then transformed into XL1-Blue supercompetent cells (Stratagene, USA). The mutations were later verified by sequencing.

Table 4.2. Mutagenesis primers used in this study. Underlined residues are mutated.

Annotation	**Primer Name**	**Mutagenesis Primers (5'-3')**
SIK2(K49M)	K49M-Fw	CCAAGACGGAGGTGGCAATAATGATAATCGATAAGTCTCAGC
	K49M-Rw	GCTGAGACTTATCGATTATCATTATTGCCACCTCCGTCTTGG

4.8. Expression of GST Fusion Proteins in *E.coli* BL21

E.coli BL21 strain transformed with the pGEX recombinant plasmids grown overnight in LB with 100 µg/ml ampicillin were inoculated into 12 ml LB containing 100 µg/ml ampicillin with 1:100 ratio and allowed to grow until OD_{600} of 0.5 reached. The fusion protein expression was induced by adding 0.2 mM IPTG, subsequently bacteria were allowed to grow at 28°C for 2 hours. Bacteria were sedimented by centrifugation at 5000 xg for 2 minutes. The bacterial pellet was resuspended in 600 µl of ice-cold resuspension buffer containing protease inhibitors (10 µg/ml leupeptin, and 5 µg/ml aprotinin and 1mM PMSF) in PBS. For lysis, cells were sonicated 3 times for 3 minutes duration each at 95 V on ice, 1% TritonX-100 was added and incubated on ice for 30 minutes. After solubilization of proteins, cell debris was pelleted with centrifugation at 5000 xg at 4^0C for 45 minutes. The supernatant containing the expressed fusion proteins was transferred to fresh tube and stored -80^0C until purification by GST- affinity column chromatography.

4.9. Affinity Purification of GST Fusion Proteins

GST fusion proteins were purified from bacterial cell extract using Glutathione Sepharose 4B MicroSpin affinity columns (Amersham, USA). Bacterial sonicates were loaded onto the columns and incubated at room temperature with delicate shaking for 10 minutes to allow GST fusion proteins bind glutathione sepharose 4B resin. Then, to remove residual unbound proteins the column was centrifuged at 3000 xg for a minute and washed with 600 µl of PBS three times. Bound proteins were released with the addition of elution buffer, 10 mM glutathione in 50 mM Tris-Cl (pH 8.0), and collected by centrifugation for a minute at 3000 xg.

4.10. Transfection of pEGFP-SIK2 and pcDNA3/HisMax-SIK2 Vectors to MIO-M1 Cells

One day before the transfection MIO-M1 cell density was measured with haemocytometer. 5 x 10^5 cells were seeded on 6-well plates, and grown in DMEM containing 10% FBS and 0.1% streptomycin/penicillin. At the day of transfection, pEGFP-SIK2 and only pEGFP plasmids were diluted in 250 µl of DMEM as 20 µg/ml concentration. The FugeneHD transfection reagent (Roche, Germany): plasmid DNA ratio was used at 4:1 and the complex in DMEM was incubated for 15 minutes at room temperature. Then, all of it was added to the wells in a drop-wise manner. The plate contents were swirled on a rotating platform shaker for 30 seconds at room temperature. 24 hour after transfection culture medium was decanted and cells were washed three times with PBS and serum-starved overnight. The next day, cells were treated with FGF2 or insulin as described before.

The same procedure was followed to transfect pcDNA3/HisMax-SIK2 vector to MIO-M1 cells.

4.11. SIK2 Gene Silencing in MIO-M1 cells via shSIK2

SIK2 shRNA (human) lentiviral particles were purchased from Santa Cruz (USA). This is a pool of concentrated, transduction-ready viral particle mixture containing three

target-specific constructs that encode 19-25 nucleotides (plus a loop) shRNA designed to knock down gene expression.

Approximately 2 x 10^5 MIO-M1 cells were grown on 10 cm culture dishes. Next day, the culture medium was changed with DMEM culture medium containing 5 µg/ml polybrene. Twenty µl of shSIK2 or scrambled shRNA vector containing lentiviral particles were thawed and added onto cells. Twenty-four hours post infection culture medium was replenished.

To select stable shSIK2 or scrambled shRNA containing colonies cells were passaged in 1:5 ratio and after 48 hours cells were transferred into culture medium containing one µg/ml puromycin. Every 3 days medium was replenished. After two weeks cell colonies were emerged. Approximately 100 cell-containing five shSIK2 and two scrambled shRNA infected colonies were collected with the help of cloning cylinders (Millipore, USA) and grown in ten cm culture dishes. In order to investigate SIK2 gene silencing in these colonies, cells were collected in ice-cold PBS and samples were analyzed by Western blotting using anti-SIK2 antibodies.

4.12. qRT-PCR

Reaction mixtures of target and reference genes were prepared using 10µl of 2x SYBR Premix Ex Taq (Takara, Japan), one µl of each primers (5 µM each), two µl of PCR grade dH_2O and 6 µl of cDNA prepared as indicated above. For negative controls, cDNA was replaced with PCR grade dH_2O. The reaction program contained an initiation step at 50°C for 2 minutes, followed by an initial denaturation step at 95°C for 10 seconds, 35 amplification cycles, a melting curve construction step and a cooling step at 40°C for 30 seconds. Each amplification cycle consists of a denaturation step at 95°C for 5 seconds, an annealing step at appropriate temperature (Table 4.3) for 10 seconds and an extension step at 72°C for 10 seconds. Data were analyzed by LinRegPCR software 7.2 (Ramakers *et al.,* 2003).

Table 4.3. Real-time PCR primers used in this study.

Real-Time Fragments	Name of Primers	Primer sequence (5'-3')	Tm (^{0}C)	bp
SIK2	SIK2-Fw SIK2-Rw	TTGCTGAACAAACAGTTGCC TCAAGCAGACAGCCATTCAC	55	207
β-Actin	β-Actin-Fw β-Actin-Rw	AAGATCAAGATCATTGCTCCTC GGGTGTAACGCAACTAAGTC	55	200
Akt1	Akt1-Fw Akt1-Rw	GCACAAACGAGGGGAGTACAT CCTCACGTTGGTCCACATC	60	161
Akt2	Akt2-Fw Akt2-Rw	CAAGCGTGGTGAATACATCAAGA GCCTCTCCTTGTACCCAATGA	60	86
Akt3	Akt3-Fw Akt3-Rw	CTCAACAACTTTTCAGTGGCAAA GCCTGGATAGCTTCTGTCCATT	60	113

4.13. Bicinchoninic acid (BCA) Assay

For determination of the concentration of proteins, BCA Assay kit was used. Unknowns and bovine serum albumin (BSA) dilutions ranging from 0.025 to 2 mg/ml were mixed with 170 µl of 50:1 diluted BCA Working Solution. After 30 minutes at 37^{0}C incubation, absorbance measured at 595 nm. Unknown sample concentrations were extrapolated from the standard curve.

4.14. SDS-PAGE and Western Blot

Immunoprecipitated proteins or cell lysates fractionated on 8 % polyacrylamide gels (8% acrylamide:bisacrylamide (29:1), 375 mM Tris-HCl (pH 8.8), 0.1% SDS, 0.1% ammonium persulfate, 0.1% N,N,N',N'-tetramethylethylenediamine) with 5% stacking gel (5% acrylamide:bisacrylamide (29:1), 125 mM Tris-HCl (pH 6.8), 0.1% SDS, 0.1% ammonium persulfate, 0.1% N,N,N',N'-tetramethylethylenediamine). Samples were boiled in 6X sample buffer (300 mM Tris-Cl, pH 6.8, 600 mM DTT, 10% SDS, 0.6% bromophenol blue, 50% glycerol) at 95^{0}C for 5 minutes before loading. The gels were run in 25 mM Tris-HCl, 250 mM glycine and 0.2% SDS buffer at 100-120 V.

Coomassie Blue staining was done after incubation of the gel in fixing solution (50% methanol, 10% acetic acid in water) for 1 hour. Subsequently, gel was gently shaken in coomassie blue solution (50% methanol, 0.05% Coomassie R250, 10% acetic acid) for at

least 2 hours. Gels were rinsed with fixing solution for 5 minutes, then, washed extensively with destaining solution (5% methanol, 7% acetic acid in water).

For Western blotting, the samples fractionated on polyacrylamide gels were electroblotted to PVDF membranes (Roche, Germany) in transfer buffer (200 mM glycine, 25 mM Tris.HCl, 15% methanol) at 100 V for 1-1.5 hours. To equilibrate the membrane was washed in tris buffered saline-tween (TBST) solution (150 mM NaCl, 20 mM Tris.HCl, pH 8.0, 0.1 % Tween 20) three times for total of 30 minutes. The membrane was incubated in blocking solution (1% BSA or 1% - 5% skimmed milk powder in TBST) for 1 hour at room temperature with gentle shaking. The membrane was left overnight in the blocking solution containing appropriate antibodies at 4^0C, where the antibodies were diluted as given in Table 4.4. Subsequently, the membrane was washed with TBST three times for 5 minutes each to remove unbound antibody and incubated in Lumi-light Western blotting substrate (Santa Cruz, USA) for 1 minute and images were captured using Stella imaging system (Raytest, Germany) with 1 minute intervals.

Table 4.4. Antibodies, their Brands, applications, dilutions and band sizes used.

Antibody	Source	Application	Antibody dilution	MW (kDa)
Gab1	SantaCruz	IP, WB	1/25, 1/1000	115
IRS1	SantaCruz	IP, WB	1/25, 1/1000	170
Grb2	Upstate	WB	1/500	25
pThr	Zymed	WB	1/1000	
pSer	Zymed	WB	1/1000	
pY(4G10)	SantaCruz	WB	1/1000	
Anti-SIK2 serum	Gift from Dr. Takemori	IP	1/125	120
SIK2	Novusbio	WB	1/2500	120

Table 4.4. Antibodies, their brands, applications, dilutions and band sizes used. (cont.)

SIK3	Abcam	WB	1/2500	170
p85	Millipore	WB	1/500	85
Shp2	SantaCruz	WB	1/500	70
pERK	SantaCruz	WB	1/1000	42-44
ERK	SantaCruz	WB	1/1000	42-44
pAKT(T308)	Cell Signaling	WB	1/1000	60
pAKT(S473)	Cell Signaling	WB	1/2000	60
panAKT	Cell Signaling	WB	1/1000	60
Akt1	Cell Signaling	IP, WB	1/50, 1/1000	60
Akt2	Cell Signaling	IP, WB	1/50, 1/1000	60
Akt3	Cell Signaling	IP, WB	1/100, 1/1000	60

4.15. Cell Proliferation Assay

Approximately $3x10^4$ shSIK2 or scrambled shRNA containing MIO-M1 cells were seeded on round coverslips in a 24-well tissue culture dish and were grown in DMEM supplemented with 10 % FBS for one day. Next day after washing with PBS, the cells were serum-starved 16 hours. The following day cells were incubated media containing 1 ng/ml or 100 ng/ml FGF2 containing 100 µg/ml heparin, or 10 nM insulin or PBS for 24 hours. Then 10 µM BrdU solution were added to the culture medium 5 h before fixation of the cells with 4 % paraformaldehyde and they were permeabilized with trypsin solution for 8 minutes at 37^0C and treated with 4 M HCl for 10 minutes at room temperature for denaturation. The cells were washed three times with PBS to bring the pH of the medium above 6.5. After incubation with blocking solution for 10 minutes, the cells were incubated in FITC-conjugated anti-BrdU antibody for one hour at room temperature in the dark. To

visualize the nuclei, cells were incubated with DAPI for 5 minutes. After washing twice with PBS, the cells were observed under fluorescent microscope and 200 cells were counted in randomly selected areas.

4.16. Apoptosis Assay

Apoptotic cell death was examined by TUNEL assay using in situ cell death kit, (Roche, Germany). Cultured MIO-M1 cells seeded on round coverslips were fixed with 4% paraformaldehyde for 45 minutes and then permeabilized with 0.1% Triton X-100 in sodium citrate buffer. After washing with PBS three times, cells were incubated in TUNEL labeling solution for one hour in the dark at 37^0C. To visualize the nuclei, cells were incubated with DAPI for 5 minutes. After washing twice with PBS, the cells were observed under fluorescent microscope and 200 cells were counted in randomly selected areas.

4.17. Gab1 and IRS1 Protein Coimmunoprecipitation

Fifty µl of recombinant protein A–Agarose (Roche) beads slurry (50%) was prepared with washing in ice-cold immunoprecipitation (IP) buffer (20 mM HEPES (pH 7.4), 150 mM NaCl, 0.1% Triton-X and 10% glycerol) twice and preincubated with 8 µg the anti-Gab1 antibody or anti-IRS1 (Santa Cruz) while gently mixing for 2 hours at room temperature.

Untreated or growth factor treated cells were lysed in lysis buffer (50 mM Tris-Cl (pH 8.0), 300 mM NaCl, 5 mM EDTA, 5 mM EGTA, 2 mM DTT and 0.5% TritonX-100) with protease and phosphatase inhibitor cocktail for 1 hour on ice by shaking gently. Then cell lysates were centrifuged at 10000 xg for 20 minutes to remove cell debris. The supernatant was incubated with 20 µl pre-cleared Protein-A Agarose beads for 30 minutes by gentle mixing at 4^0C and then centrifuged at 10000 xg for 1 minute. The beads were discarded. Protein concentration in the supernatants was measured by BCA kit (Pierce, USA).

The beads were incubated with 500 µg of total lysate protein for 4 h at 4^0C. After the incubation, the beads were washed twice with ice-cold IP buffer with protease and phosphatase inhibitor cocktail and once with PBS. The proteins were eluted in 2x SDS sample buffer, heated for 5 min at 75^0C and spun down for 1 minute at 10000 xg.

4.18. Coimmunoprecipitation of SIK2 Protein with Gab1

After 10^6 MIO-M1 cells were harvested in PBS with protease inhibitor cocktail, cells were pelleted by centrifuging at 750 xg for 5 minutes at 4^0C and then lysed in five packed-cell volume of EBC buffer (20 mM Tris-Cl pH 8.0, 125 mM NaCl, 0.5% NP-40, 2 mM EDTA, 20 mM NaF, 0.2 mM Na_3VO_4). Total protein concentration was determined and 500 µg total protein were precleared with 80 µl of Protein A agarose slurry per 1 ml lysate. After preclearance the lysate was incubated with anti-Gab1 antibody for 2 hours at 4^0C on a rotator, then another 2 hours with 30 µl of protein A agarose slurry. Agarose beads were collected by centrifugation at 800 xg for 3 minutes and the supernatant was carefully aspirated. The beads were washed four times with ice-cold EBC buffer with protease inhibitor cocktail. After the last wash, to remove residual wash buffer the tubes were centrifuged one more time at 800 xg for 1 minute at 4^0C. The pellet was resuspended in 50 µl of 2x sample buffer and boiled for 5 minutes at 95^0C to dissociate the beads. Then the beads were collected by centrifugation and the supernatant fraction was transferred to a new tube and stored at -80^0C for later use.

4.19. Immunoprecipitation of SIK2 Protein

To be used in *in vitro* kinase assays SIK2 was immunoprecipitated as described by Horike *et al*. (2004) using antiserum kindly donated by Dr. Takemori (National Institute of Biomedical Innovation, Osaka, Japan). Anti-SIK2 anti-serum pre-incubated with insoluble fraction of *E. coli* lysate was incubated with protein A-agarose beads at 4^0C for four hours, beads were washed and 50% suspension was prepared in lysis buffer containing 50 mM Tris-HCl (pH 8.0), 150 mM NaCl, 1% NP40 with protease and phosphatase inhibitor cocktails. After insulin or FGF2 treatments, approximately 10^6 MIO-M1 cells were harvested. The cell pellet was resuspended in 1 ml of cold lysis buffer containing protease inhibitor cocktail. The cells were kept on ice for 30 minutes with occasional mixing,

spinned at 10000 xg for 15 minutes at 4^0C, and the supernatant was collected. A 50 µl aliquot of Protein A agarose beads (Roche, Germany) was equilibrated with washing the beads with 450 µl cold lysis buffer and spinned at 10000 xg for 30 seconds. The washing was repeated, the beads were resuspended in 50 µl of cold lysis buffer. This Protein A slurry and 500 µg of cell lysate were mixed and incubated on ice for one hour. The mixture was then spinned at 10000 xg for 10 minutes at 4^0C and the supernatant was transferred carefully to a fresh tube. SIK2 antibody conjugated protein A-agarose slurry was incubated with the supernatant for two hours at 4^0C. The beads were collected, washed and resuspended in the kinase buffer (50 mM Tris-Cl, pH 7.4, 1 mM DTT, 10 mM $MgCl_2$, 10 mM $MnCl_2$). Half the samples were analyzed by western blotting, the remaining was stored at -80^0C for *in vitro* kinase assay.

4.20. In vitro Kinase Assay

The *in vitro* autophosphorylation and kinase assays were performed according to the method of Feldman *et al.* (2000). Briefly, reactions containing approximately 1 µg of immunoprecipitated Gab1 and IRS1 proteins, 1 µl of radioactive ATP cocktail containing 100 µM cold ATP (Amersham, USA), 1 µCi [γ^{32}P]ATP 3000 Ci/mmol (Isotop, Hungary) and kinase buffer (50 mM Tris-Cl, pH 7.4, 1 mM DTT, 10 mM $MgCl_2$, 10 mM $MnCl_2$) were set up at 30^0C. The reactions were initiated by the addition of 0.25 µg of purified GST-SIK2-(KD/UBA). For SIK2 activity assay, to 20 µl of immunoprecipitated SIK2 proteins one µCi [γ32P]-ATP (3000 Ci/mmol) and 500 ng of purified recombinant GST-IRS1 were added. The kinase reaction was allowed to proceed at 30^0C for one hour, and terminated by the addition of the SDS sample buffer. The beads were removed by centrifugation, the supernatants were run on 8% SDS-PAGE. The gels were fixed, dried and exposed to X-ray film (Amersham, UK) for varying times at -80^0C.

4.21. Statistical analysis

Experimental groups were compared statistically using the Mann-Whitney test (one-tailed) or one-way ANOVA. Means with $P < 0.05$ were considered statistically significant.

5. RESULTS

5.1. The Potential Role of SIK2 in the FGF Signal Transduction Pathway

The possible involvement of SIK2 in the FGF signal transduction pathway was initially explored by studying temporal changes in the SIK2 phosphorylation and activation status upon FGF2 treatment in MIO-M1 cells. Subsequently FGF2-dependent ERK and Akt activation profiles were defined and possible modulations in these profiles by SIK2 was investigated through SIK2 overexpression and knockdown studies. Effect of SIK2 silencing on FGF2 induced Müller cell proliferation was also included in these studies. In the final part we expanded our earlier work (Küser, 2006) suggesting that Gab1 is the potential target of SIK2 in the FGF/ERK and FGF/Akt pathways.

5.1.1. Modulation of SIK2 Phosphorylation and Activity upon FGF2 Treatment in MIO-M1 Cells

To investigate possible FGF2 dependent changes in the serine and threonine phosphorylation profile and activity of SIK2, MIO-M1 cells were treated with the FGF2 factor for 0-60 min. The SIK2 protein immunoprecipitated from the cell lysates was subjected to immunoblot analysis with anti-pSer or anti-pThr antibodies and used in *in vitro* kinase assays where GST-IRS1 was included as the substrate in the presence of radiolabelled ATP. For the immunoblot studies stripped membranes were reprobed with anti-SIK2, pSer and pThr band intensities were normalized to that of the corresponding SIK2 bands. For comparative analysis of SIK2 activity reaction mixtures were resolved on PAGE and subjected to autoradiography, the band intensities of GST-IRS1 bands were normalized to that of SIK2 bands in matching samples as revealed by immunoblotting. Three independent experiments were performed.

The immunoblotting results (Figure 5.1) indicated a modest decline in serine phosphorylation of SIK2 starting 5 minutes after FGF2 induction and the minimum levels (0,5-fold decrease) were reached at 10 minutes; by 60 minutes of induction basal levels were restored. On the other hand, threonine phosphorylation levels of SIK2 began to

increase 5 minutes after induction and at 10 minutes threonine phosphorylated SIK2 level was at the highest (about 1,65-fold of resting cells), and remained about the same level thereafter (Figure 5.1). In matching samples the SIK2 activity was doubled at 10 minutes of FGF2 induction, then gradually returned to basal level in 60 minutes (Figure 5.2). The profile is reminiscent of the FGF2-dependent ERK activation profile.

The phosphorylation and activity data taken together support the involvement of SIK2 in the FGF2 pathway. It is conceivable that concurrent threonine hyperphosphorylation and serine hypophosphorylation of SIK2 in response to FGF2 leads to a rapid increase in the kinase activity of the protein, and as the pSer:pThr ratio increases the activity of the enzyme declines.

(a)

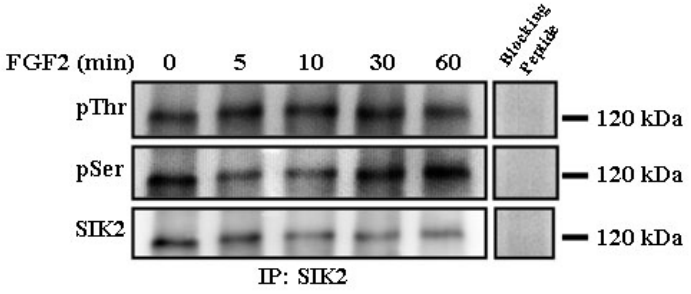

(b)

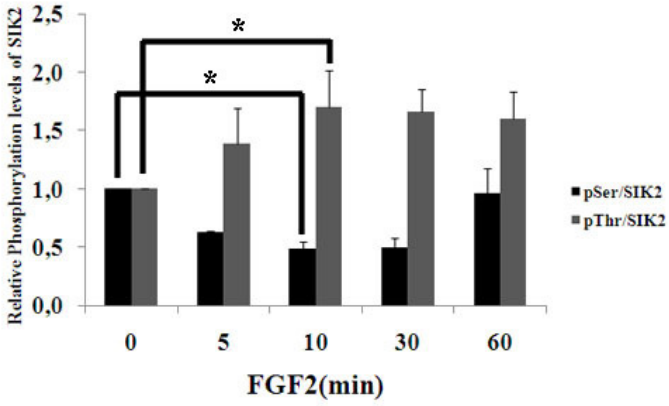

Figure 5.1. FGF2-dependent serine and threonine phosphorylation profiles of SIK2. MIO-M1 cells were treated with FGF2 for indicated times. (a) Immunoprecipitated SIK2 was immunoblotted with anti-pThr, anti-pSer and anti-SIK2 antibodies, in lane C antibodies were preincubated with corresponding blocking peptides. (b) Graphic representation of SIK2 phosphorylation levels normalized to that of corresponding SIK2. * $P < 0.05$ compared to corresponding untreated samples.

(a)

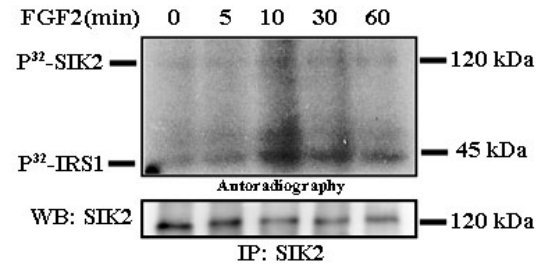

(b)

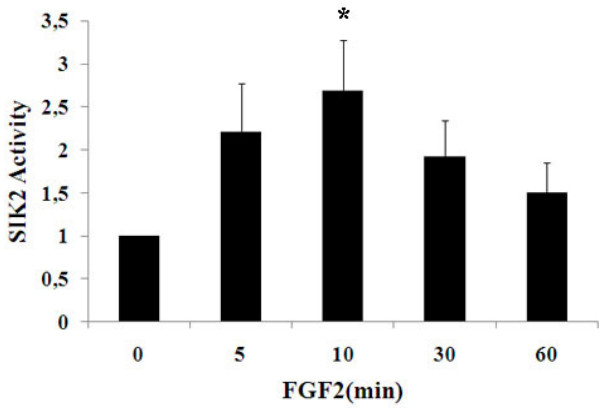

Figure 5.2. FGF2-dependent SIK2 activity modulation. MIO-M1 cells were treated with FGF2 for indicated times, (a) GST-IRS1 phosphorylation by immunoprecipitated SIK2 was assayed *in vitro* followed by PAGE and autoradiography. Input levels of SIK2 were revealed by Western blot analysis using anti-SIK2 antibody. (b) Graphic representation of pGST-IRS1 band intensities normalized to that of SIK2 levels in the same samples * $P < 0.05$ compared to untreated levels.

5.1.2. Effect of SIK2 Knockdown and Overexpression on pERK levels and Müller Cell Proliferation

5.1.2.1. Effect of FGF2 on ERK Phosphorylation Profile in MIO-M1 Cells. The profile of ERK activation was studied in MIO-M1 cells that received an FGF2 stimulus for 0-60 min. The pERK and total ERK levels were evaluated by immunoblotting, and pERK band intensities were normalized to that of ERK in the same samples. Three independent experiments were performed.

The results showed that pERK levels peaked (4-fold of basal level) within 10 minutes of FGF2 treatment and began to return to basal level after 60 minutes of induction

(Figure 5.1). These findings are consistent with earlier results obtained in our laboratory (Çinaroğlu, unpublished data).

(a)

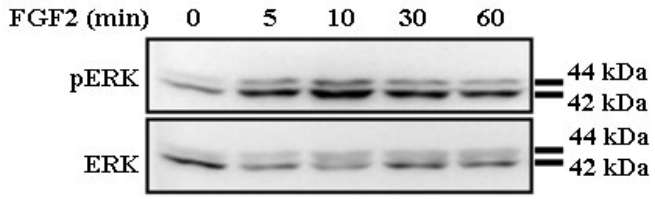

(b)

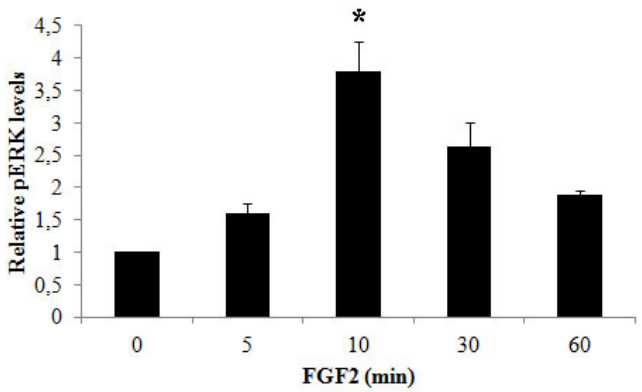

Figure 5.3. FGF2-dependent ERK phosphorylation profile in MIO-M1 cells. Serum starved cells were treated with FGF2 for indicated times. (a) Western blot analysis was performed with anti-pERK, anti-ERK was the loading control. (b) Graphic representation of relative pERK band intensities normalized to that of corresponding ERK. * $P < 0.05$ compared to untreated levels.

5.1.2.2. Effect of SIK2 Overexpression on FGF2-induced ERK Phosphorylation Levels.

For transient SIK2 overexpression, MIO-M1 cells were transfected with pEGFP-SIK2 vector, while control cells received an empty vector. The transfection efficiencies were around 40%, as judged by GFP-expressing cell numbers compared to the total cells in the dish. Modulations in FGF2-dependent ERK phosphorylation was examined 48 h after transfection as described in Section 5.1.2.1. Three independent experiments were performed.

In cells expressing only GFP, the obtained ERK phosphorylation profile was similar to that of untransfected cells, 4-fold increase at 10 min and returning to basal level at 60

minutes after FGF2 stimulation (Figure 5.3 and Figure 5.4). However, in SIK2-overexpressing cells we observed no significant upregulation in ERK phosphorylation above basal levels at any time point examined. When the overexpression study was carried out with His-tagged SIK2, similar results were obtained (data not shown).

These results indicate that enhanced expression of SIK2 prevents FGF2-induced ERK phosphorylation in MIO-M1 cells.

(a)

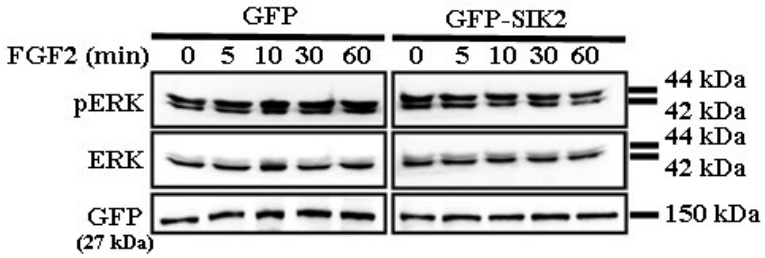

(b)

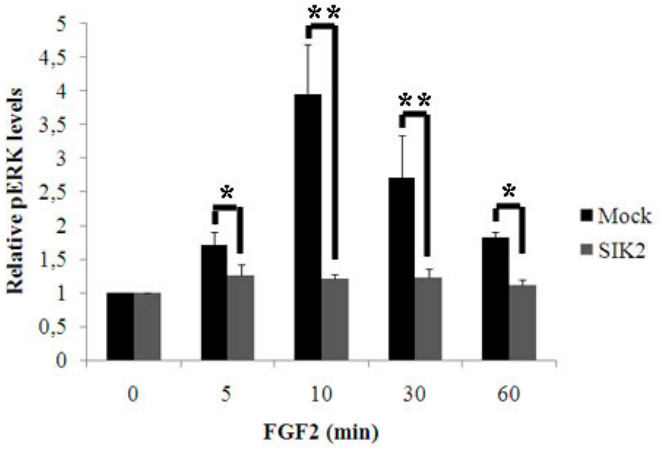

Figure 5.4. Effect of SIK2 overexpression on FGF2-induced ERK phosphorylation levels in MIO-M1 cells. Cells were transfected with either pEGFP-SIK2 or only GFP vector, and 2 days post-transfection they were treated with FGF2 for 0-60 minutes. (a) pERK profile was elucidated by Western blotting with anti-pERK antibody. Anti-ERK and anti-GFP were used as loading control. (b) Graphic representation of pERK band intensities normalized to that of ERK levels in the same samples. $*P < 0.1$, $*P < 0.05$ compared to corresponding mock transfected samples.

5.1.2.3. Effect of SIK2 Knockdown on FGF2-induced ERK Phosphorylation Levels. To further verify that SIK2 negatively regulates FGF2 induced ERK signaling, SIK2 knockdown was performed. MIO-M1 cells were infected with shSIK2 or scrambled RNA containing lentiviral particles and stably transduced cells were puromycin selected for 2 weeks. Puromycine-resistant single cell isolates were expanded. In this study, shSIK2 transduced clone number 3 and scrambled shRNA transduced clone number 5 were exposed to FGF2 and modulations in ERK activation were assesed by immunoblotting as described above. Three independent experiments were performed. Anti-SIK2 probing showed downregulation of SIK2 expression in the order of 60% at the protein level, though SIK3 protein levels were unaffected (Figure 5.5a). Scrambled shRNA expressing cells showed similar ERK activation to uninfected cells. SIK2 silencing increased pERK levels dramatically (2-4 fold) upon FGF2 induction at all time points examined (Figure 5.5c), and remained at significantly higher levels even at 60 min post induction. Taken together overexpression and the knockdown data suggest that SIK2 restrains FGF2 induced ERK activation in MIO-M1 cells.

5.1.2.4. Effect of SIK2 Gene Silencing on FGF2-Induced Müller Cell Proliferation. It has been suggested that FGF2 induces proliferation of MIO-M1 cells mediated via of ERK1/2 activation (Hollborn *et al*., 2004). Thus we explored if, along with inhibition of ERK activation, SIK2 has a negative effect on FGF2-induced Müller cell proliferation. To address this possibility cells stably transduced with shSIK2 or scrambled RNA, subsequent to overnight serum starvation, were treated with 1 or 100 ng/ml FGF2 for 24 hours. Proliferation was evaluated by a BrdU incorporation assay and compared to untreated cells. Three independent experiments were performed. The fraction of BrdU incorporated cells were increased in an FGF2 concentration-dependent manner in both control and SIK2 silenced cells (Figure 5.6). In scrambled shRNA transduced cells the observed increase was comparable to untransduced cells (Çınaroglu, 2005). In all cases, untreated and treated groups alike, SIK2 silencing significantly increased the proportion of BrdU-positive cells compared to the controls. The most striking difference was seen in cells treated with 100 ng/ml FGF2, where 13% of the control cells and 33% SIK2-silenced cells appeared to be proliferating. This proliferation result in combination with the previous ERK activation data (Figure 5.3 and 5.6) strongly suggest that SIK2 has an inhibitory role on FGF2-induced Müller cell proliferation via ERK activity regulation.

(a)

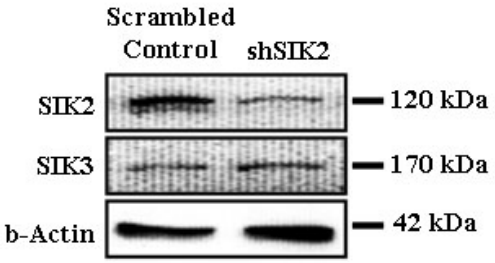

(b)

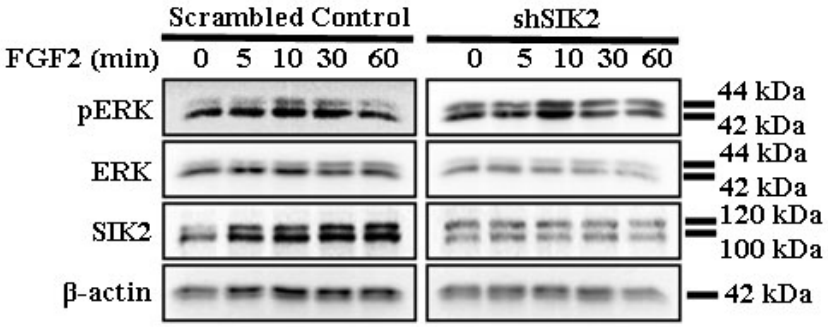

(c)

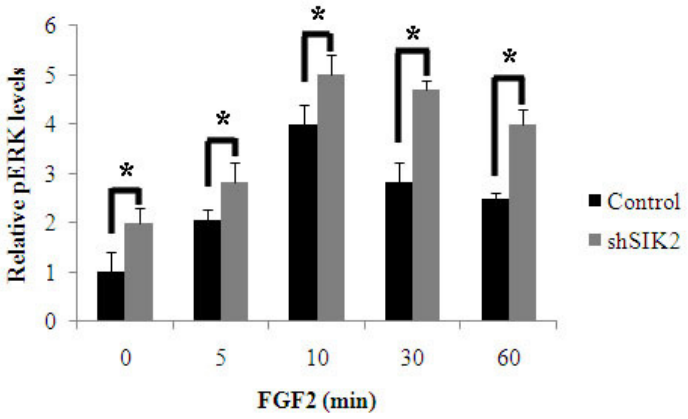

Figure 5.5. Effect of SIK2 knockdown on FGF2-induced ERK phosphorylation levels in MIO-M1 cells. (a) Knockdown of SIK2 gene was done by infecting cells with lentiviral particles carrying shSIK2 or scrambled shRNA. Silencing was verified using anti-SIK2 antibody and β-actin as loading control. (b) The cells were treated with 1ng/ml FGF2 for the indicated times. pERK levels were evaluated by anti-pERK, anti-ERK, or anti-β-actin used as loading, or anti-SIK2 for silencing control. (b) Graphic representation of pERK band intensities normalized to that of ERK levels in the same samples. $*P < 0.05$ compared to the corresponding control samples.

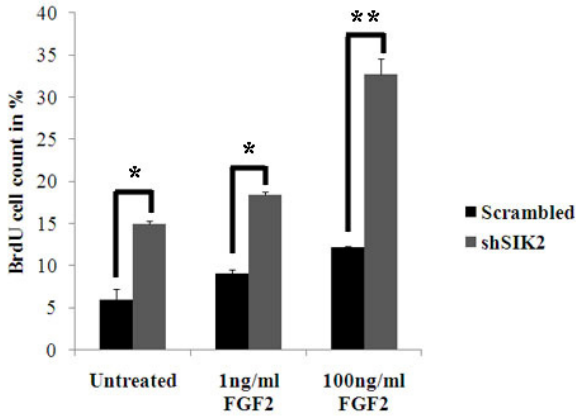

Figure 5.6. Effect of SIK2 gene silencing on FGF2-induced BrdU incorporation in MIO-M1 cells. Knockdown of SIK2 was done by infecting cells with lentiviral particles carrying shSIK2 or scrambled shRNA. Stably transduced were cells serum-starved overnight and were either untreated or treated with 1 or 100 ng/ml FGF2 for 24 hours. Proliferation was evaluated by a BrdU incorporation assay. *$P < 0.05$, **$P < 0.01$ compared to the scrambled control samples.

5.1.3. Effect of SIK2 Knockdown and Overexpression on pAkt Levels in MIO-M1 Cells

5.1.3.1. Effect of FGF2 on Akt Phosphorylation Profile in MIO-M1 Cells. Reduced FGF2-dependent proliferation of MIO-M1 cells observed in the presence of PI3K inhibitor, LY294002 implicates Akt pathway in this mitogenic response (Hollborn *et al.*, 2004; Çınaroğlu, unpublished data). The profile of Akt activation was studied in MIO-M1 cells that received a FGF2 stimulus for 0-60 min. The pAkt(S473) and panAkt levels were evaluated by immunoblotting, and pAkt band intensities were normalized to that of panAkt in the same samples (Figure 5.7). Three independent experiments were performed. Relative pAkt levels halved at 10 minutes of FGF2-induction, turned to basal level after 30 minutes and peaked (3-fold of basal level) at 60 minutes.

5.1.3.2. Effect of SIK2 Overexpression on FGF2-induced Akt Phosphorylation Levels. In order to investigate whether SIK2 is involved in the regulation of FGF2-induced Akt signaling, a SIK2 overexpression study was performed in MIO-M1 cells as described in 5.1.2.2 and modulations in FGF2-dependent Akt phosphorylation were examined 48 hrs after transfection as described in 5.1.3.1. Three independent experiments were performed.
In cells expressing only GFP, Akt phosphorylation profile was similar to its normal profile, peaking to 3-fold level at 60 min after FGF2 stimulation (Figure 5.7 and Figure 5.8). However, SIK2 overexpression does not allow significant upregulation of Akt activation

when compared to that of mock-transfected cells. The same overexpression study was carried out with His-tagged SIK2 proteins and similar results were obtained (data not shown). These results indicate that enhanced expression of SIK2 prevents FGF2-induced Akt phosphorylation in MIO-M1 cells.

5.1.3.3. Effect of SIK2 Knockdown on FGF2-induced Akt Phosphorylation Levels. In this study clone number 3 and 5 were exposed to FGF2 and modulations in Akt activation were assessed by immunoblotting as described above (Figure 5.10). Three independent experiments were performed. SIK2 silencing, in the order of 60%, increases pAkt levels dramatically (2-3 fold) at all time points after FGF2 induction, although scrambled shRNA infected cells show a similar Akt activation profile upon FGF2 treatment. Previous SIK2 overexpression and this knockdown data overall suggest that SIK2 negatively regulates FGF2-induced Akt activation in MIO-M1 cells.

(a)

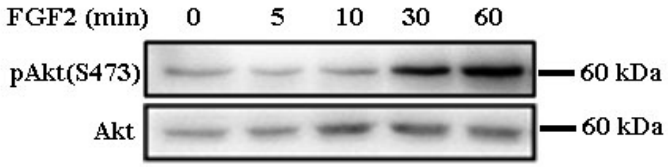

(b)

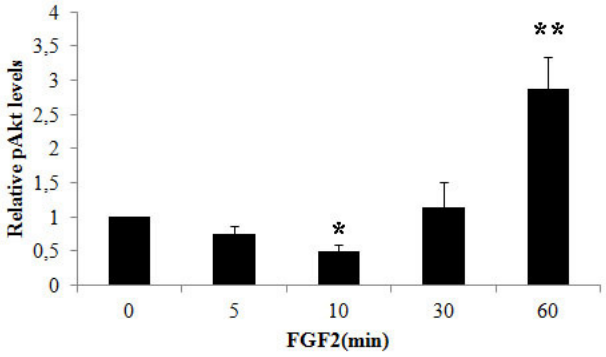

Figure 5.7. FGF2-dependent Akt phosphorylation profile in MIO-M1 cells. Serum starved cells were treated with FGF2 for indicated times. (a) Western blot analysis was performed with anti-pAkt and anti-Akt represents the loading control. (b) Graphic representation of relative pAkt band intensities normalized to that of corresponding panAkt. * $P < 0.05$ and ** $P < 0.01$ compared to untreated levels.

(a)

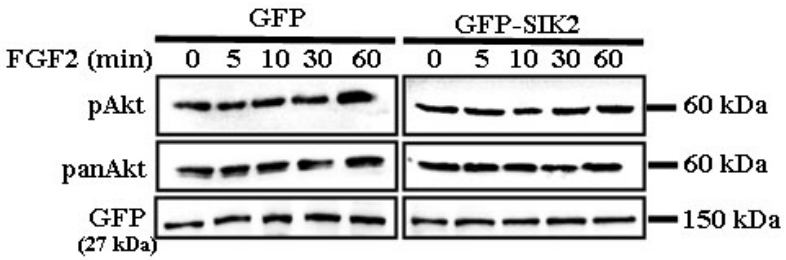

(b)

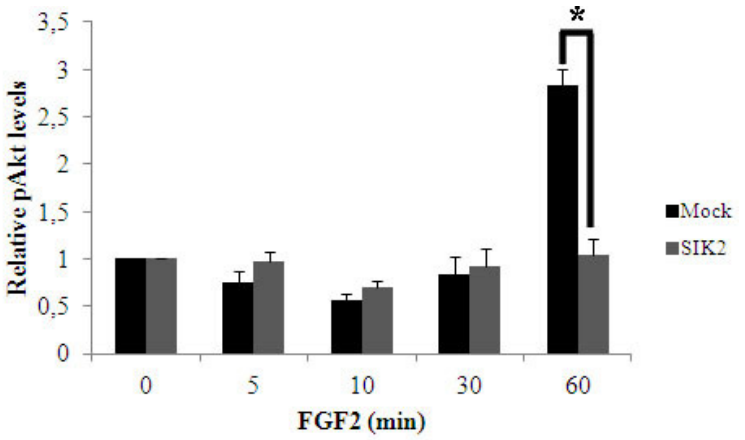

Figure 5.8. Effect of SIK2 overexpression on FGF2-induced Akt phosphorylation levels in MIO-M1 cells. Cells were transfected with either pEGFP-SIK2 or only GFP vector, and 2 days post-transfection they were treated with FGF2 for 0-60 minutes. (a) pAkt profile was elucidated by Western blotting with anti-pAkt(S473) antibody. Anti-panAkt and anti-GFP were used as loading controls. (b) Graphic representation of pERK band intensities normalized to that of ERK levels in the same samples. *$P < 0.01$ compared to mock transfected samples.

5.1.4. Gab1 Phosphorylation by SIK2 *in Vitro*

Our earlier work identified the presence of a SIK2 phosphorylation motif, L[(B)X or X(B)][S/T]X**S**XXXL in Gab1 and the motif containing fragment of the protein (nucleotide: 680-1253) was phosphorylated by SIK2 *in vitro* (Küser, 2006). As Gab1, an adaptor protein that relays FGFR signals into cycle cycle progression (Mood *et al.,* 2006), we considered it to be a strong SIK2 target candidate in the context of our study.

(a)

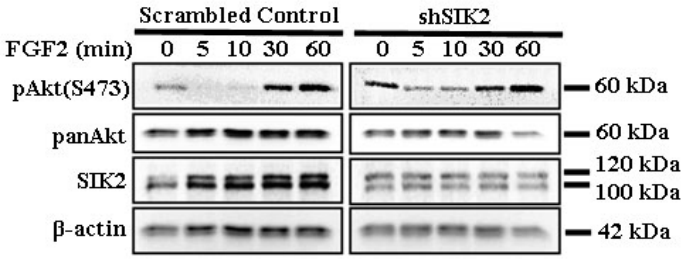

(b)

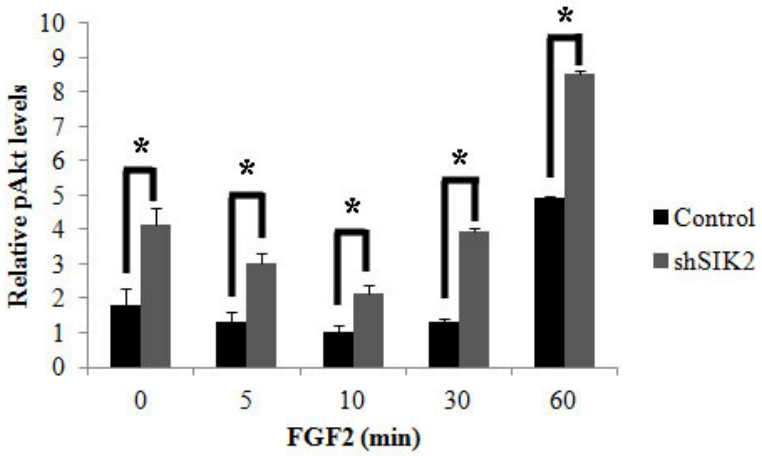

Figure 5.9. Effect of SIK2 knockdown on FGF2-induced Akt phosphorylation levels in MIO-M1 cells. (a) Knockdown of SIK2 gene was performed by infecting cells with lentiviral particles carrying shSIK2 or scrambled shRNA. The cells were treated with 1ng/ml FGF2 for the indicated times. pAkt levels were evaluated by anti-pAkt(S473), anti-panAkt, or anti-β-actin used as loading, or anti-SIK2 for silencing control. (b) Graphic representation of pERK band intensities normalized to that of ERK levels in the same samples. * $P < 0.05$ compared to the control samples.

To further verify that SIK2 phosphorylates Gab1 *in vitro*, GST-SIK2-(WT) recombinant protein and immunoprecipitated Gab1 from MIO-M1 cells were incubated in kinase buffer containing [^{32}P]γ-ATP. SIK2 activity was assesed on its autophosphorylation levels. The known SIK2 substrate IRS1 constituted the positive and kinase-inactive mutant of SIK2, GST-SIK2-(KI) the negative control of the experiment. While an autophosphorylation signal was detected when recombinant GST-SIK2-(WT) protein was used, no signal was detectable in GST-SIK2-(KI) samples (Figure 5.10a), while GST-SIK2-(WT) phosphorylates IRS1 as expected. Immunoprecipitated Gab1 was also phosphorylated by the wildtype SIK2 *in vitro*, but not by GST-SIK2-(KI), confirming our earlier findings (Figure 5.10b).

(a)

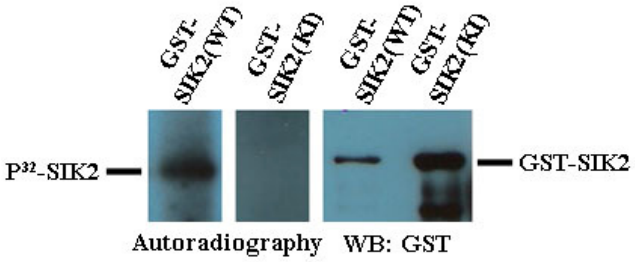

(b)

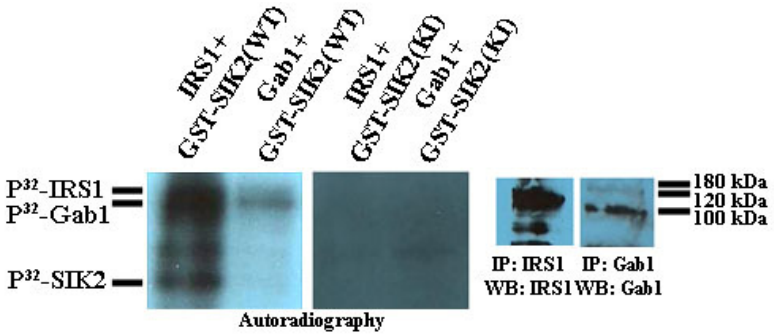

Figure 5.10. Gab1 phosphorylation by SIK2 *in vitro*. Bacterially expressed GST-SIK2(WT) and GST-SIK2(KI) recombinant proteins were affinity-purified on glutathione columns and used in *in vitro* kinase assays (a) SIK2 autophosphorylation (b) kinasing of immunoprecipitated Gab1 and IRS1 with GST-SIK2 (WT), and GST-SIK2 (KI) recombinant proteins. The input was assessed by immunoblotting using anti-GST, anti-IRS1 or anti-Gab1 antibodies as indicated.

5.1.5. FGF2-Dependent Gab1 Interaction with SIK2

To verify the SIK2 and Gab1 interaction *in vivo*, MIO-M1 cells were serum-starved overnight and either left untreated or exposed to 1 ng/ml FGF2 for 10 minutes where SIK2 activity is at maximum. Subsequently, lysates were coimmunoprecipitated with anti-Gab1 antibody. The association of SIK2 with Gab1 was elucidated by Western blotting using anti-SIK2 antibody. Anti-Gab1 antibody was used as immunoprecipitation control.

As seen in Figure 5.11, SIK2 protein was coimmunoprecipitated with Gab1 in MIO-M1 cells treated with FGF2 for 10 minutes. We detected no Gab1 signal in Gab1/SIK2 coimmunoprecipitation experiments in serum-starved cells.

These data strongly suggest *in vivo* FGF-dependent interaction of Gab1 and SIK2, and supports our previous finding that Gab1 is an *in vivo* substrate for SIK2.

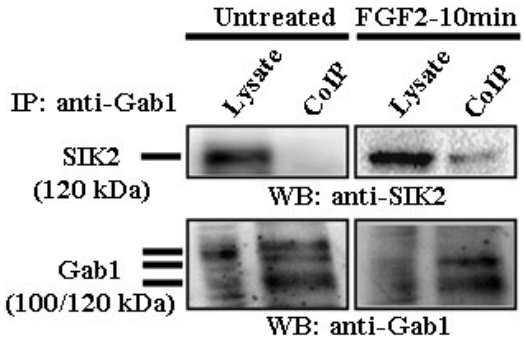

Figure 5.11. Coimmunoprecipitation of SIK2 with Gab1 upon FGF2 treatment in MIO-M1 cells. Serum starved cells were either untreated or treated with FGF2 for 10 minutes, immunoprecipitations were carried out with anti-Gab1 antibody and immunoprecipitates were analyzed by immunoblotting using anti-SIK2 antibody.

5.1.6. Effect of FGF2 on Gab1 Phosphorylation and Binding Partner Association in MIO-M1 Cells

FRS2 and Gab1 docking proteins relay signals from FGF to ERK and Akt (Kouhara *et al.*, 1997; Ong *et al.*, 2001; Krejci *et al.*, 2007). Gab1/Grb2 and Gab1/Shp2 associations lead to Ras/ERK pathway activation, whereas p85 binding is directly involved in PI3K/Akt pathway activation in signaling of various growth factors, including HGF, EGF, insulin and FGF (Holgado-Madruga *et al.*, 1996; Ong *et al.*, 2001).

However, there is complete lack of data on Gab1 involvement in FGF induced ERK and Akt pathways in Müller glial cells. In order to test Gab1 involvement in FGF/ERK and FGF/Akt signaling pathways in Müller cells, we investigated serine and tyrosine phosphorylation profiles of Gab1 and Gab1/Grb2 and Gab1/p85 associations upon FGF2 stimulation in MIO-M1 cells. Cells were treated as described before. After endogeneous Gab1 proteins were immunoprecipitated with anti-Gab1 antibody. Anti-pSer and anti-pTyr antibodies were used to detect the Gab1 phosphorylation status in these cells. Grb2 and p85 binding to Gab1 were analyzed using anti-p85 and anti-Grb2 antibodies. Anti-Gab1 antibody was used as immunoprecipitation control (Figure 5.12a). pSer, pTyr, Grb2 and

p85 levels were normalized to that of corresponding immunoprecipitated Gab1 levels in the same samples and the results of three independent experiments were graphically presented (Figure 5.12b).

Tyrosine and serine phosphorylation level of Gab1 peaked at 10 minutes of FGF2 treatment and turned to basal levels 60 minutes after induction (Figure 5.13). In the same vein, Grb2/Gab1 binding reached maxima at 10 minutes after induction and declined to basal level after 30 minutes. These patterns resemble the ERK activation profile (Figure 5.1 and 5.12). p85/Gab1 binding was doubled at 60 minutes after induction that is reminiscent of the Akt activation profile after FGF2 induction in MIO-M1 cells (Figure 5.7 and Figure 5.12).

From this data we can conclude that the phosphorylation profile of Gab1 is modulated by FGF2 induction in MIO-M1 cells. This is consistent with the FGF2 signal being relayed to ERK through Gab1/Grb2 association and Akt activation which is facilitated via Gab1/p85 binding.

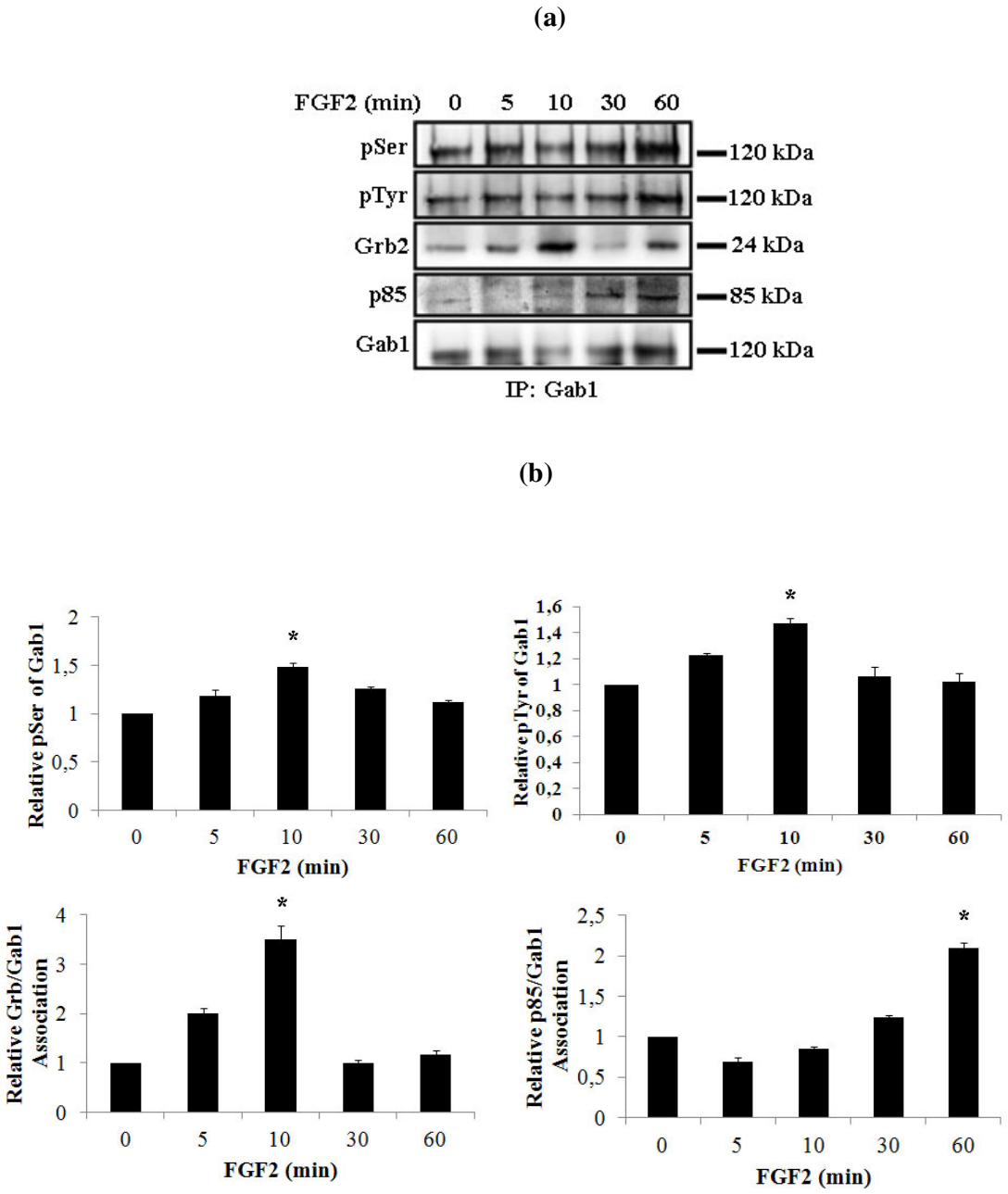

Figure 5.12. Effect of FGF2 on Gab1 phosphorylation and its association with its partners. Gab1 was immunoprecipitated by using anti-Gab1 antibody from lysates of MIO-M1 cells treated with 1 ng/ml FGF2 for 0-60 minutes subsequent to overnight serum starvation. (a) Immunoprecipitates were analyzed by Western blotting using anti-pTyr and anti-pSer, anti-Grb2, anti-p85 and anti-Gab1 antibodies as indicated. (b) Graphic representation of indicated band intensities normalized to that of immunoprecipitated Gab1 levels in the same samples. * $P < 0.05$ compared to the control samples.

5.1.7. Effect of SIK2 Gene Silencing on Gab1 Docking Partner Interactions

In order to test our hypothesis that SIK2 exerts its negative effect on FGF2-induced ERK and Akt activation, thereby Müller cell proliferation, via Gab1 serine phosphorylation

and modulation of its interaction with the docking partners, Gab1 protein was immunoprecipitated from both control and SIK2-silenced cells treated with FGF2 for 10 minutes. Its serine and tyrosine phosphorylation levels and the presence of p85, Shp2 and Grb2 proteins in the immunecomplexes were detected by Western blot analysis using anti-pSer, anti-pTyr, anti-p85, anti-Shp2 and anti-Grb2 antibodies (Figure 5.13). pTyr, pSer, Grb2, p85 and Shp2 levels were normalized to that of corresponding immunoprecipitated Gab1 levels in the same samples and the results of three independent experiments were graphically presented (Figure 5.13b).

As seen in Figure 5.13, in SIK2-silenced cells overall serine phosphorylation level of Gab1 is downregulated 95% upon FGF stimulation, whereas overall tyrosine phosphorylation is upregulated 3.5-fold. In parallel, Grb2, p85 and Shp2 in immune-complexes are increased significantly in control cells compared to the scrambled samples.

This result strongly supports our hypothesis that SIK2 may be involved in the negative regulation of FGF2-induced ERK and Akt pathway and thereby Müller cell proliferation by phosphorylating Gab1, most probably on serine 266 residue that results in prevention of tyrosine hypophosphorylation and Gab1 binding of p85, Shp2 and Grb2 proteins. p85 has a pivotal role in FGF induced Akt signaling, whereas Shp2 and Grb2 are essential parts of the ERK cascade.

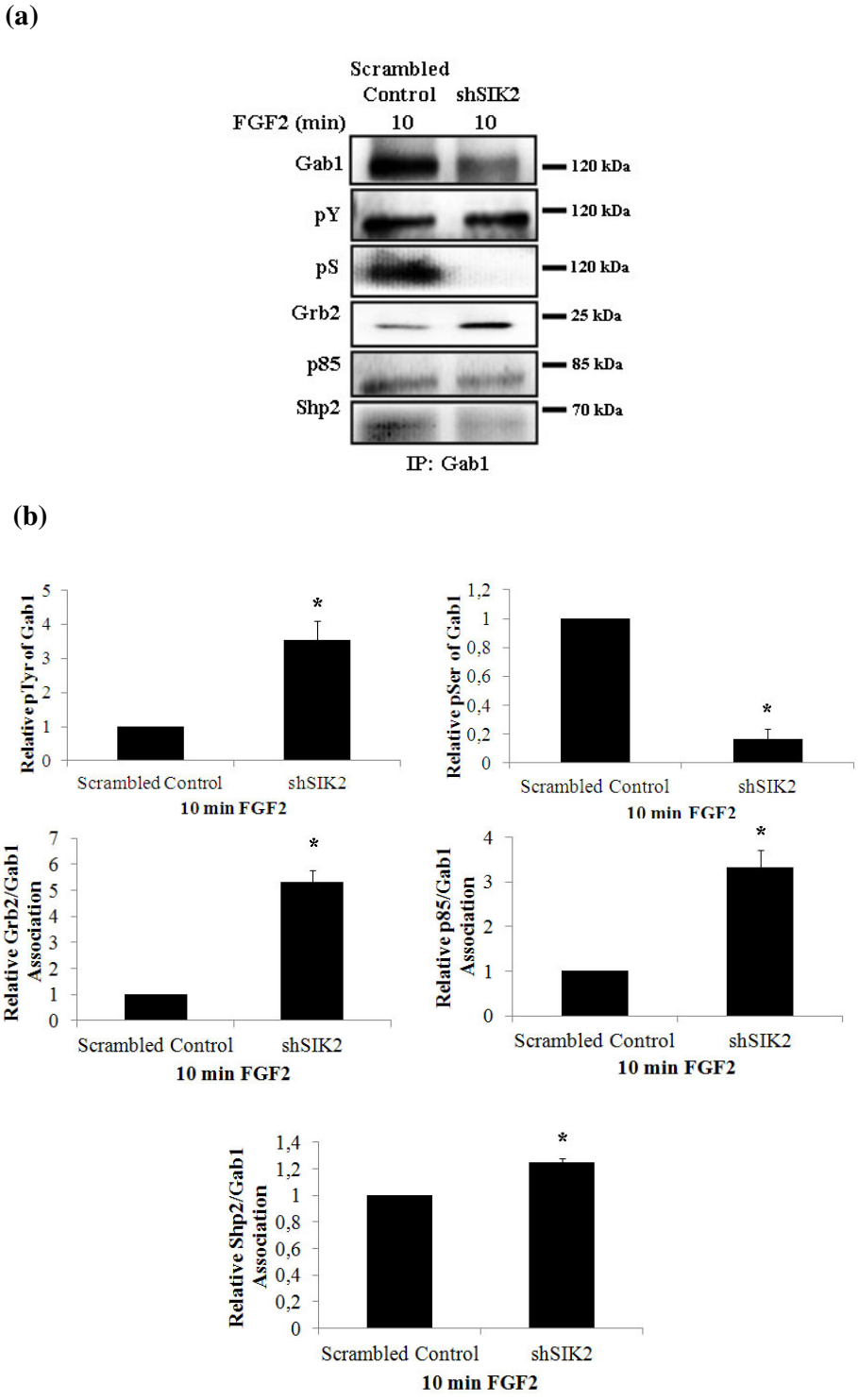

Figure 5.13. Effect of SIK2 gene silencing on Gab1 docking partner interactions. Overnight serum starved MIO-M1 cells stably transduced with scrambled RNA or shSIK2 were treated with 1 ng/ml FGF2 for 10 minutes, Gab1 was immunoprecipitated using anti-Gab1 antibody. Immune complexes were subjected to Western blot analysis using anti-Gab1, anti-pSer and anti-pTyr, anti-Grb2 and anti-p85 antibodies. (b) Graphic representation of indicated band intensities normalized to that of immunoprecipitated Gab1 levels in the same samples. * $P < 0.05$ compared to the control samples.

5.2. The Potential Role of SIK2 in Insulin Dependent Müller Cell Survival under Normal and Diabetic Conditions

Though insulin receptor and IRS proteins are expressed in Müller cells, there is a lack of data on insulin response and elements regulating this pathway in these cells. In ther vertebrate retina insulin is thought to evoke a survival response, rather than regulating glucose metabolism. Therefore, we hypothesized that SIK2 takes part in the modulation of insulin-dependent Müller cell survival mediated by the IRS1/Akt axis and may be involved in hyperglycemia-induced Müller cell apoptosis via Akt inactivation. In initial experiments, insulin-dependent Akt activation, IRS1 phosphorylation and Müller cell survival were studied. Subsequently, the insulin responsive Akt isoform was identified. We analyzed modulations of the insulin-dependent phosphorylation and activation profile of SIK2 and its interaction with IRS1 which is the critical mediator of the insulin signaling pathway. The involvement of SIK2 in insulin-dependent Müller cell survival via Akt activity modulation was studied through SIK2 overexpression and silencing experiments. The possible role of SIK2 in chronic hyperglycemia-induced Akt inactivation and Müller cell apoptosis were studied through SIK2 overexpression and knockdown experiments in MIO-M1 cells. Finally, IRS1 phosphorylation and protein levels were examined in MIO-M1 cells grown under hyperglycemic conditions. SIK2 activity changes in retina were tested using type 1 diabetic animals.

5.2.1. Akt and ERK Phosphorylation Profiles upon Insulin Treatment in MIO-M1 Cells

To establish insulin-dependent Akt and ERK activation profiles in MIO-M1 cells, cells were treated as discussed before (section 5.1.2.1). For the Akt phosphorylation experiment, cell extracts were immunoblotted with anti-pAkt(S473) and anti-pAkt(T308). For loading control, anti-pan-Akt was used. For ERK phosphorylation kinetics, the same cell extracts were immunoblotted with anti-pERK and anti-ERK antibodies. pAkt or pERK levels were normalized to that of corresponding Akt and ERK levels in the same samples and the results of three independent experiments were graphically presented (Figure 5.14b and Figure 5.14d).

As expected the Akt phosphorylation status changes in an insulin-dependent manner in MIO-M1 cells (Figure 5.14a,b). The data demonstrated that pAkt levels increased 2-fold within 10 min and reached a maximum level, 5-fold, at 60 minutes after insulin induction. A decrease is evident at 120 minutes post-insulin treatment. However, pERK levels did not change significantly upon the insulin stimulus in MIO-M1 cells (Figure 5.14c,d).

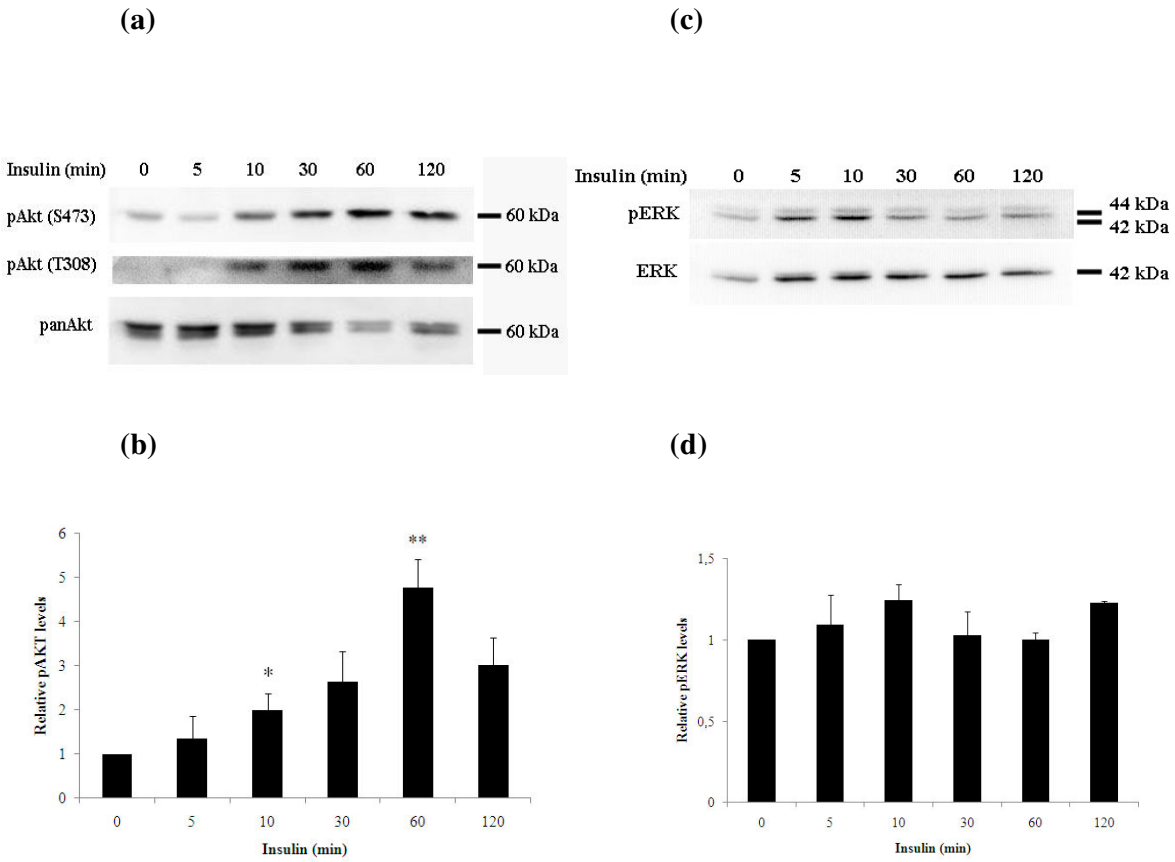

Figure 5.14. Effect of insulin treatment on Akt and ERK activity in MIO-M1 cells. Overnight serum starved cells were treated with 100 pM insulin for indicated times, lysates were analyzed by Western blotting with (a) anti-pAkt(S473), anti-pAkt(T308) and anti-panAkt or (b) anti-pERK and ERK. Relative phosphorylated protein levels were graphically represented following normalization of (c) pAkt(475) band intensities to that of pan-Akt, (d) pERK to Erk in the same samples. $*P < 0.05$, $**P < 0.05$ compared to untreated samples.

5.2.2. Akt Isoform Expression and Activation Kinetics upon Insulin Treatment in MIO-M1 Cells

The Akt family comprises three members, Akt1-3. In the retina all of the isoforms are expressed (Reiter *et al.*, 2003). In this part of the study, we aimed to identify Akt

isoform expression in MIO-M1 cells using RT-PCR and Western blot using Akt1, 2 and 3-specific primers and anti-Akt1, anti-Ak2 and anti-Akt3 antibodies, respectively.

Both RT-PCR and Western blot analysis of Akt isoforms showed that all Akt isoforms are expressed in MIO-M1 cells (Figure 5.15).

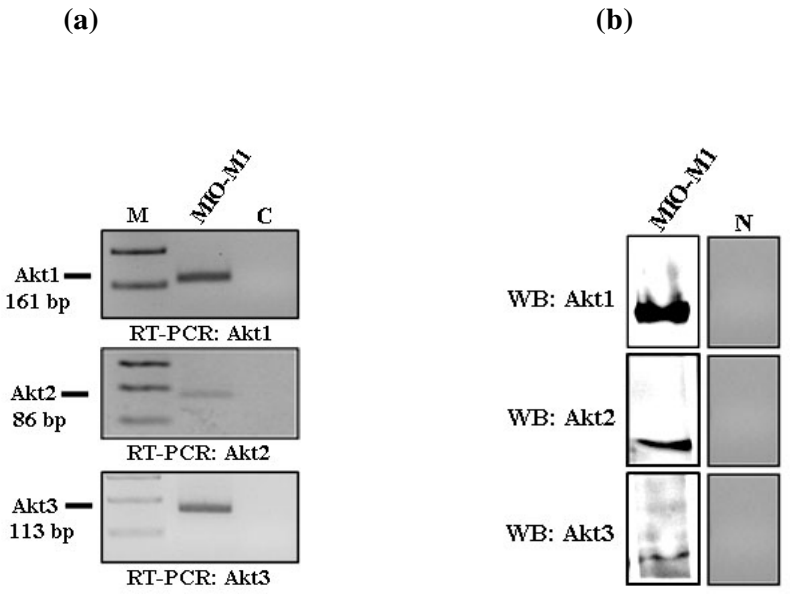

Figure 5.15. Akt isoforms expressed in MIO-M1 cells. (a) cDNA was prepared by reverse transcription of total RNA. The predicted 161 bp, 86 bp, 113 bp amplification product for Akt1, Akt2 and Akt3 were obtained, in that order, by RT-PCR. In lane C reverse transcriptase was omitted. M: 100 bp DNA size marker. (**b**) MIO-M1 cell lysates were immunoblotted using anti-Akt1, Akt2 and Akt3 antibodies. Primary antibodies that were pre-incubated with their corresponding blocking peptides were used in lane N.

Although all Akt isoforms are expressed in the retina, insulin acts on retinal neuronal cell survival through Akt1 activation (Reiter *et al.*, 2003). In order to identify the isoform(s) that is/are activated by insulin in MIO-M1 cells, cells were treated with physiological levels (100 pM) of insulin for 0, 5, 10, 30, 60 and 120 minutes and Akt isoforms were immunoprecipitated using anti-Akt1, Akt2 and Akt3 antibodies followed by immunoblotting with anti-pAkt(S473) antibody. Stripped membranes were reprobed with anti-Akt1, Akt2 and Akt3 antibodies to evaluate loading levels.

The results indicated only one of the Akt isoforms, Akt3, could be phosphorylated upon giving an insulin stimulus in MIO-M1 cells (Figure 5.16). No Akt1 and Akt2 signal was detected. These data suggest that insulin relays the signal through Akt3, but not Akt1

and Akt2 in MIO-M1 cells. The Akt3 phosphorylation profile is reminiscent of the general Akt phosphorylation profile, peaking at 60 minutes and turning back to basal levels at 120 minutes after insulin treatment (Figure 5.7b and Figure 5.16c).

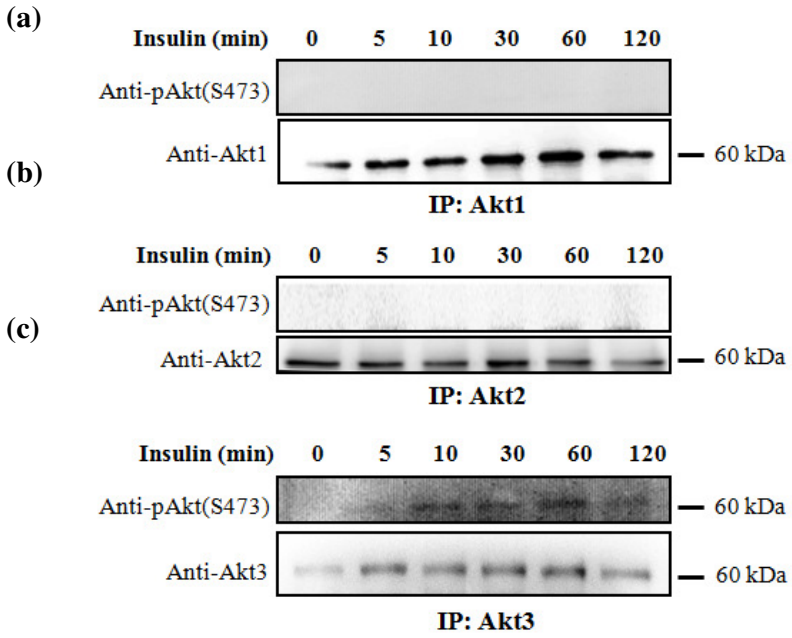

Figure 5.16. Activity profiles of Akt isoforms upon insulin treatment in MIO-M1 cells. Overnight serum starved cells were treated with 100 pM insulin for indicated times. (a) Akt1 (b) Akt2 and (c) Akt3 protein immunoprecipitates from the lysates were immunoblotted with anti-pAkt(S473) antibody. Anti-Akt1, Akt2 and Akt3 antibodies were used as loading controls.

5.2.3. Müller Glia Cell Survival and Proliferation upon Insulin Stimulus

It is widely accepted that insulin acts as a trophic factor in the retina rather than a regulator of energy homeostasis as in metabolically active tissues (Reiter and Gardner, 2003). In line with this view we analyzed insulin (10 nM)-dependent cell survival and proliferation in MIO-M1 cells using TUNEL and BrdU assays, respectively.

We observed that 24 hour insulin treatment enhanced cell survival 20 fold as evaluated by TUNEL assay (Figure 5.17a). A BrdU incorporation assay under the same conditions revealed no insulin-dependent change in proliferation of these cells (Figure 5.17b).

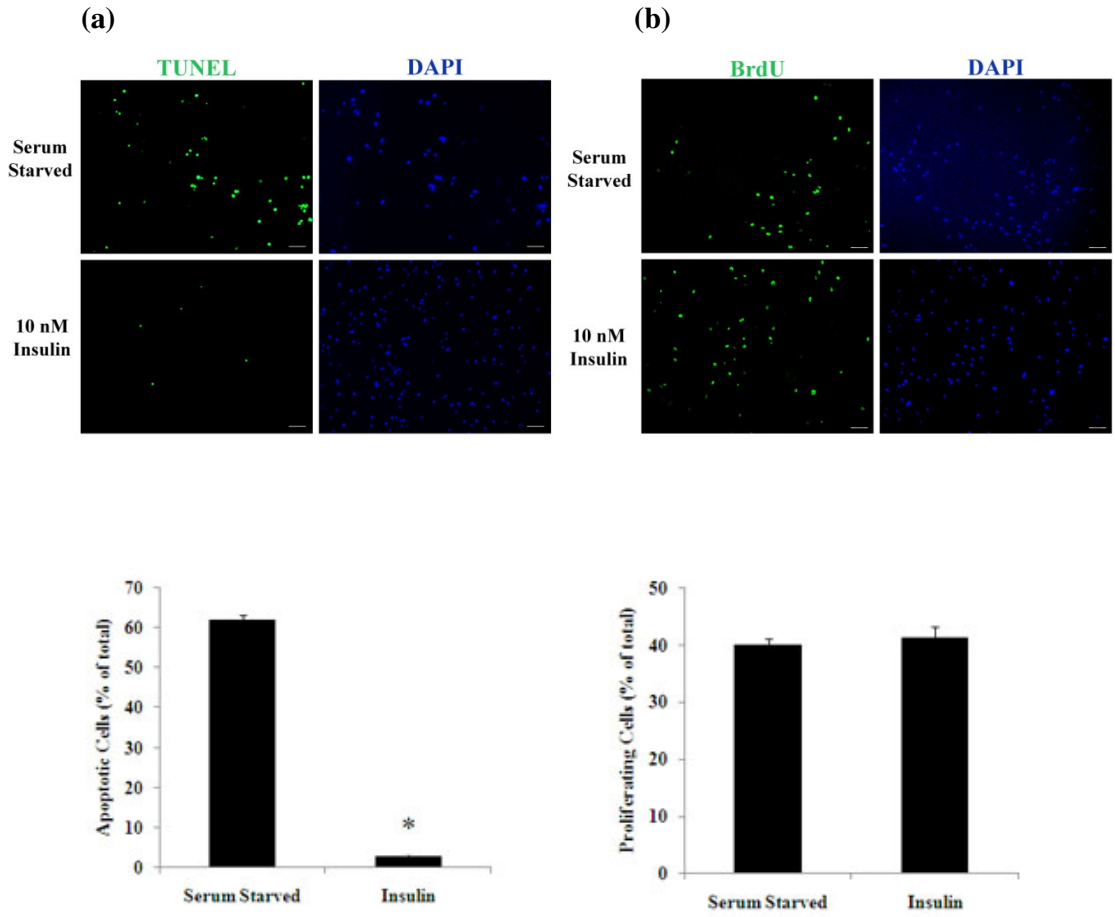

Figure 5.17. Effect of insulin on survival and proliferation of MIO-M1 cells. After overnight serum starvation cells were treated with 10 nM insulin for 24 hours. **(a)** Apoptotic cells were assessed by a TUNEL assay. **(b)** Proliferation was evaluated by a BrdU incorporation assay. Mean values of fraction of apoptotic or proliferating cells in triplicates were graphically presented in lower panels. Cell nuclei were stained with DAPI, at least 200 cells were counted for each triplicate sample. Scale bar = 50 µm.

5.2.4. Serine/Threonine Phosphorylation Profile of SIK2 upon Insulin Treatment in MIO-M1 Cells

In order to provide evidence that SIK2 is involved in insulin dependent signaling in MIO-M1 cells, as a first step, we investigated the serine/threonine phosphorylation profile of SIK2 upon insulin stimulation. Cells were treated with 100 pM insulin for 0, 5, 10, 30, 60 and 120 minutes. Using anti-SIK2 antiserum, endogenous SIK2 proteins were immunoprecipitated from the cell lysates and immunoblotted with anti-phosphoserine and anti-phosphothreonine antibodies to reveal SIK2's phosphorylation status upon insulin treatment in time. The results of three independent experiments are shown in the graph by

normalizing the band intensities of pSer and pThr to that of corresponding immunoprecipitated SIK2 proteins (Figure 5.18).

The threonine phosphorylation level of SIK2 began to decrease at 10 minutes of insulin treatment to 80% of control. At 30 minutes, its level further dropped to 50% and was remained the same upto 120 minutes when compared to that of untreated cells. In parallel, the serine phosphorylation level of SIK2 drops to 35% at 5 minutes and remained constant after that time point upto 120 minutes of insulin treatment.

(a)

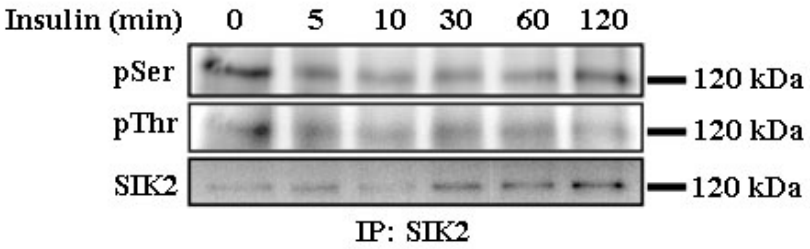

(b)

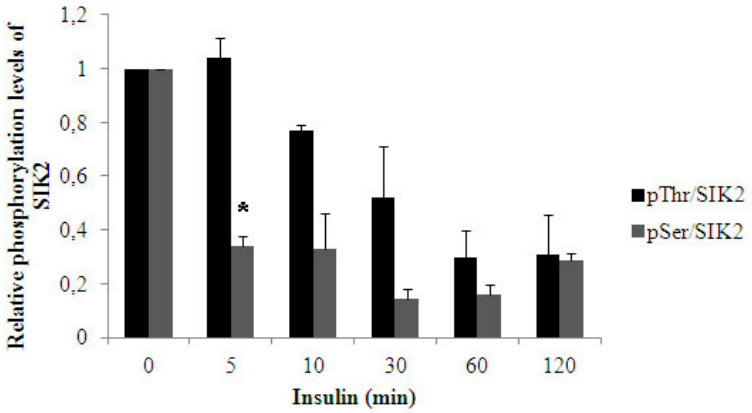

Figure 5.18. Serine and threonine phosphorylation profile of SIK2 upon insulin stimulation in MIO-M1 cells. Overnight serum starved cells were treated with 100 pM insulin for indicated times followed by immunoprecipitation using anti-SIK2 antiserum and subjected to (a) Western bloting using anti-phosphoserine, anti-phosphothreonine and anti-SIK2 antibodies **(b)** Relative SIK2 phosphorylations were shown in the graph by normalizing pSer and pThr band intensities to that of corresponding SIK2 bands. *$P <$ 0.05 compared to untreated samples.

5.2.5. Activity and Expression Profiles of SIK2 upon Insulin Treatment in MIO-M1 Cells

MIO-M1 cells were treated with 100 pM insulin for 0 to 120 minutes. Then, with anti-SIK2 antiserum endogenous SIK2 proteins were immunoprecipitated and *in vitro* kinase assay was performed to investigate the SIK2 activity profile upon insulin treatment in time. GST-IRS1 was used as the SIK2 substrate, and the band intensities of this protein were normalized to that of immunoprecipitated SIK2 proteins in the sample in order to evaluate relative SIK2 activities (Figure 5.19a). For SIK2 protein level analysis, the same cell extracts were immunoblotted with anti-SIK2 antibody. Anti-β-Actin was used as loading control. The results of three independent experiments were plotted on the graph after normalizing SIK2 band intensities to that of corresponding β-actin levels (Figure 5.19b).

SIK2 activity was doubled at 5 minutes of insulin treatment in MIO-M1 cells (Figure 5.19a). Its level began to decrease to 1.5 fold at 10 minutes and turned to basal level at 60 minutes of induction. SIK2 protein level was significantly increased (1.6-fold) at 120 minutes post insulin stimulation in MIO-M1 cells (Figure 5.19b).

As in FGF2 stimulation, threonine hyper- and serine hypo-phosphorylation reflect directly at SIK2 activity increase upon insulin stimulation in MIO-M1 cells.

5.2.6. Tyrosine Phosphorylation Profile and SIK2 interaction of IRS1 upon Insulin Stimulation in MIO-M1 Cells

In cultured Müller glia insulin treatment was reported to enhance tyrosine phosphorylation of IRS-1 (Ola *et al.*, 2011). SIK2 was shown to phosphorylate IRS1 at S794 and as such implicated in downregulation of insulin signaling in adipocytes (Horike *et al.*, 2003). In order to test whether insulin acts on Akt activation through IRS1 tyrosine phosphorylation in MIO-M1 cells, overnight serum starved cells were treated with 100 pM of insulin for 0, 5, 10, 30, 60 and 120 minutes. IRS1 was immunoprecipitated using anti-IRS1 antibody from cell extracts and immunoblotted with anti-pTyr and anti-SIK2 antibody. *In vivo* SIK2-IRS1 interaction was studied by coimmunoprecipitation assays.

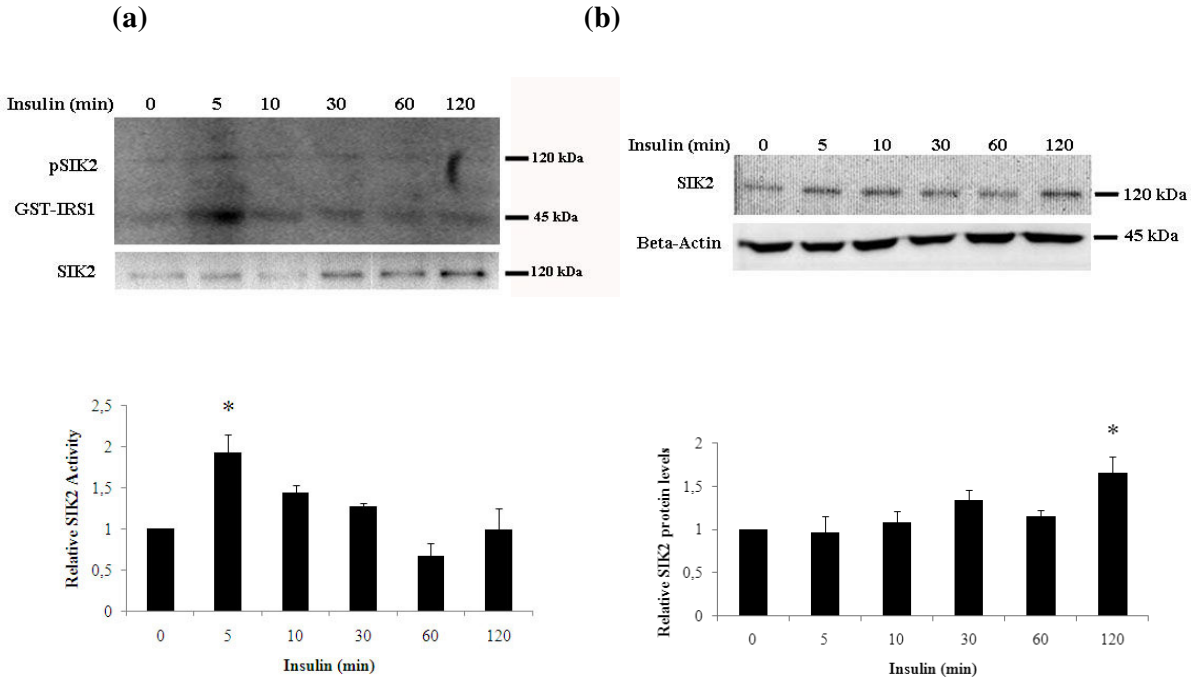

Figure 5.19. Activity and expression profile of SIK2 upon insulin stimulation in MIO-M1 cells. Overnight serum starved cells were treated with 100 pM insulin for indicated times and SIK2 was immunoprecipated. (a) *In vitro* kinase assays carried out in the presence of γ-^{32}PATP, GST-IRS1, were followed by PAGE and autoradiography. Relative SIK2 activity was graphically presented after normalization of GST-IRS1 band intensities to that of corresponding SIK2 on the western blots. (b) Relative SIK2 levels were assessed by Western bloting using anti-SIK2 and β-Actin antibody. SIK2 band intensities were normalized to that of corresponding β-Actin. *$P < 0.05$ compared to untreated samples.

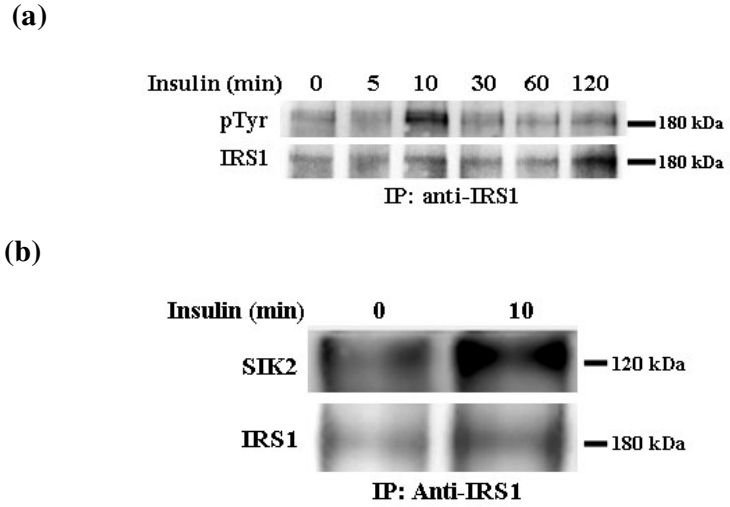

Figure 5.20. Tyrosine phosphorylation of IRS1 and SIK2-IRS1 interaction upon insulin treatment in MIO-M1 cells. Overnight serum starved cells were treated with 100 pM insulin for indicated times followed by immunoprecipitation using anti-IRS1 antibody. (a) Tyrosine phosphorylation of IRS1 was assesed by Western blot analysis using anti-p-Tyr antibody, and IRS1 antibody used as the loading control. (b) Coimmunoprecipitated SIK2 proteins were visualized using anti-SIK2 antibody. IRS1 in the same samples were visualized using anti-IRS1 antibody.

In MIO-M1 cells tyrosine phosphorylation of IRS1 is induced within 10 minutes after insulin treatment and returns to basal levels after 60 minutes (Figure 5.20a). At 10 min insulin-dependent SIK2-IRS1 interaction was evident in coimmunoprecipitation assays (Figure 5.20b).

5.2.7. Effect of SIK2 Overexpression and Silencing on Insulin Dependent Akt Activation.

SIK2 has been suggested to take part in Akt downregulation in the insulin pathway (Horike *et al*., 2003). Thus, the potential role of SIK2 on insulin-dependent Akt activation in MIO-M1 cells was investigated through over-expression and sh-RNA mediated gene knockdown studies. For the overexpression study, cells transfected with GFP-SIK2 or GFP vector (mock transfection) were left untreated or treated with 100 pM insulin for 60 minutes and cell lysates were immunoblotted with anti-pAkt(S473) and pan-Akt. For silencing experiments, we used the same MIO-M1 clonesas described in Section 5.1.2.3. Overnight serum-starved cells were treated with 100 pM insulin for 5 min. Cell lysates were immunoblotted with anti-pAkt(S473) and pan-Akt as loading control. The results of three independent experiments were plotted on after normalizing pAkt(S473) band intensities to that of corresponding panAkt levels.

When SIK2 was overexpressed, the insulin-dependent increase in pAkt levels reached 2 fold of the basal levels. This represents 2 fold lower activation levels compared to mock transfection cases (Figure 5.21a, lanes 3 and 4). In complementary experiments where SIK2 expression was downregulated 60%, pAkt levels were upregulated 4 fold that of controls (Figure 5.21b).

These results are consistent with SIK2 being a negative modulator of insulin-dependent Akt activation in MIO-M1 cells.

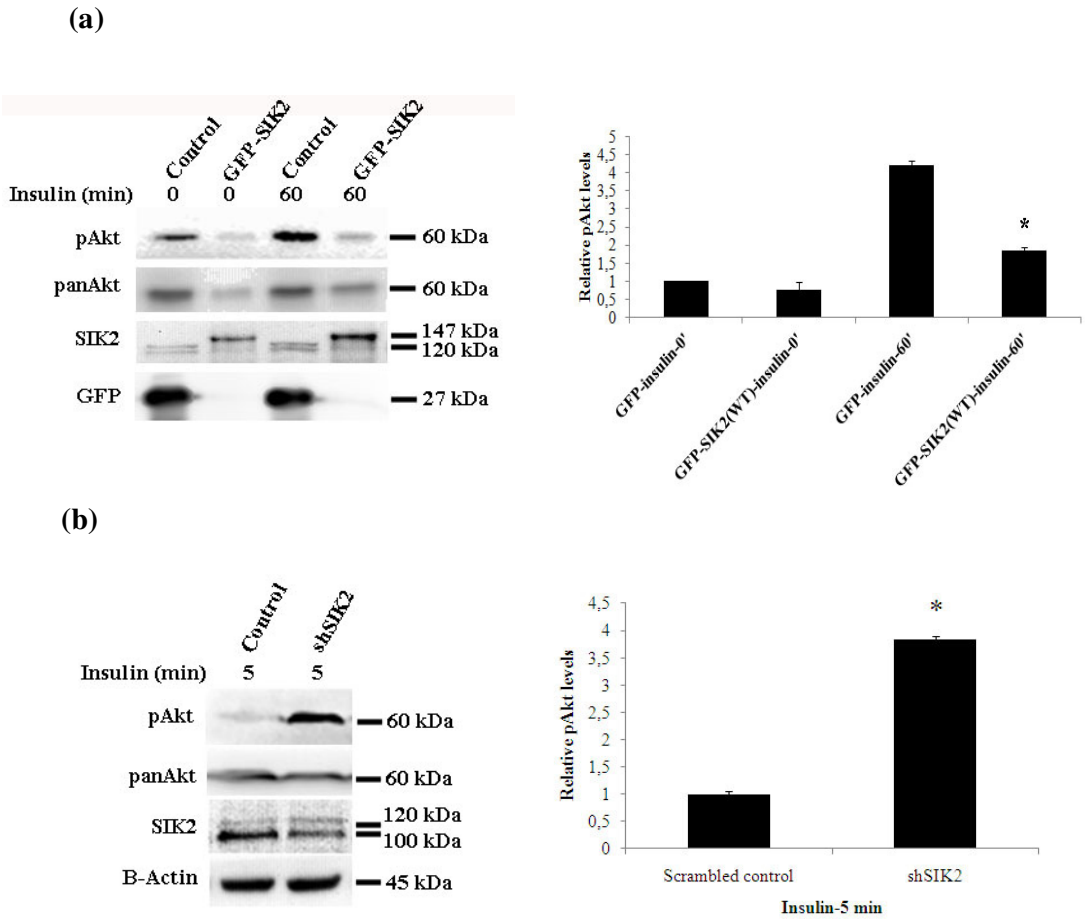

Figure 5.21. Effect of SIK2 overexpression and silencing on insulin-dependent Akt activation. MIO-M1 cells **(a)** GFP-SIK2 or mock transfected and **(b)** transduced with shSIK2 or scrambled shRNA treated with 100 pM insulin for the indicated times. Immunoblots were evaluated by anti-pAkt(S473), anti-pan-Akt, anti-β-actin, anti-GFP or anti-SIK2. Relative pAkt levels were plotted after pAkt(S473) band intensities were normalized to that of corresponding pan-Akt. $*P < 0.05$ compared to the untreated samples.

5.2.8. Effect of SIK2 Overexpression on Insulin-Dependent Müller Cell Survival

In order to see the modulatory effect of SIK2 on Müller cell survival upon insulin treatment, MIO-M1 cells transfected with GFP-SIK2 or GFP vector were treated with 10 nM insulin for 24 hours. Cell death was assesed by the TUNEL assay. Insulin-induced cell survival rates were calculated by dividing insulin-induced to uninduced apoptotic cell percentages. Three independent experiments were carried out.

Consistent with insulin-dependent Akt phosphorylation data obtained with untransfected cells, the TUNEL assay revealed that in mock-transfected cells insulin enhanced survival by 20 fold, (Figure 5.17 and Figure 5.22). But insulin-dependent

increase in survival in SIK2 overexpressing cells was limited to 5 fold that of untreated cells, 4 fold less than the controls.

Overall our data suggest that SIK2 is involved in a negative feedback mechanism of an insulin-induced Akt-mediated Müller glial survival pathway.

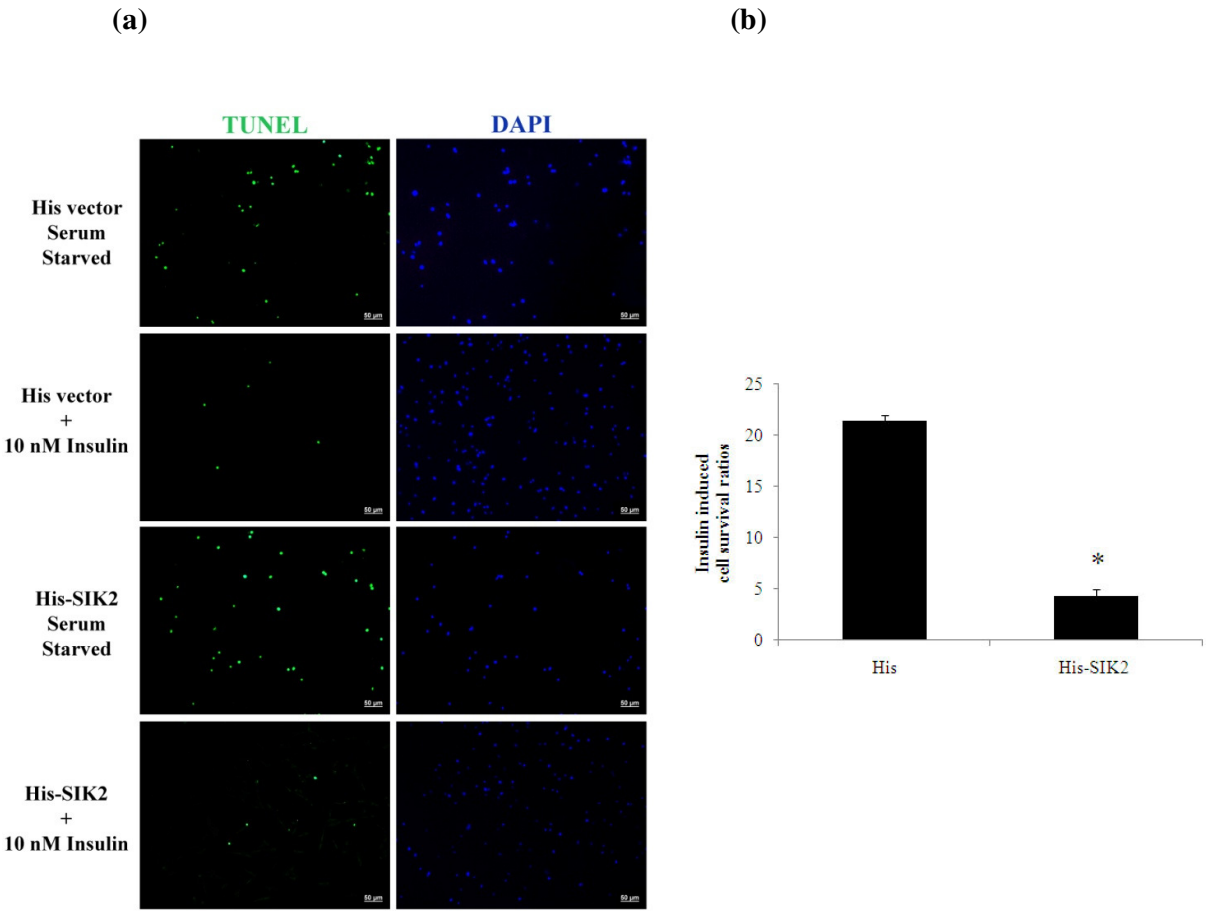

Figure 5.22. Effect of SIK2 overexpression on insulin dependent Müller cell survival. (a) MIO-M1 cells transfected with SIK2 or empty vector, after overnight serum starvation, were treated with 10 nM insulin for 24 hours. Apoptotic cells were assessed by TUNEL assay, nuclei were stained with DAPI. (b) The graphical represents ratio of apoptotic cell numbers of untreated samples to that of treated ones. *$P < 0.05$ compared to the mock transfected samples.

5.2.9. Effect of Chronic Hyperglycemia on Basal and Insulin-Induced Akt Activation and SIK2 Activity/ Expression levels in MIO-M1 Cells

The recent article published by Xi *et al*. (2005), showed that Akt was significantly inactivated, 52%, and thereby apoptosis level was increased 40% in primary rat Müller

cells cultured in elevated glucose compared to that cultured in normal glucose for 48 h. Consistent with this *in vitro* results, a significant decrease in Akt activity was observed in Müller cells in the retina of longterm diabetic animals (Xi *et al*., 2005). However, the underlying mechanism of hyperglycemia-induced Akt inactivation in Müller cells has not been identified yet. The negative effect of SIK2 on insulin-induced Akt activation and cell survival has been shown previously in Section 5.2.6 and 5.2.7. Based on these findings, we explored SIK2 involvement in hyperglycemia-induced Akt inactivation and apoptosis in MIO-M1 cells.

Before the analysis of SIK2 involvement in this apoptosis process, we investigated the effect of hyperglycemia on both basal and insulin-induced Akt activation in MIO-M1 cells. Briefly, cells were grown in 5.5 mM or 25 mM glucose medium with or without 100 pM insulin for 2 days and cell lysates were immunoblotted with anti-pAkt(S473), anti-pan-Akt antibodies. pAkt levels were normalized to that of corresponding Akt levels and the results of three independent experiments were plotted.

The basal Akt phosphorylation level was decreased 40% in cells grown under chronic hyperglycemic conditions in MIO-M1 cells (Figure 5.23, lane 1 and lane 2). Even in the presence of insulin, under chronic hyperglycermia Akt phosphorylation level remained at 40% of the controls (Figure 5.23, lane 3 and lane 4). These data suggest that chronic hyperglycemia attenuates both basal and insulin-induced Akt activation in MIO-M1 cells.

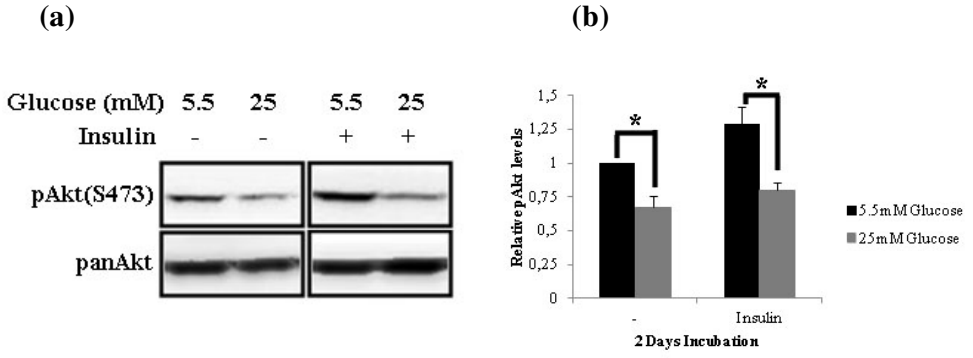

Figure 5.23. Akt phosphorylation levels of MIO-M1 cells grown under normal or hyperglycemic conditions. Cells under normoglycemic or hyperglycemic conditions were grown for 2 days in the absence or presence of insulin. (a) lysates were immunoblotted with anti-pAkt(S473), anti-pan-Akt antibodies. (b) Graphic representation of pAkt levels normalized to that of Akt. *$P < 0.05$ compared to the cells grown under 5.5 mM glucose conditions without and with insulin treatment, respectively.

In order to investigate whether SIK2 is involved in chronic hyperglycemia-induced Akt inactivation, its activity and expression changes upon hyperglycemia in MIO-M1 cells were investigated. After 2 days in culture, SIK2 was immunoprecipitated from the cell lysates with anti-SIK2 serum and its activity was tested in *in vitro* kinase assays using GST-IRS1 as the substrate. GST-IRS1 band intensities were normalized to that of the corresponding immunoprecipitated SIK2 levels analyzed by Western blotting. The results of three independent experiments were plotted (Figure 5.24b). In the matching samples, in order to investigate possible changes in SIK2 expression at the mRNA level, quantitative real-time PCR method was used. Coamplified β-actin was used as the internal control and the results of three independent cDNAs were plotted (Figure 5.25).

SIK2 activity was doubled in cells allowed to grow in high glucose conditions for 2 days when compared to that of normal glucose conditions (Figure 5.24). The presence of insulin did not change the profile.

mRNA level of SIK2 increased 40% in cells grown under hyperglycemia when compared to that of normoglycemia, even in the presense of insulin (Figure 5.25). After two-days insulin treatment under normal glucose conditions SIK2 level dropped 25% (Figure 5.25). This drop corresponds to the pAkt level increase seen in insulin-treated cells growing under normal conditions.

Overall these data suggest that chronic hyperglycemia-induced basal and insulin-induced Akt inactivation in MIO-M1 cells may be due to the higher activity and expression level of SIK2 in cells grown under hyperglycemic conditions.

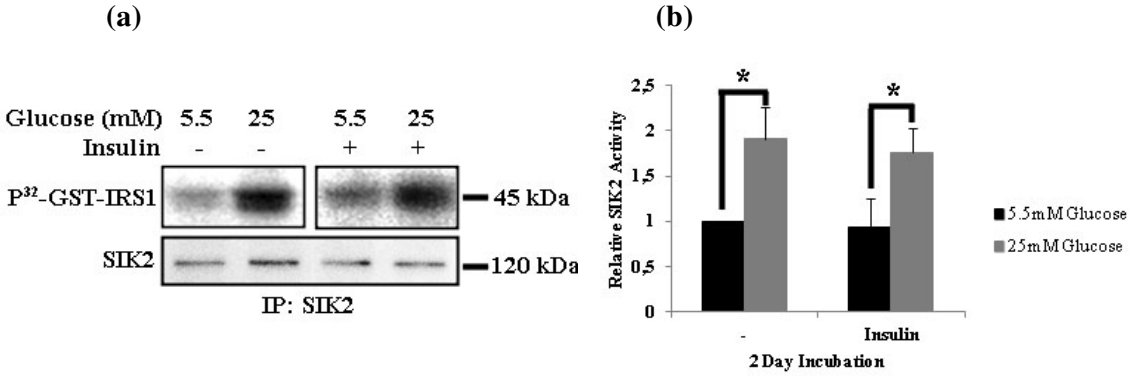

Figure 5.24. Effect of hyperglycemia on SIK2 activity in MIO-M1 cells. Cells were grown under normal or hyperglycemic conditions for 2 days in the absence or presence of 100 pM insulin. (a) SIK2 immunoprecipitated from the lysates was used in kinase assays. GST-IRS1 kinasing was visualized by autoradiography following PAGE. SIK2 levels in matching samples evaluated by Western blotting using anti-SIK2 antibody. (b) Relative SIK2 activity levels were plotted by normalizing GST-IRS1 band intensities to that of corresponding SIK2. *$P < 0.05$ compared to the cells grown under normoglycemia without and with insulin treatment, respectively.

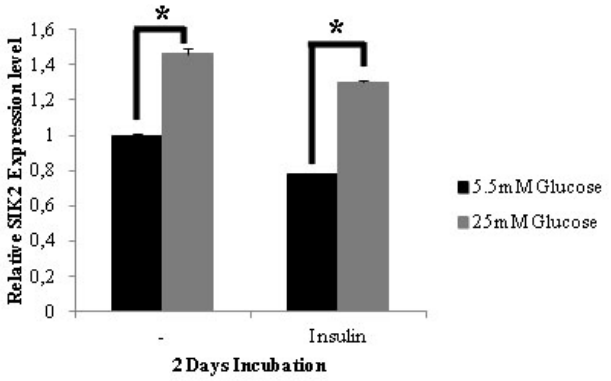

Figure 5.25. Effect of hyperglycemia on SIK2 expression in MIO-M1 cells. Cells were grown under normal or hyperglycemic conditions for 2 days in the absence or presence of 100 pM insulin. Relative SIK2 transcript levels were evaluated by qRT-PCR using primers specific to SIK2 and β-actin. *$P < 0.05$ compared to the cells grown under normoglycemia without and with insulin treatment, respectively.

5.2.10. Effect of SIK2 Overexpression and Knockdown on pAkt Levels in MIO-M1 Cells

To further investigate the potential role of SIK2 in hyperglycemia-induced Akt inactivation in Müller cells, MIO-M1 cells were transfected with GFP-SIK2 or GFP and were grown under 5.5 mM or 25 mM glucose conditions for 2 days and the cell lysates were immunoblotted using anti-pAkt(S473) and panAkt antibodies. The results of three independent experiments were plotted after normalizing pAkt(S473) band intensities to that of panAkt levels (Figure 5.26b).

As expected, in mock transfected cells 2 day-hyperglycemia diminished the pAkt level by 25%. On the other hand, SIK2 overexpression decreased Akt phosphorylation 45% in MIO-M1 cells grown under normal glucose conditions when compared to mock-transfected cells grown using the same glucose concentration (Figure 5.26). The transfection efficiency was nearly 35% in this experiment.

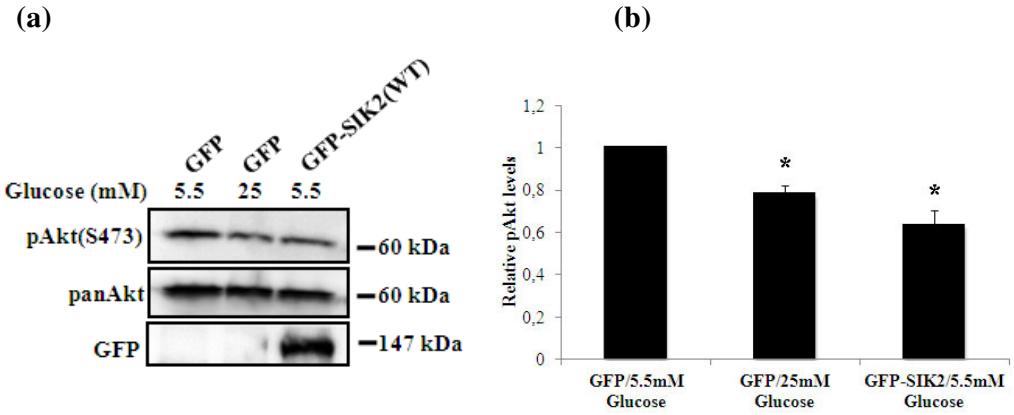

Figure 5.26. Effect of SIK2 overexpression on pAkt levels in MIO-M1 cells. (a) After transfection with GFP-SIK2 or GFP vector, cells were grown in 5.5 mM or 25 mM glucose for 3 days. pAkt levels were evaluated by anti-pAkt(S473) antibody. Anti-pan-Akt antibody was used as loading, anti-GFP for transfection control. (b) Relative Akt phosphorylation levels were plotted on the graph after pAkt(S473) band intensities were normalized to that of corresponding pan-Akt. *$P < 0.05$ compared to the cells grown in 5.5 mM glucose.

In SIK2 silenced cases stable MIO-M1 clone number 3 and the scrambled control clone number 5 were treated as described in Section 5.1.2.3 above.

A 35% decrease was observed in pAkt level upon hyperglycemia in MIO-M1 cells. Silencing of SIK2 in cells grown under hyperglycemia increased pAkt levels 2.7-fold. Even under normal glucose conditions SIK2 silencing increased Akt activation 3-fold (Figure 5.27).

In conclusion, these data suggest that SIK2 is likely to block both basal and insulin-induced Akt activation and therefore apoptosis under hyperglycemia in MIO-M1 cells by its enhanced activity and expression.

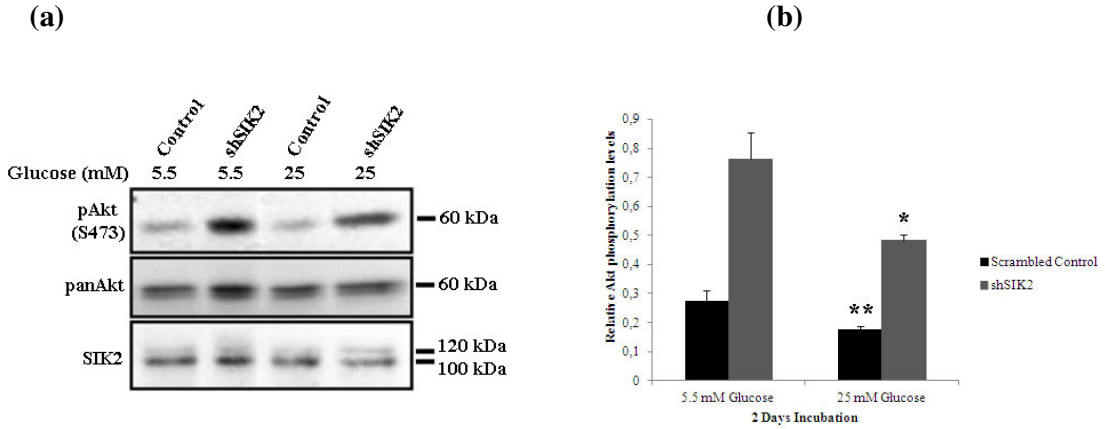

Figure 5.27. Effect of SIK2 knockdown on pAkt levels in MIO-M1 cells. Knockdown of SIK2 gene was done by infecting cells with lentiviral particles carrying shSIK2 or scrambled shRNA. The cells were either grown under 5.5 mM or 25 mM glucose conditions for 2 days. pAkt levels were evaluated by anti-pAkt(S473), anti-pan-Akt antibody used as loading, anti-SIK2 for knockdown control. (b) Relative Akt phosphorylation levels were plotted on the graph after pAkt(S473) band intensities were normalized to that of corresponding pan-Akt. *$P < 0.01$, **$P < 0.05$ compared to the cells grown in 5.5 mM glucose.

5.2.11. Effect of SIK2 Overexpression on MIO-M1 Cell Apoptosis

The potential role of SIK2 in hyperglycemia-induced Müller cell apoptosis was studied by TUNEL assay in His-SIK2 or mock transfected cells grown under 5.5 mM or 25 mM glucose conditions for 2 days. Quantitation of apoptosis was done by dividing TUNEL positive cell nuclei by DAPI positive total cell number and multiplying with 100. Three independent experiments were carried out (Figure 5.28).

As predicted from the previous Akt phosphorylation data, the apoptosis level was increased 2.5-fold, in cells grown under hyperglycemic conditions when compared to those grown under normal glucose concentrations. In MIO-M1 cells overexpressing SIK2, even under normal glucose conditions, the apoptosis level was increased 2.5-fold compared to the mock transfected cells grown under normal glucose conditions (Figure 5.29b).

Taken together the data support SIK2 involvement in negative regulation of Akt inactivation, and therefore apoptosis in hyperglycemia.

(a)

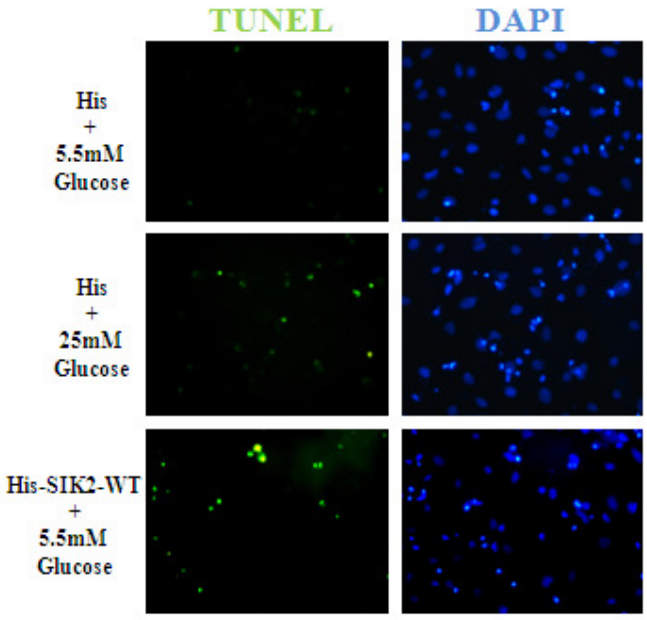

(b)

Figure 5.28. Effect of SIK2 overexpression on MIO-M1 cell apoptosis. MIO-M1 cells overexpressing SIK2 were grown under hyperglycemic conditions for 2 days. Mock transfected cells grown under normal glucose conditions constituted the control. (a) Apoptotic cells were assessed by TUNEL assay, nuclei were stained with DAPI. (b) The graph represents apoptotic cell numbers in percent of total cell numbers. *$P < 0.05$ compared to the cells His transfected and grown in 5.5 mM glucose.

5.2.12. IRS1 Protein Degradation and Tyrosine Phosphorylation upon Chronic Hyperglycemia in MIO-M1 Cells

IRS1 is a scaffold protein that conveys the signal from insulin down to glucose uptake via Akt phosphorylation/activation. As in insulin-resistant rats S789

phosphorylation of IRS1 is found to be elevated and SIK2 expression and activity were induced markedly in the white adipose tissue of diabetic mice (Horike *et al*., 2003), and it was suggested that SIK2 might be involved in development of type 2 diabetes (Horike *et al*., 2003). Generally, serine/threonine phosphorylation of IRS1 protein causes insulin-mediated signal attenuation by increasing degradation of IRS1 and/or blocking its tyrosine phosphorylation required for proper insulin/Akt signal transduction (Boura-Halfon and Zick, 2009).

In this section of the study, we examined whether pTyr and IRS1 protein levels change in cells exposed to elevated glucose levels compared to the controls. Subsequent to growing MIO-M1 cells under normal or hyperglycemic conditions for 2 days, IRS1 protein levels were assessed by immunoblotting with anti-IRS1 antibody. To evaluate tyrosine phosphorylation under the same conditions, immunoprecipitated IRS1 with anti-IRS1 were immunoblotted using anti-pTyr antibody. Relative IRS1 and pTyr-IRS1 levels were quantified by measuring their band intensities and normalized to pan-Actin and immunoprecipitated IRS1 proteins, respectively.

The results indicated a 50% decrease in IRS1 protein level (Figure 5.29) in cells under hyperglycemia. A 38% decrease in pTyr-IRS1 level was observed under chronic hyperglycemic conditions when compared to that of grown under normal glucose conditions (Figure 5.30).

Based on these data we can suggest that the observed Akt inactivation under chronic hyperglycemia may be due to decreased IRS1 protein stability and tyrosine phosphorylation.

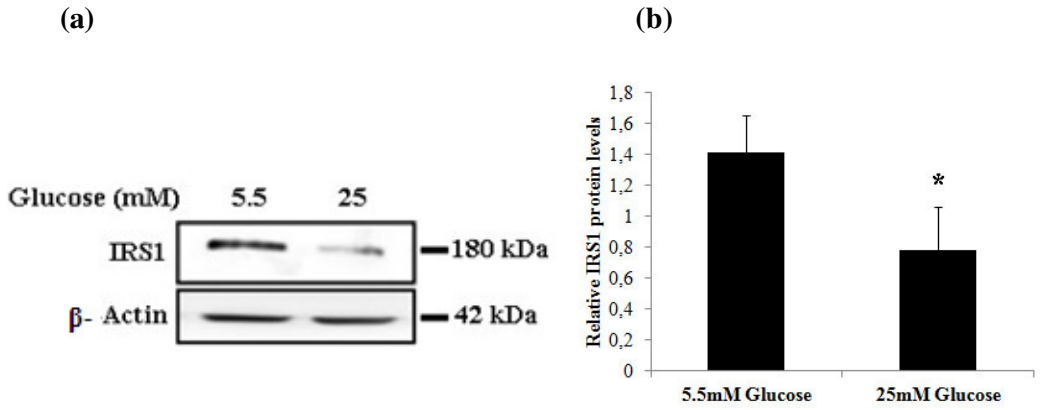

Figure 5.29. Change in IRS1 levels under chronic hyperglycemia. MIO-M1 cells were grown under 5.5 or 25 mM glucose for 2 days. (a) Relative IRS1 protein levels in the lysates were assessed by Western blot analysis using anti-IRS1 antibody, β-Actin was used as the loading control and (b) IRS1 band intensities were normalized to that of corresponding β-Actin bands. *P < 0.05 compared to normoglycemia samples.

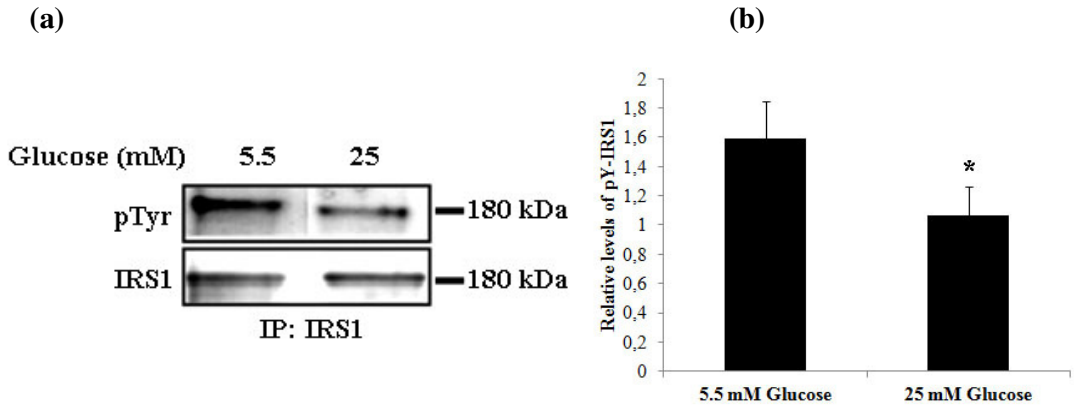

Figure 5.30. Change in pTyr -IRS1 levels under chronic hyperglycemia. MIO-M1 cells were grown under 5.5 or 25 mM glucose conditions for 2 days. (a) Tyrosine phosphorylation was assesed by Western blotting of immunoprecipitated IRS1 using anti-pTyr antibody, anti-IRS1 antibody was used as loading control. (d) Relative pTyr-IRS1 levels were plotted by normalizing pTyr band intensities to that of corresponding IRS1 bands. *P < 0.01 compared to 5.5 mM glucose conditioned samples.

5.2.13. SIK2 Phosphorylation and Activity Levels in Type 1 Diabetic Rats

In order to test whether SIK2 activity is modulated by hyperglycemia in the retina *in vivo* as observed in MIO-M1 cells *in vitro* in Section 5.2.8, we generated diabetic rats as our *in vivo* diabetic model system and investigated SIK2 activity and phosphorylation levels in their retinae.

The most common animal model of human diabetes is streptozotocin (STZ)-induced diabetes in the rat. Diabetes can be induced by selective destruction of the insulin-

producing β-cells of the pancreas with a single dose injection of STZ, a glucose moiety with a very reactive nitrosourea group from the mould *Streptomyces griseus* (Wei *et al*, 2003).

To test SIK2 activity change in retina under hyperglycemic conditions *in vivo*, male albino Wistar rats were injected with STZ in 10 mM citrate buffer (diabetic group), or 10 mM citrate buffer alone (control group) intravenously. Their fasted blood glucose levels ranged from 65 to 80 mg/dl at the beginning of the experiment. At the next day of injection fasting blood glucose levels of rats that were higher than 200 were accounted as diabetic. The diabetic and control rats were sacrificed after 2 weeks and their retinae were taken. Serine and threonine phosphorylation levels of SIK2 were analyzed by immonoblotting with anti-pThr and anti-pSer antibodies and SIK2 activities were tested with *in vitro* kinase assay using GST-IRS1 peptide as substrate after immunoprecipitating SIK2 proteins from diabetic and control retinae.

Rats in the diabetic group showed weight loss (188 g) compared to the control group (210 g) on average and diabetic fasted blood glucose levels were 246 mg/dl on average, whereas those of the control group was 86 mg/dl after 2 weeks of STZ or vehicle injection, respectively (Table 5.1).

As observed in Müller cells grown under hyperglycemic conditions *in vitro,* SIK2 activity was increased in diabetic rat retina, whereas its serine phosphorylation level was diminished and its threonine phosphorylation level was conserved (Figure 5.31b).

Table 5.1. Average weights and fasted blood glucose levels of male albino Wistar rats before and after STZ or vehicle injection.

Average Weight before STZ injection (n=8)	Average Weight after 2 weeks of STZ injection (n=8)	Average Weight before vehicle injection (n=6)	Average Weight after 2 weeks of vehicle injection (n=6)	Average Fasted Blood Glucose before STZ injection (n=8)	Average Fasted Blood Glucose after 2 weeks of STZ injection (n=8)	Average Fasted Blood Glucose before vehicle injection (n=6)	Average Fasted Blood Glucose after 2 weeks of vehicle injection (n=6)
216	188	202	210	77	246	68	86

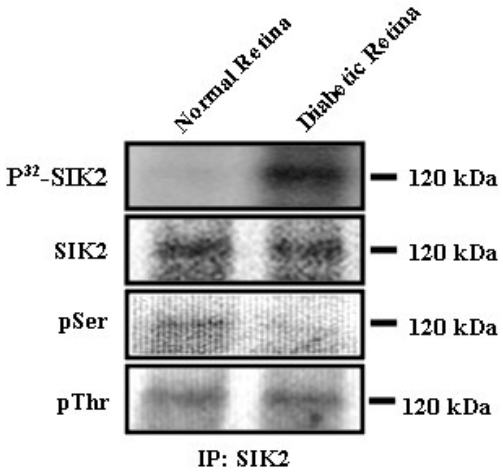

Figure 5.31. SIK2 phosphorylation and activity change in STZ injected rats. Male albino Wistar rats were injected with streptozotocin (diabetic group), or vehicle alone (control group) intravenously. The rats were sacrified after 2 weeks. SIK2 immunoprecipitated from the retina lysates were used in kinase assays in the presence of radiolabelled ATP. Reaction products were fractionated on PAGE visualized by autoradiography. SIK2 levels in matching samples were evaluated by Western blot analysis using anti-SIK2 antibody as a control. Serine and threonine phosphorylations of SIK2 was assesed by Western blot analysis using anti-phosphoserine and anti-phosphothreonine antibodies.

In conclusion, SIK2 activity is upregulated upon hyperglycemia in the retina and in MIO-M1 cells that may be responsible for hyperglycemia-induced Akt inactivation and apoptosis seen in Müller cells *in vivo* and *in vitro*.

6. DISCUSSION

Müller cells are the main glia of the retina that maintains retinal homeostasis by supporting proper neuronal and vascular functioning (Bringmann *et al*., 2006, 2009). Due to this close anatomical and functional relationship, Müller cells are implicated in nearly all retinal pathologies. Often these cells undergo an abnormal proliferation called gliosis in many forms of retinal injury and in numerous diseases (Bringmann and Reichenbach, 2001; Bringmann *et al*., 2006). The molecular mechanisms underlying this gliotic response are still not well understood. FGF2 has been suggested as one of the signaling molecules that may be important in the development of Müller gliosis (Geller *et al*., 2001). In diabetic retinopathy however, glial cell degenerations are evident early on in the course of diabetes (Barber *et al*., 1998). It is widely accepted that insulin acts as survival factor in the retina, (Barber *et al*., 2001), though its role in Müller cell survival is not known. In addition, these two factors together stimulate the proliferation and dedifferentiation of Müller cells into progenitor cells in the absence of retinal damage (Fischer *et al*., 2002). Thus, both the FGF and insulin signaling are critical for the maintenance of proper Müller cell function during the normal and diseased states, and possibly in retinal regeneration.

The aim of this work is to identify the potential role of SIK2 in the FGF2 signal transduction pathway and if it is involved in the modulation of insulin-dependent Müller cell survival and in chronic hyperglycemia-induced Akt inactivation and apoptosis in MIO-M1 cells. FGF2 was chosen because SIK2 was obtained in a yeast two-hybrid screen of a retinal cDNA library using the cytoplasmic domain of FGFR2 as bait in our laboratory (Özcan, 2003). We focused on insulin since SIK2 has been implicated in the downregulation of insulin signaling (Horike *et al*., 2003) and little is known about the downstream of insulin signaling in Müller cells.

Possible involvement of SIK2 in the FGF signal transduction pathway was initially explored by studying temporal changes in the SIK2 phosphorylation and activation status upon FGF2 treatment of MIO-M1 cells. Subsequently, FGF2-dependent ERK and Akt activation profiles were defined and possible modulations in these profiles by SIK2 was investigated through SIK2 overexpression and knockdown studies. Effect of SIK2

silencing on FGF2 induced Müller cell proliferation was also included in these studies. In the final part, Gab1/SIK2 interaction was verified by coimmunoprecipitation study. Gab1 binding partner associations upon FGF2 were tested and effect of SIK2 silencing on these associations was also included.

In the initial experiments we have shown that SIK2 phosphorylation and thereby activity were modulated by FGF2 in MIO-M1 cells. Based on the Thr/Ser phosphorylation and activity profiles of SIK2 upon FGF2 treatment, we hypothesized that hyper-threonine and hypo-serine phosphorylation may lead to enhanced SIK2 activation. Recent findings from our laboratory in the framework of FGF2 signaling suggesting ERK as an upstream activatory threonine kinase of SIK2 (Ejder, 2011), lends support to this hypothesis. Studies to reveal the exact ERK phosphorylation sites on SIK2 are under investigation. We also have evidence implicating the serine kinases, Akt and PKA, in downregulation of SIK2 activity in FGF2 induced MIO-M1 cells (Ejder, 2011). Other than ERK, PKA and Akt, there might be other kinases involved. One strong candidate is the well established SIK2 upstream activatory kinase LKB1 (Lizcano *et al*., 2004). As its activity is modulated by FGF2 (Esteve-Puig et al., 2009) and it is expressed in MIO-M1 cells (data not shown), LKB1 is highly likely to contribute to the FGF dependent SIK2 activation observed in this study. LKB1 and PKA are well known regulators of energy metabolism (Katoh *et al*., 2006), thus suggesting that SIK2 may be implicated in the crosstalk position between FGF and energy metabolism. SIK2 has been shown to be involved in insulin signaling in earlier reports (Horike *et al*., 2003). Here in this study we have shown for the first time its involvement in another RTK, FGFR, signaling pathway.

The intensity and duration of ERK signaling proposed to be important in shaping cellular response to growth factors (Kaplan *et al*., 1998). Differential negative feedback inhibition of the ERK cascade is the most important determining factor for ERK signal duration (Brightman and Fell, 2000). In agreement with the Hollborn *et al*. (2004) and Çınaroğlu (2005) data indicating that ERK and Akt activations are required for MIO-M1 cell proliferation, here in this study we showed transient ERK activation profile upon FGF2 treatment in MIO-M1 cells results in cell proliferation. When we compare FGF dependent ERK and SIK2 activation profiles, they appear very similar, peaking at 10 min. and turning to basal rapidly. However, temporal decrease in SIK2 activity is paralleled by

increase in Akt activation. Later in this study, we have identified the negative regulatory effect of SIK2 on FGF2-induced ERK and Akt signaling by SIK2 overexpression and knockdown studies. Both ERK and Akt activity levels were reduced significantly by SIK2 overexpression and on the contrary, the intensity and the duration of active ERK and Akt levels increased by SIK2 knockdown indicating a negative feedback exerted by SIK2 on FGF2-induced Ras/ERK and PI3K/Akt pathways. As predicted from our observed ERK and Akt activation data, SIK2 silencing dramatically increased FGF2-dependent Müller cell proliferation rate. Based on findings, we suggest that SIK2 is part of the negative-feedback mechanism in FGF2-induced ERK and Akt signaling pathways, and directly reflected on Müller cell proliferation.

It has been suggested that Gab1 contributes to PI3K/Akt activation through Gab1/p85 binding and Ras/ERK pathway activation through Gab1/Shp2 upon FGF2 stimulation (Ong *et al*., 1997; Ong *et al*., 2001; Krejci *et al*., 2007; and Lamothe *et al*., 2004). Later, studies have proposed that Shp2 mediates a basal level of Ras/MAPK signaling in Müller glial cells during postnatal development and in the adult retina (Cai *et al*., 2011). Gab1 has been identified recently as the potential substrate of SIK2 *in vitro* (Küser, 2006). In order to test whether SIK2 exerts its negative effect on FGF2-induced ERK and Akt signaling pathways via Gab1, first of all, Gab1 phosphorylation by SIK2 was verified *in vitro* and FGF2-dependent Gab1/SIK2 interaction was demonstrated by coimmunoprecipitation study. Further analysis in our laboratory supported our data and identified that SIK2 phosphorylated Gab1 on serine 266 residue (Yılmaz-Sert, 2011).

Due to lack of information on the involvement of Gab1 in the regulation of FGF induced ERK and Akt activations in Müller cells, first FGF2-induced tyrosine and serine phosphorylation profiles of Gab1 were investigated. Then, Grb2/Gab1 and p85/Gab1 associations were studied in MIO-M1 cells. pTyr and pSer kinetics of Gab1 protein are similar, peaking at 10 min. and returning to basal afterwards. When the p85/Gab1 association and Akt activation profiles upon FGF2 exposure are compared, they bear resemblance where their levels were halved at 10 min and peaked at 60 min-FGF2 treatment, suggesting that Gab1 can contribute to FGF/Akt signaling through p85 association. Gab1/Grb2 association kinetics, on the other hand, resembled to ERK activation profile, peaking at 10 min-FGF2 and returning to basal levels, suggesting that

Gab1 may enhance FGF/ERK pathway transduction via Grb2 binding. Due to the anti-Shp2 antibody problems we could not test Shp2/Gab1 association kinetics in our cells upon FGF2 treatment. Thus, based on the data provided by this study demonstrate Gab1 involvement in FGF signaling of MIO-M1 cells. FRS2 may also contribute to FGF-induced ERK and Akt activations in these cells, however, we have not tested its involvement in this study.

Finally, through SIK2 silencing experiments, pSer and pTyr levels of Gab1 and its binding partner associations (p85, Grb2 and Shp2) at 10 min. FGF2 treatment were investigated. In aggrement with our data, suggesting SIK2 being a Gab1 kinase, pSer of Gab1 was diminished significantly by SIK2 silencing. At the same time frame, pTyr levels and binding partner associations (p85/Gab1, Shp2/Gab1, Grb2/Gab1) were increased. These data are consistent with Gual *et al.* (2001) in that Gab1 hyperphosphorylation on serine/threonine residues attenuates tyrosine phosphorylation which in turn prevents interaction with partners, possibly due to conformational change that renders kinase domain of growth factor receptors inaccessible. In support of our SIK2 silencing data, complementary studies conducted in our laboratory indicate that Gab1-S266A mutants have enhanced Gab1/Shp2 and Gab1/Grb2 interaction in MIO-M1 cells upon FGF2 stimulation (Yılmaz-Sert, 2011). These findings taken together suggest that SIK2 downregulates Ras/ERK pathway via pertubing Shp2/Gab1 and Grb2/Gab1 association in our cells. On the other hand, SIK2 by interfering with Gab1/p85 association attenuates PI3K/Akt signaling.

To date, only ERK and PKC have been identified as Gab1 negative regulators in RTK signaling (Gual *et al*., 2001, Lehr *et al*., 2004). These enzymes phosphorylate serine residues on Gab1 that attenuates signal transduction downstream of EGF and HGF (Gual *et al*., 2001; Lehr *et al*., 2004). Here we identified SIK2 protein as a novel Gab1 negative regulator in FGF signal transduction. We also confirmed that the serine phosphorylation of Gab1 by SIK2 protein may downregulate FGF signaling. It is conceivable that SIK2 can also act downstream of other RTK pathways in order to modulate the ERK signal duration and Akt signal intensity through Gab1, because Gab1 is directly involved in numerous RTK signaling pathways (Liu and Rohrschneider, 2002; Kiyatkin *et al*., 2006; Ong *et al*., 2001; Krejci *et al*., 2007).

In this study, we have shown that SIK2 silencing in MIO-M1 cells increased Gab1/Shp2, Gab1/Grb2 and Gab1/p85 associations, thereby ERK and Akt activity levels and to some extent the duration of ERK signal (up to 60 minutes of FGF2) and proliferation rate of MIO-M1 cells. Thus, we suggest that SIK2 may act as a tumor-suppressor. It should be further studied whether the duration of ERK signaling is modulated with SIK2 silencing in longer term (up to 48 hours) and the cell invasion/ motiliy assays should be done to determine the role of SIK2 in tumorogenicity of MIO-M1 cells. SIK2 expression levels should also be examined in different cancer types with deregulated RTK signaling. Gab1 overexpression is also implicated in breast cancer (Sachs *et al*., 2000). A recent study found that in individuals with Noonan syndrome associated with juvenile myelomonocytic leukemia, activated Shp2 mutants had prolonged binding to Gab1 (Wang *et al*., 2009). Gab1 and its inhibitory kinases have potential as therapeutic targets for tumors with deregulated RTK signaling.

MIO-M1 cells differentiate into retinal neurons when exposed to FGF2 for 7 days (Lawrence *et al*., 2007). The prerequisite of transdifferentiation is cell proliferation. After proliferation ceases, cells start to differentiate. One month of cultured SIK2 silenced MIO-M1 clones showed some neurite extensions after their high rate of proliferations (data not shown), while, Müller glia marker expression levels, vimentin and glutamine synthase were dropped (data not shown). Put together, these data suggest that SIK2 protein may be involved in Müller cell transdifferentiation process under diseased states or long-term FGF2 stimulation. Whether SIK2 activity or protein levels are modulated when MIO-M1 cells are exposed to FGF2 for 7 days has not been addressed yet.

In summary, in this study we are proposing a new negative feedback mechanism contributing to fine-tuning of ERK signal duration and intensity in MIO-M1 cells upon FGF2 treatment leading to Müller cell proliferation. Our working model proposes (Figure 6.1), upon FGF2 stimulation ERK is activated within 5 minutes, and targets SIK2 on threonine residues leading to its activation. Fully active SIK2, at 10 min., in turn, phosphorylates Gab1, most probably on serine 266 residue. Resulting hyperserine phosphorylated and hypotyrosine phosphorylated Gab1 has reduced association with Grb2

and Shp2. This may result in the downregulation of ERK signaling after 10 minutes of FGF2 induction in MIO-M1 cells.

SIK2 activity appeared higher than its basal level all the time points until 30 min. of FGF2 stimulation, however, Akt activity levels were below their basal level during this interval. When the SIK2 activity was returned almost to the basal level at 60 min. of FGF2 treatment, robust and sudden Akt activation was evident. We observed a 50 min. of Akt activation delay in MIO-M1 cells when compared to that of ERK. Based on SIK2 overexpression and silencing data we can propose that SIK2 may be responsible for this delay via restraining Akt activation by modulating Gab1/p85 association within the first 30 min of FGF2 stimulation (Figure 6.1). Retinal explant culture experiments are under investigation to test our working model and verify SIK2 effect on Müller cell proliferation *in vivo*.

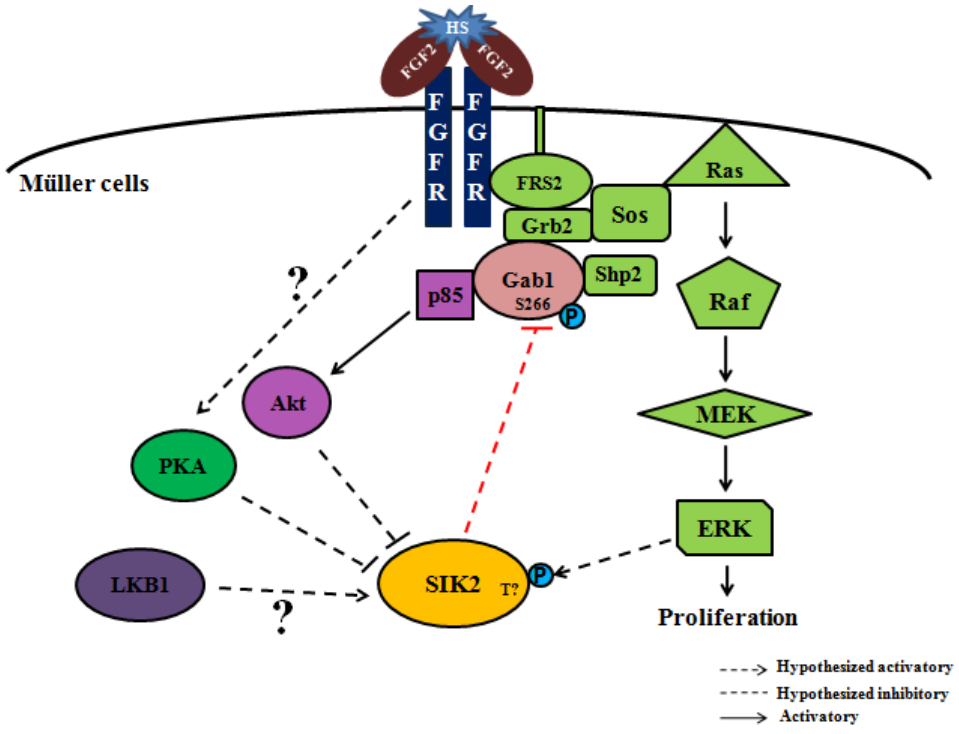

Figure 6.1. Our proposed model for the negative-feedback regulation of FGF signaling pathway by SIK2.

In the second part of the study we investigated whether SIK2 is engaged in the modulation of insulin-dependent Müller cell survival via IRS1/Akt axis and in chronic hyperglycemia-induced Akt inactivation and apoptosis in MIO-M1 cells.

As the information on insulin pathway and the resulting response in the context of Müller cells is scarce, the initial experiments directed to establish whether IRS1 and Akt are associated in this process and if the end result is a survival response. The results showed that insulin treatment leads to enhanced tyrosine phosphorylation of IRS1 rapidly, with subsequent Akt activation resulting in increased Müller cell survival. We detected no insulin dependent ERK activation or increase in proliferation. Our data is consistent with the previous report indicating that whole retina responds to insulin *in vitro* with significant elevation in Akt phosphorylation, while the Ras/ERK pathway is relatively insensitive to insulin stimulation (Diaz *et al*., 2000). Thus, we concluded that insulin evokes survival response in Müller cells via IRS1/Akt activation. Although IRS2 is also expressed in Müller cells (data not shown), we did not investigate its involvement.

SIK2 has been implicated in downregulation insulin signaling via phosphorylating IRS1 on Ser789 in adipocytes (Horike *et al*., 2003). In this study we show that insulin treatment results in a rapid and transient activation of SIK2 in MIO-M1 cells. SIK2/IRS1 interaction was demonstrated by coimmunoprecipitation assay, for the first time to our knowledge. Their enhanced interaction by insulin treatment supports IRS1 being an *in vivo* SIK2 substrate in Müller cells. We attempted to test whether SIK2 target on IRS1 is Ser789, unfortunately the available antibody did not react with human p789-IRS1. An alternative approach would involve comparative analysis of kinasing profile of S789A mutant of IRS1.

When temporal modulations in SIK2 and Akt activation in Müller glial cells compared, we can argue that SIK2 acts upstream of Akt in insulin signaling. This would be in line with the report that in ovarian cancer cells SIK2 activation is required for Akt phosphorylation (Ahmed *et al*., 2010). However, in the frame of insulin response of liver, HEK293T and brown adipocytes Akt2 was proposed as the upstream activatory kinase of SIK2 (Muraoka *et al*., 2009, Dentin *et al*., 2007). In such core insulin responsive tissues insulin acts as a regulator of energy metabolism, thus the discrepancy may be due to the differences in the nature of the cellular responses, and may be reflecting the differences of Akt isoforms involved, as in our system Akt3 not Akt2 is activated in insulin dependent manner.

The possible modulatory role of SIK2 on transduction of insulin signaling in Müller cells was analyzed by SIK2 knockdown and overexpression studies. SIK2 knockdown leads to earlier Akt activation, within 5 min. as oppose to 60 min of induction observed in untransfected cells. In line with these results in cells overexpressing SIK2, pAkt levels remain close to the basal levels even at 60 min. and TUNEL analysis revealed that insulin-induced Müller cell survival was significantly reduced. Based on these observations, we suggest that SIK2 is a negative modulator of insulin-induced IRS1/Akt mediated Müller glial survival pathway. Knockdown studies implicated SIK2 in TORC1/CREB dependent survival of cortical neurons (Sasaki *et al*., 2011). It should be interesting to investigate the contribution of SIK2/TORC1/CREB-mediated pathway to Müller glia survival in addition to SIK2/IRS1/Akt axis upon insulin stimulation revealed in this study.

Diabetes has been reported to accelerate Müller glia apoptosis *in vivo* (Hammes *et al*., 1995) and hyperglycemia induced apoptosis in cultured Müller glia via inactivation of Akt has been reported (Xi *et al*., 2005). We also find that chronic hyperglycemia attenuates both basal and insulin-induced Akt activation in MIO-M1 cells. It is possible that this attenuation stems from the observed higher activity and expression level of SIK2 in cells grown hyperglycemic conditions. Restored pAkt level by SIK2 gene silencing under hyperglycemia support this possibility. In line with this result under normoglycemia cells overexpressing SIK2, Akt phosphorylation was decreased and apoptosis increased almost to the same level observed in cells grown under hyperglycemic conditions.

Recent studies have shown that IRS1 becomes serine phosphorylated after prolonged exposure to glucose and consequently IRS1 fails to become tyrosyl-phosphorylated that results in attenuation of insuling signaling or in degradation of IRS1, leading to the so-called insulin resistance (Ricort *et al*, 1995; Hotamisligil *et al*., 1996; Tanti *et al*., 1991; Haystead *et al*., 1990; Khan *et al*., 1989; Kroder *et al*., 1996; Kanety *et al*., 1995; Feinstein *et al*., 1993; Li *et al*., 1999). We observed tyrosine hypophosphorylation of IRS1 and its protein level decrease in cells under hyperglycemia. This observation taken together with the rest of the data addressed above, it is conceivable that enhanced SIK2 activity/level may result in enhanced IRS1 serine phosphorylation, thus hampers Akt activation. This may be the underlying mechanism of hyperglycemia-induced insulin resistance and

resulting in Müller apoptosis. Other than IRS1, Gab1 is also involved in insulin mediated PI3K/Akt signaling and survival in several cell types (Rocchi *et al*., 1998). As our results in the first part of the study revealed Gab1 as an SIK2 substrate, its involvement cannot be excluded in this process.

Hyperglycemia dependent changes in SIK2 activity observed in culture prompted us to look into diabetic rats. In the type 1 diabetic rats where hyperglycemia was evident, retinal SIK2 activity was upregulated, whereas its serine phosphorylation level was diminished and threonine phosphorylation level was conserved. We have shown that pSer levels of SIK2 is inversely proportional to its activity upon FGF2 and insulin stimulus as well as under hyperglycemia. Thus, this upregulation of SIK2 activity *in vivo* in diabetic rats may stem from the decline in inhibitory serine phosphorylation. Hyperglycemia in general, induces the O-N-acetylglucosamine (O-GlcNAc) addition to serines or threonines on proteins, which hinders phosphorylations of these sites by serine/threonine kinases (Yoshida-Moriguchi *et al*., 2010). It is possible that downregulation of SIK2 pSer levels is due this O-linked glycosylation process. More detailed investigation should be performed in order to verify the involvement of SIK2 in diabetic retinopathy in the Müller cell context.

It has been suggested that both hyperglycemia and hypoinsulinemia in diabetes contribute to retinal neuronal cell death by Akt inactivation. In this study, we provided evidence that hyperglycemia contribution to Müller cell death by Akt inactivation and excessive glucose disrupts the insulin action via SIK2 overactivation/overexpression in Müller cells. Therefore, we suggest that SIK2 may contribute directly to diabetic retinopathy (Figure 6.2). Similar mechanism may function in retinal neurons, excessive glucose may perturb the insulin action promoting cell survival by Akt or alter glycosylation of proteins that maintain neuronal survival (Nakamura *et al*., 2001).

In conclusion, in this study we have identified two distinct roles of SIK2 in insulin and FGF signaling. In insulin signaling, SIK2 negatively regulates insulin action to promote cell survival by Akt in Müller cells grown under both normal conditions and chronic hyperglycemia. It is also involved in FGF signaling, as a negative feedback regulator of FGF2-induced ERK and Akt signaling to promote Müller cell proliferation.

One would expect SIK2 activity should be tightly controlled in Müller cells for the maintenance of the healthy retina, because of the intimate interaction of Müller glia with neurons and endothelial cells. In addition to diabetic retinopathy, inappropriate SIK2 activation in Müller cells may contribute to various other retinal pathologies, such as Müller cell sheen dystrophy, retinoschisis, macular hole formation, and retinitis pigmentosa.

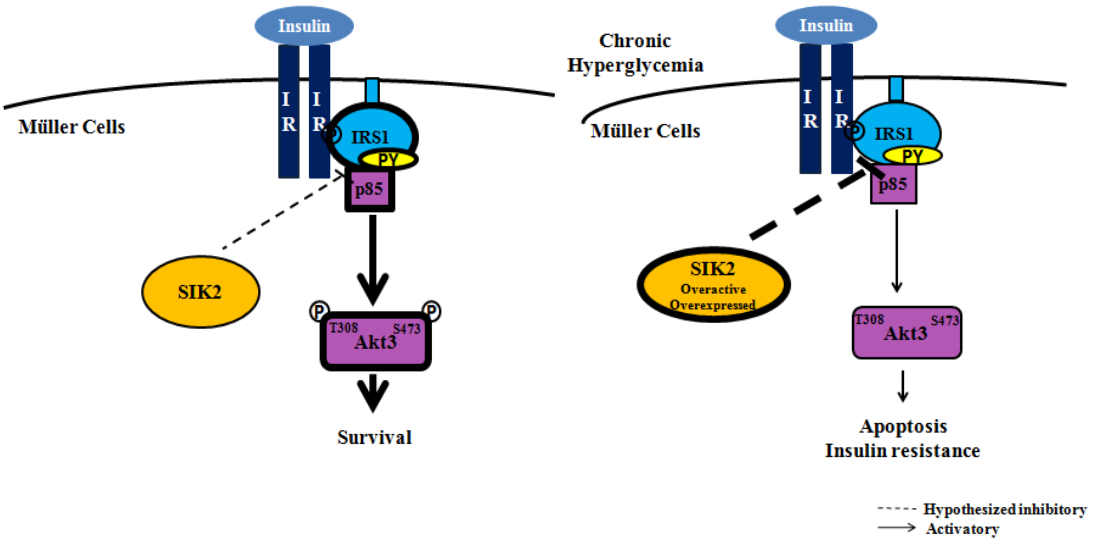

Figure 6.2. Proposed model for the negative regulation of Müller cell insulin signaling under normal and chronic hyperglycemic conditions.

REFERENCES

Abu El-Asrar, A. M., S. Desmet, A. Meersschaert, L. Dralands, L. Missotten, and K. Geboes, 2001, "Expression of the Inducible Isoform of Nitric Oxide Synthase in the Retinas of Human Subjects with Diabetes Mellitus", *American Journal of Ophthalmology,* Vol. 132, No. 4, pp. 551-556.

Ahmed, A. A., Z. Lu, N. B. Jennings, D. Etemadmoghadam, L. Capalbo, R. O. Jacamo, N. Barbosa-Morais, X. F. Le, P. Vivas-Mejia, G. Lopez-Berestein, G. Grandjean, G. Bartholomeusz, W. Liao, M. Andreeff, D. Bowtell, D. M. Glover, A. K. Sood, and R. C. Bast, Jr., 2010, "SIK2 is a Centrosome Kinase Required for Bipolar Mitotic Spindle Formation that Provides a Potential Target for Therapy in Ovarian Cancer", *Cancer Cell,* Vol. 18, No. 2, pp. 109-121.

Akiyama, H., T. Nakazawa, M. Shimura, H. Tomita, and M. Tamai, 2002, "Presence of Mitogen-Activated Protein Kinase in Retinal Müller Cells and its Neuroprotective Effect Ischemia-Reperfusion Injury", *Neuroreport,* Vol. 13, No. 16, pp. 2103-2107.

Allen, M., L. Svensson, M. Roach, J. Hambor, J. McNeish, and C. A. Gabel, 2000, "Deficiency of the Stress Kinase P38alpha Results in Embryonic Lethality: Characterization of the Kinase Dependence of Stress Responses of Enzyme-Deficient Embryonic Stem Cells", *Journal of Experimental Medicine,* Vol. 191, No. 5, pp. 859-870.

Amin, R. H., R. N. Frank, A. Kennedy, D. Eliott, J. E. Puklin, and G. W. Abrams, 1997, "Vascular Endothelial Growth Factor is Present in Glial Cells of the Retina and Optic Nerve of Human Subjects with Nonproliferative Diabetic Retinopathy", *Investigative Ophthalmology and Visual Science,* Vol. 38, No. 1, pp. 36-47.

Anderson, D. H., C. J. Guerin, P. A. Erickson, W. H. Stern, and S. K. Fisher, 1986, "Morphological Recovery in the Reattached Retina", *Investigative Ophthalmology and Visual Science,* Vol. 27, No. 2, pp. 168-183.

Anderson, L. J., C. Tsou, R. A. Parker, T. L. Chorba, H. Wulff, P. Tattersall, and P. P. Mortimer, 1986, "Detection of Antibodies and Antigens of Human Parvovirus B19 by Enzyme-Linked Immunosorbent Assay", *Journal of Clinical Microbiology,* Vol. 24, No. 4, pp. 522-526.

Araki, T., H. Nawa, and B. G. Neel, 2003, "Tyrosyl Phosphorylation of Shp2 is Required for Normal Erk Activation in Response to Some, But Not All, Growth Factors", *Journal of Biological Chemistry,* Vol. 278, No. 43, pp. 41677-41684.

Barber, A. J., D. A. Antonetti, T. S. Kern, C. E. Reiter, R. S. Soans, J. K. Krady, S. W. Levison, T. W. Gardner, and S. K. Bronson, 2005, "The Ins2akita Mouse as a Model of Early Retinal Complications in Diabetes", *Investigative Ophthalmology and Visual Science,* Vol. 46, No. 6, pp. 2210-2218.

Barber, A. J., T. W. Gardner, and S. F. Abcouwer, 2011, "The Significance of Vascular and Neural Apoptosis to the Pathology of Diabetic Retinopathy", *Investigative Ophthalmology and Visual Science,* Vol. 52, No. 2, pp. 1156-1163.

Barber, A. J., E. Lieth, S. A. Khin, D. A. Antonetti, A. G. Buchanan, and T. W. Gardner, 1998, "Neural Apoptosis in the Retina during Experimental and Human Diabetes. Early Onset and Effect of Insulin", *Journal of Clinical Investigation,* Vol. 102, No. 4, pp. 783-791.

Barber, A. J., M. Nakamura, E. B. Wolpert, C. E. Reiter, G. M. Seigel, D. A. Antonetti, and T. W. Gardner, 2001, "Insulin Rescues Retinal Neurons from Apoptosis by a Phosphatidylinositol 3-Kinase/Akt-Mediated Mechanism that Reduces the Activation of Caspase-3", *Journal of Biological Chemistry,* Vol. 276, No. 35, pp. 32814-32821.

Barnett, N. L., and D. V. Pow, 2000, "Antisense Knockdown of Glast, a Glial Glutamate Transporter, Compromises Retinal Function", *Investigative Ophthalmology and Visual Science,* Vol. 41, No. 2, pp. 585-591.

Baumann, C. A., V. Ribon, M. Kanzaki, D. C. Thurmond, S. Mora, S. Shigematsu, P. E. Bickel, J. E. Pessin, and A. R. Saltiel, 2000, "CAP Defines a Second Signalling Pathway Required for Insulin-Stimulated Glucose Transport", *Nature,* Vol. 407, No. 6801, pp. 202-207.

Bignami, A., and D. Dahl, 1979, "The Radial Glia of Müller in the Rat Retina and Their Response to Injury. An Immunofluorescence Study with Antibodies to the Glial Fibrillary Acidic (GFA) Protein", *Experimental Eye Res,* Vol. 28, No. 1, pp. 63-69.

Boura-Halfon, S., and Y. Zick, 2009, "Phosphorylation of Irs Proteins, Insulin Action, and Insulin Resistance", *American Journal of Physiological Endocrinology and Metabolism,* Vol. 296, No. 4, pp. E581-591.

Bricambert, J., J. Miranda, F. Benhamed, J. Girard, C. Postic, and R. Dentin, 2010, "Salt-Inducible Kinase 2 Links Transcriptional Coactivator P300 Phosphorylation to the Prevention of Chrebp-Dependent Hepatic Steatosis in Mice", *Journal of Clinical Investigation,* Vol. 120, No. 12, pp. 4316-4331.

Bright, N. J., C. Thornton, and D. Carling, 2009, "The Regulation and Function of Mammalian AMPK-Related Kinases", *Acta Physiologica (Oxf),* Vol. 196, No. 1, pp. 15-26.

Brightman, F. A., and D. A. Fell, 2000, "Differential Feedback Regulation of the MAPK Cascade Underlies the Quantitative Differences in EGF and NGF Signalling in PC12 Cells", *FEBS Letters,* Vol. 482, No. 3, pp. 169-174.

Bringmann, A., T. Pannicke, B. Biedermann, M. Francke, I. Iandiev, J. Grosche, P. Wiedemann, J. Albrecht, and A. Reichenbach, 2009, "Role of Retinal Glial Cells in Neurotransmitter Uptake and Metabolism", *Neurochemistry International,* Vol. 54, No. 3-4, pp. 143-160.

Bringmann, A., T. Pannicke, J. Grosche, M. Francke, P. Wiedemann, S. N. Skatchkov, N. N. Osborne, and A. Reichenbach, 2006, "Müller Cells in the Healthy and Diseased Retina", *Progress in Retininal and Eye Research,* Vol. 25, No. 4, pp. 397-424.

Bringmann, A., and A. Reichenbach, 2001, "Role of Müller Cells in Retinal Degenerations", *Frontiers in Bioscience,* Vol. 6, No., pp. E72-92.

Bugra, K., and D. Hicks, 1997, "Acidic And Basic Fibroblast Growth Factor Messenger RNA and Protein Show Increased Expression in Adult Compared to Developing Normal and Dystrophic Rat Retina", *Journal of Molecular Neuroscience,* Vol. 9, No. 1, pp. 13-25.

Bugra, K., L. Oliver, E. Jacquemin, M. Laurent, Y. Courtois, and D. Hicks, 1993, "Acidic Fibroblast Growth Factor is Expressed Abundantly by Photoreceptors within the Developing and Mature Rat Retina", *European Journal of Neuroscience,* Vol. 5, No. 12, pp. 1586-1595.

Burgess, W. H., C. A. Dionne, J. Kaplow, R. Mudd, R. Friesel, A. Zilberstein, J. Schlessinger, and M. Jaye, 1990, "Characterization and cDNA Cloning of Phospholipase C-Gamma, a Major Substrate for Heparin-Binding Growth Factor 1 (Acidic Fibroblast Growth Factor)-Activated Tyrosine Kinase", *Molecular Cell Biology,* Vol. 10, No. 9, pp. 4770-4777.

Burke, J. M., and J. M. Smith, 1981, "Retinal Proliferation in Response to Vitreous Hemoglobin or Iron", *Investigative Ophthalmology and Visual Science,* Vol. 20, No. 5, pp. 582-592.

Cai, Z., D. L. Simons, X. Y. Fu, G. S. Feng, S. M. Wu, and X. Zhang, 2011, "Loss Of Shp2-Mediated Mitogen-Activated Protein Kinase Signaling in Müller Glial Cells Results in Retinal Degeneration", *Molecular Cell Biology,* Vol. 31, No. 14, pp. 2973-2983.

Cao, W., R. Wen, F. Li, M. M. Lavail, and R. H. Steinberg, 1997, "Mechanical Injury Increases bFGF And CNTF mRNA Expression in the Mouse Retina", *Experimental Eye Research,* Vol. 65, No. 2, pp. 241-248.

Cardone, M. H., N. Roy, H. R. Stennicke, G. S. Salvesen, T. F. Franke, E. Stanbridge, S. Frisch, and J. C. Reed, 1998, "Regulation of Cell Death Protease Caspase-9 by Phosphorylation", *Science,* Vol. 282, No. 5392, pp. 1318-1321.

Chakrabarti, S., A. A. Sima, J. Lee, P. Brachet, and E. Dicou, 1990, "Nerve Growth Factor (NGF), proNGF and NGF Receptor-like Immunoreactivity in BB Rat Retina", *Brain Research,* Vol. 523, No. 1, pp. 11-15.

Chen, W. S., P. Z. Xu, K. Gottlob, M. L. Chen, K. Sokol, T. Shiyanova, I. Roninson, W. Weng, R. Suzuki, K. Tobe, T. Kadowaki, and N. Hay, 2001, "Growth Retardation and Increased Apoptosis in Mice with Homozygous Disruption of the Akt1 Gene", *Genes & Development,* Vol. 15, No. 17, pp. 2203-2208.

Cho, H., J. Mu, J. K. Kim, J. L. Thorvaldsen, Q. Chu, E. B. Crenshaw, 3rd, K. H. Kaestner, M. S. Bartolomei, G. I. Shulman, and M. J. Birnbaum, 2001, "Insulin Resistance and a Diabetes Mellitus-like Syndrome in Mice Lacking the Protein Kinase Akt2 (PKB Beta)", *Science,* Vol. 292, No. 5522, pp. 1728-1731.

Condon, G. P., S. Brownstein, N. S. Wang, J. A. Kearns, and C. C. Ewing, 1986, "Congenital Hereditary (Juvenile X-linked) Retinoschisis. Histopathologic and Ultrastructural Findings in Three Eyes", *Archives of Ophthalmology,* Vol. 104, No. 4, pp. 576-583.

Crawley, J. B., L. Rawlinson, F. V. Lali, T. H. Page, J. Saklatvala, and B. M. Foxwell, 1997, "T Cell Proliferation in Response to Interleukins 2 And 7 Requires P38MAP Kinase Activation", *Journal of Biological Chemistry,* Vol. 272, No. 23, pp. 15023-15027.

Crossley, P. H., and G. R. Martin, 1995, "The Mouse Fgf8 Gene Encodes a Family of Polypeptides and is Expressed in Regions that Direct Outgrowth and Patterning in the Developing Embryo", *Development,* Vol. 121, No. 2, pp. 439-451.

Cunnick, J. M., L. Mei, C. A. Doupnik, and J. Wu, 2001, "Phosphotyrosines 627 and 659 of Gab1 Constitute a Bisphosphoryl Tyrosine-Based Activation Motif (BTAM) Conferring Binding and Activation of SHP2", *Journal of Biological Chemistry,* Vol. 276, No. 26, pp. 24380-24387.

Çınaroğlu, A., 2005, *Müller Cells as Potential Targets of FGF9 in Rodent Retina*, Ph.D. Thesis, Boğaziçi University.

Çınaroglu, A., Y. Ozmen, A. Ozdemir, F. Ozcan, C. Ergorul, P. Cayirlioglu, D. Hicks, and K. Bugra, 2005, "Expression and Possible Function of Fibroblast Growth Factor 9 (FGF9) And its Cognate Receptors FGFR2 And FGFR3 in Postnatal and Adult Retina", *Journal of Neuroscience Research,* Vol. 79, No. 3, pp. 329-339.

Das, A., B. Pansky, and G. C. Budd, 1987, "Demonstration of Insulin-specific mRNA in Cultured Rat Retinal Glial Cells", *Investigative Ophthalmology and Visual Science,* Vol. 28, No. 11, pp. 1800-1810.

Datta, S. R., H. Dudek, X. Tao, S. Masters, H. Fu, Y. Gotoh, and M. E. Greenberg, 1997, "Akt Phosphorylation ff Bad Couples Survival Signals to the Cell-Intrinsic Death Machinery", *Cell,* Vol. 91, No. 2, pp. 231-241.

de Jong, P. T., E. Zrenner, G. J. van Meel, J. E. Keunen, and D. van Norren, 1991, "Mizuo Phenomenon in X-linked Retinoschisis. Pathogenesis of the Mizuo Phenomenon", *Archives of Ophthalmology,* Vol. 109, No. 8, pp. 1104-1108.

Dentin, R., Y. Liu, S. H. Koo, S. Hedrick, T. Vargas, J. Heredia, J. Yates, 3rd, and M. Montminy, 2007, "Insulin Modulates Gluconeogenesis by Inhibition of the Coactivator TORC2", *Nature,* Vol. 449, No. 7160, pp. 366-369.

Diaz, B., J. Serna, F. De Pablo, and E. J. de la Rosa, 2000, "*In Vivo* Regulation of Cell Death by Embryonic (Pro)insulin and the Insulin Receptor during Early Retinal Neurogenesis", *Development,* Vol. 127, No. 8, pp. 1641-1649.

Du, J., Q. Chen, H. Takemori, and H. Xu, 2008, "SIK2 Can Be Activated by Deprivation of Nutrition and it Inhibits Expression of Lipogenic Genes in Adipocytes", *Obesity (Silver Spring),* Vol. 16, No. 3, pp. 531-538.

Du, K., S. Herzig, R. N. Kulkarni, and M. Montminy, 2003, "TRB3: a Tribbles Homolog that Inhibits Akt/PKB Activation by Insulin in Liver", *Science,* Vol. 300, No. 5625, pp. 1574-1577.

Dummler, B., and B. A. Hemmings, 2007, "Physiological Roles of PKB/Akt Isoforms in Development and Disease", *Biochemical Society Transactions,* Vol. 35, No. 2, pp. 231-235.

Eisenfeld, A. J., A. H. Bunt-Milam, and P. V. Sarthy, 1984, "Müller Cell Expression of Glial Fibrillary Acidic Protein after Genetic and Experimental Photoreceptor Degeneration in the Rat Retina", *Investigative Ophthalmology and Visual Science,* Vol. 25, No. 11, pp. 1321-1328.

Ejder, F., 2011, *ERK, Akt and PKA as Regulatory Kinases of SIK2 in FGF Signaling in Müller Cells*, M.S. Thesis, Boğaziçi University.

Eriksson, A. E., L. S. Cousens, L. H. Weaver, and B. W. Matthews, 1991, "Three-Dimensional Structure of Human Basic Fibroblast Growth Factor", *Proceedings of National Academy of Sciences U S A,* Vol. 88, No. 8, pp. 3441-3445.

Esteve-Puig, R., F. Canals, N. Colome, G. Merlino, and J. A. Recio, 2009, "Uncoupling of the LKB1-AMPKalpha Energy Sensor Pathway by Growth Factors and Oncogenic BRAF", *Public Library of Science One,* Vol. 4, No. 3, pp. 4771.

Farooq, A., G. Chaturvedi, S. Mujtaba, O. Plotnikova, L. Zeng, C. Dhalluin, R. Ashton, and M. M. Zhou, 2001, "Solution Structure of ERK2 Binding Domain of MAPK Phosphatase MKP-3: Structural Insights into MKP-3 Activation by ERK2", *Molecular Cell,* Vol. 7, No. 2, pp. 387-399.

Fawcett, J. W., and R. A. Asher, 1999, "The Glial Scar and Central Nervous System Repair", *Brain Research Bulletin,* Vol. 49, No. 6, pp. 377-391.

Feinstein, R., H. Kanety, M. Z. Papa, B. Lunenfeld, and A. Karasik, 1993, "Tumor Necrosis Factor-Alpha Suppresses Insulin-Induced Tyrosine Phosphorylation of Insulin Receptor and its Substrates", *Journal of Biological Chemistry,* Vol. 268, No. 35, pp. 26055-26058.

Feldman, J. D., L. Vician, M. Crispino, W. Hoe, M. Baudry, and H. R. Herschman, 2000, "The Salt-Inducible Kinase, SIK, is Induced by Depolarization in Brain", *Journal of Neurochemistry,* Vol. 74, No. 6, pp. 2227-2238.

Fischer, A. J., C. R. McGuire, B. D. Dierks, and T. A. Reh, 2002, "Insulin and Fibroblast Growth Factor 2 Activate a Neurogenic Program in Müller Glia of the Chicken retina", *Journal of Neuroscience,* Vol. 22, No. 21, pp. 9387-9398.

Fischer, A. J., M. A. Scott, and W. Tuten, 2009, "Mitogen-Activated Protein Kinase-Signaling Stimulates Müller Glia to Proliferate in Acutely Damaged Chicken Retina", *Glia,* Vol. 57, No. 2, pp. 166-181.

Folli, F., L. Bonfanti, E. Renard, C. R. Kahn, and A. Merighi, 1994, "Insulin Receptor Substrate-1 (IRS-1) Distribution in the Rat Central Nervous System", *Journal of Neuroscience,* Vol. 14, No. 11, pp. 6412-6422.

Fort, P. E., M. K. Losiewicz, C. E. Reiter, R. S. Singh, M. Nakamura, S. F. Abcouwer, A. J. Barber, and T. W. Gardner, 2011, "Differential Roles Of Hyperglycemia and Hypoinsulinemia in Diabetes induced Retinal Cell Death: Evidence for Retinal Isulin Resistance", *Public Library of Science One,* Vol. 6, No. 10, pp. 26498.

Frame, S., and P. Cohen, 2001, "GSK3 Takes Centre Stage More Than 20 Years after its Discovery", *Biochemistry Journal,* Vol. 359, No. 1, pp. 1-16.

Francke, M., F. Makarov, J. Kacza, J. Seeger, S. Wendt, U. Gartner, F. Faude, P. Wiedemann, and A. Reichenbach, 2001, "Retinal Pigment Epithelium Melanin Granules are Phagocytozed by Müller Glial Cells in Experimental Retinal Detachment", *Journal of Neurocytology,* Vol. 30, No. 2, pp. 131-136.

Francke, M., S. Uhlmann, T. Pannicke, I. Goczalik, O. Uckermann, M. Weick, W. Hartig, P. Wiedemann, A. Reichenbach, and A. Bringmann, 2003, "Experimental Dispase-induced Retinopathy Causes Up-Regulation of P2Y Receptor-Mediated Calcium Responses in Müller Glial Cells", *Ophthalmic Research,* Vol. 35, No. 1, pp. 30-41.

Frasson, M., S. Picaud, T. Leveillard, M. Simonutti, S. Mohand-Said, H. Dreyfus, D. Hicks, and J. Sabel, 1999, "Glial Cell Line-Derived Neurotrophic Factor Induces Histologic and Functional Protection of Rod Photoreceptors in the Rd/Rd Mouse", *Investigative Ophthalmology and Visual Science,* Vol. 40, No. 11, pp. 2724-2734.

Friedman, J. E., T. Ishizuka, S. Liu, C. J. Farrell, D. Bedol, R. J. Koletsky, H. L. Kaung, and P. Ernsberger, 1997, "Reduced Insulin Receptor Signaling in the Obese Spontaneously Hypertensive Koletsky Rat", *American Journal of Physiology,* Vol. 273, No. 5, pp. 1014-1023.

Gao, H., and J. G. Hollyfield, 1992, "Basic Fibroblast Growth Factor (bFGF) Immunolocalization in the Rodent Outer Retina Demonstrated with an Anti-Rodent bFGF Antibody", *Brain Research,* Vol. 585, No. 1-2, pp. 355-360.

Gao, T., F. Furnari, and A. C. Newton, 2005, "PHLPP: a Phosphatase that Directly Dephosphorylates Akt, Promotes Apoptosis, and Suppresses Tumor Growth", *Molecular Cell,* Vol. 18, No. 1, pp. 13-24.

Garcia, M., V. Forster, D. Hicks, and E. Vecino, 2002, "Effects of Müller Glia on Cell Survival and Neuritogenesis in Adult Porcine Retina *in Vitro*", *Investigative Ophthalmology and Visual Science,* Vol. 43, No. 12, pp. 3735-3743.

Garcia, M., and E. Vecino, 2003, "Role of Müller Glia in Neuroprotection and Regeneration in the Retina", *Histology and Histopathology,* Vol. 18, No. 4, pp. 1205-1218.

Gass, J. D., 1999, "Müller Cell Cone, an Overlooked Part of the Anatomy of the Fovea Centralis: Hypotheses Concerning its Role in the Pathogenesis of Macular Hole and Foveomacualr Retinoschisis", *Archives of Ophthalmology,* Vol. 117, No. 6, pp. 821-823.

Geller, S. F., G. P. Lewis, and S. K. Fisher, 2001, "FGFR1, Signaling, and AP-1 Expression after Retinal Detachment: Reactive Müller and RPE Cells", *Investigative Ophthalmology and Visual Science,* Vol. 42, No. 6, pp. 1363-1369.

Gerhardinger, C., M. B. Costa, M. C. Coulombe, I. Toth, T. Hoehn, and P. Grosu, 2005, "Expression of Acute-Phase Response Proteins in Retinal Müller Cells in Diabetes", *Investigative Ophthalmology and Visual Science,* Vol. 46, No. 1, pp. 349-357.

Gotoh, N., 2008, "Regulation of Growth Factor Signaling by FRS2 Family Docking/Scaffold Adaptor Proteins", *Cancer Science,* Vol. 99, No. 7, pp. 1319-1325.

Goureau, O., D. Hicks, Y. Courtois, and Y. De Kozak, 1994, "Induction and Regulation of Nitric Oxide Synthase in Retinal Müller Glial Cells", *Journal of Neurochemistry,* Vol. 63, No. 1, pp. 310-317.

Goureau, O., F. Regnier-Ricard, and Y. Courtois, 1999, "Requirement for Nitric Oxide in Retinal Neuronal Cell Death Induced by Activated Müller Glial Cells", *Journal of Neurochemistry,* Vol. 72, No. 6, pp. 2506-2515.

Gu, H., and B. G. Neel, 2003, "The "Gab" in Signal Transduction", *Trends in Cell Biology,* Vol. 13, No. 3, pp. 122-130.

Gu, H., J. C. Pratt, S. J. Burakoff, and B. G. Neel, 1998, "Cloning of p97/Gab2, the Major SHP2-Binding Protein in Hematopoietic Cells, Reveals a Novel Pathway for Cytokine-Induced Gene Activation", *Molecular Cell,* Vol. 2, No. 6, pp. 729-740.

Gual, P., S. Giordano, S. Anguissola, P. J. Parker, and P. M. Comoglio, 2001, "Gab1 Phosphorylation: A Novel Mechanism for Negative Regulation of HGF Receptor Signaling", *Oncogene,* Vol. 20, No. 2, pp. 156-166.

Gual, P., Y. Le Marchand-Brustel, and J. F. Tanti, 2005, "Positive and Negative Regulation of Insulin Signaling Through IRS-1 Phosphorylation", *Biochimie,* Vol. 87, No. 1, pp. 99-109.

Gustafson, T. A., W. He, A. Craparo, C. D. Schaub, and T. J. O'Neill, 1995, "Phosphotyrosine-Dependent Interaction of SHC and Insulin Receptor Substrate 1 with the NPEY Motif of the Insulin Receptor via a Novel Non-SH2 Domain", *Molecular Cell Biology,* Vol. 15, No. 5, pp. 2500-2508.

Hadari, Y. R., N. Gotoh, H. Kouhara, I. Lax, and J. Schlessinger, 2001, "Critical Role for the Docking-Protein FRS2 Alpha in FGF Receptor-Mediated Signal Transduction Pathways", *Proceedings National Academy of Sciences U S A,* Vol. 98, No. 15, pp. 8578-8583.

Hammes, H. P., H. J. Federoff, and M. Brownlee, 1995, "Nerve Growth Factor Prevents both Neuroretinal Programmed Cell Death and Capillary Pathology in Experimental Diabetes", *Molecular Medicine,* Vol. 1, No. 5, pp. 527-534.

Harada, C., T. Harada, B. S. Slusher, K. Yoshida, H. Matsuda, and K. Wada, 2000, "N-Acetylated-Alpha-Linked-Acidic Dipeptidase Inhibitor Has a Neuroprotective

Effect on Mouse Retinal Ganglion Cells after Pressure-Induced Ischemia", *Neuroscience Letters,* Vol. 292, No. 2, pp. 134-136.

Hardie, D. G., 2004, "AMP-Activated Protein Kinase: A Master Switch in Glucose and Lipid Metabolism", *Reviews in Endocrine and Metabolic Disorders,* Vol. 5, No. 2, pp. 119-125.

Hawkins, P. T., H. Welch, A. McGregor, A. Eguinoa, S. Gobert, S. Krugmann, K. Anderson, D. Stokoe, and L. Stephens, 1997, "Signalling via Phosphoinositide 3OH Kinases", *Biochemical Society Transactions,* Vol. 25, No. 4, pp. 1147-1151.

Haystead, T. A., J. E. Weiel, D. W. Litchfield, Y. Tsukitani, E. H. Fischer, and E. G. Krebs, 1990, "Okadaic Acid Mimics the Action of Insulin in Stimulating Protein Kinase Activity in Isolated Adipocytes. The Role of Protein Phosphatase 2A in Attenuation of the Signal", *Journal of Biological Chemistry,* Vol. 265, No. 27, pp. 16571-16580.

Hernandez-Sanchez, C., A. Lopez-Carranza, C. Alarcon, E. J. de La Rosa, and F. de Pablo, 1995, "Autocrine/Paracrine Role of Insulin-Related Growth Factors in Neurogenesis: Local Expression and Effects on Cell Proliferation and Differentiation in Retina", *Proceedings National Academy of Sciences U S A,* Vol. 92, No. 21, pp. 9834-9838.

Hicks, D., and Y. Courtois, 1992, "Fibroblast Growth Factor Stimulates Photoreceptor Differentiation *in Vitro*", *Journal of Neuroscience,* Vol. 12, No. 6, pp. 2022-2033.

Holgado-Madruga, M., D. R. Emlet, D. K. Moscatello, A. K. Godwin, and A. J. Wong, 1996, "A Grb2-Associated Docking Protein in EGF- and Insulin-Receptor Signalling", *Nature,* Vol. 379, No. 6565, pp. 560-564.

Hollborn, M., K. Jahn, G. A. Limb, L. Kohen, P. Wiedemann, and A. Bringmann, 2004, "Characterization of the Basic Fibroblast Growth Factor-Evoked Proliferation of

the Human Müller Cell Line, MIO-M1", *Graefes Archive for Clinical and Experimental Ophthalmology,* Vol. 242, No. 5, pp. 414-422.

Honjo, M., H. Tanihara, N. Kido, M. Inatani, K. Okazaki, and Y. Honda, 2000, "Expression of Ciliary Neurotrophic Factor Activated by Retinal Müller Cells in Eyes with NMDA- And Kainic Acid-Induced Neuronal Death", *Investigative Ophthalmology and Visual Science,* Vol. 41, No. 2, pp. 552-560.

Horike, N., A. Kumagai, Y. Shimono, T. Onishi, Y. Itoh, T. Sasaki, K. Kitagawa, O. Hatano, H. Takagi, T. Susumu, H. Teraoka, K. Kusano, Y. Nagaoka, H. Kawahara, and H. Takemori, 2010, "Downregulation of SIK2 Expression Promotes the Melanogenic Program in Mice", *Pigment Cell and Melanoma Research,* Vol. 23, No. 6, pp. 809-819.

Horike, N., H. Takemori, Y. Katoh, J. Doi, L. Min, T. Asano, X. J. Sun, H. Yamamoto, S. Kasayama, M. Muraoka, Y. Nonaka, and M. Okamoto, 2003, "Adipose-Specific Expression, Phosphorylation of Ser794 in Insulin Receptor Substrate-1, and Activation in Diabetic Animals of Salt-Inducible Kinase-2", *Journal of Biological Chemistry,* Vol. 278, No. 20, pp. 18440-18447.

Hotamisligil, G. S., P. Peraldi, A. Budavari, R. Ellis, M. F. White, and B. M. Spiegelman, 1996, "IRS-1-Mediated Inhibition of Insulin Receptor Tyrosine Kinase Activity in TNF-Alpha- and Obesity-Induced Insulin Resistance", *Science,* Vol. 271, No. 5249, pp. 665-668.

Huang, J., M. Mohammadi, G. A. Rodrigues, and J. Schlessinger, 1995, "Reduced Activation of RAF-1 and MAP Kinase by a Fibroblast Growth Factor Receptor Mutant Deficient in Stimulation of Phosphatidylinositol Hydrolysis", *Journal of Biological Chemistry,* Vol. 270, No. 10, pp. 5065-5072.

Inokuchi, N., T. Ikeda, Y. Imamura, C. Sotozono, S. Kinoshita, Y. Uchihori, and K. Nakamura, 2001, "Vitreous Levels of Insulin-Like Growth Factor-I in Patients with

Proliferative Diabetic Retinopathy", *Current Eye Research,* Vol. 23, No. 5, pp. 368-371.

Jaleel, M., F. Villa, M. Deak, R. Toth, A. R. Prescott, D. M. Van Aalten, and D. R. Alessi, 2006, "The Ubiquitin-Associated Domain of AMPK-Related Kinases Regulates Conformation and LKB1-Mediated Phosphorylation and Activation", *Biochemical Journal,* Vol. 394, No. 3, pp. 545-555.

Johnson, D. E., and L. T. Williams, 1993, "Structural and Functional Diversity in the FGF Receptor Multigene Family", *Advances in Cancer Research,* Vol. 60, No. 1, pp. 1-41.

Kanety, H., R. Feinstein, M. Z. Papa, R. Hemi, and A. Karasik, 1995, "Tumor Necrosis Factor Alpha-Induced Phosphorylation of Insulin Receptor Substrate-1 (IRS-1). Possible Mechanism for Suppression of Insulin-Stimulated Tyrosine Phosphorylation of IRS-1", *Journal of Biological Chemistry,* Vol. 270, No. 40, pp. 23780-23784.

Kanzaki, M., and J. E. Pessin, 2001, "Signal Integration and the Specificity of Insulin Action", *Cell Biochemistry and Biophysics,* Vol. 35, No. 2, pp. 191-209.

Kaplan, D. R., 1998, "Studying Signal Transduction in Neuronal Cells: the Trk/NGF System", *Progressive Brain Research,* Vol. 117, No. 1, pp. 35-46.

Karl, M. O., and T. A. Reh, 2010, "Regenerative Medicine for Retinal Diseases: Activating Endogenous Repair Mechanisms", *Trends in Molecular Medicine,* Vol. 16, No. 4, pp. 193-202.

Kashii, S., M. Mandai, M. Kikuchi, Y. Honda, Y. Tamura, K. Kaneda, and A. Akaike, 1996, "Dual Actions of Nitric Oxide in N-Methyl-D-Aspartate Receptor-Mediated Neurotoxicity in Cultured Retinal Neurons", *Brain Research,* Vol. 711, No. 1-2, pp. 93-101.

Katoh, Y., H. Takemori, N. Horike, J. Doi, M. Muraoka, L. Min, and M. Okamoto, 2004, "Salt-Inducible Kinase (SIK) Isoforms: Their Involvement in Steroidogenesis and Adipogenesis", *Molecular and Cellular Endocrinology,* Vol. 217, No. 1-2, pp. 109-112.

Katoh, Y., H. Takemori, X. Z. Lin, M. Tamura, M. Muraoka, T. Satoh, Y. Tsuchiya, L. Min, J. Doi, A. Miyauchi, L. A. Witters, H. Nakamura, and M. Okamoto, 2006, "Silencing the Constitutive Active Transcription Factor CREB by the LKB1-SIK Signaling Cascade", *FEBS Journal,* Vol. 273, No. 12, pp. 2730-2748.

Kawasaki, A., Y. Otori, and C. J. Barnstable, 2000, "Müller Cell Protection of Rat Retinal Ganglion Cells from Glutamate and Nitric Oxide Neurotoxicity", *Investigative Ophthalmology and Visual Science*, Vol. 41, No. 11, pp. 3444-3450.

Kellner, U., H. Kraus, H. Heimann, H. Helbig, N. Bornfeld, and M. H. Foerster, 1998, "Electrophysiological Evaluation of Visual Loss in Müller Cell Sheen Dystrophy", *British Journal of Ophthalmology,* Vol. 82, No. 6, pp. 650-654.

Khan, M. N., G. Baquiran, C. Brule, J. Burgess, B. Foster, J. J. Bergeron, and B. I. Posner, 1989, "Internalization and Activation of the Rat Liver Insulin Receptor Kinase *in Vivo*", *Journal of Biological Chemistry,* Vol. 264, No. 22, pp. 12931-12940.

Kinkl, N., J. Sahel, and D. Hicks, 2001, "Alternate FGF2-ERK1/2 Signaling Pathways in Retinal Photoreceptor and Glial Cells *in Vitro*", *Journal of Biological Chemistry,* Vol. 276, No. 47, pp. 43871-43878.

Kirsch, L. S., S. Brownstein, and D. de Wolff-Rouendaal, 1996, "A Histopathological, Ultrastructural and Immunohistochemical Study of Congenital Hereditary Retinoschisis", *Canadian Journal of Ophthalmology,* Vol. 31, No. 6, pp. 301-310.

Kiyatkin, A., E. Aksamitiene, N. I. Markevich, N. M. Borisov, J. B. Hoek, and B. N. Kholodenko, 2006, "Scaffolding Protein Grb2-Associated Binder 1 Sustains Epidermal Growth Factor-Induced Mitogenic and Survival Signaling by Multiple

Positive Feedback Loops", *Journal of Biological Chemistry,* Vol. 281, No. 29, pp. 19925-19938.

Koeberle, P. D., and A. K. Ball, 1999, "Nitric Oxide Synthase Inhibition Delays Axonal Degeneration and Promotes the Survival of Axotomized Retinal Ganglion Cells", *Experimental Neurology,* Vol. 158, No. 2, pp. 366-381.

Kouhara, H., Y. R. Hadari, T. Spivak-Kroizman, J. Schilling, D. Bar-Sagi, I. Lax, and J. Schlessinger, 1997, "A Lipid-Anchored Grb2-Binding Protein that Links FGF-Receptor Activation to the Ras/MAPK Signaling Pathway", *Cell,* Vol. 89, No. 5, pp. 693-702.

Kovalenko, D., X. Yang, R. J. Nadeau, L. K. Harkins, and R. Friesel, 2003, "Sef Inhibits Fibroblast Growth Factor Signaling by Inhibiting FGFR1 Tyrosine Phosphorylation and Subsequent Erk Activation", *Journal of Biological Chemistry,* Vol. 278, No. 16, pp. 14087-14091.

Krejci, P., B. Masri, L. Salazar, C. Farrington-Rock, H. Prats, L. M. Thompson, and W. R. Wilcox, 2007, "Bisindolylmaleimide I Suppresses Fibroblast Growth Factor-Mediated Activation of Erk Map Kinase in Chondrocytes by Preventing Shp2 Association with the Frs2 and Gab1 Adaptor Proteins", *Journal of Biological Chemistry,* Vol. 282, No. 5, pp. 2929-2936.

Kroder, G., B. Bossenmaier, M. Kellerer, E. Capp, B. Stoyanov, A. Muhlhofer, L. Berti, H. Horikoshi, A. Ullrich, and H. Haring, 1996, "Tumor Necrosis Factor-Alpha- and Hyperglycemia-Induced Insulin Resistance. Evidence for Different Mechanisms and Different Effects on Insulin Signaling", *Journal of Clinical Investigation,* Vol. 97, No. 6, pp. 1471-1477.

Küser, G., 2006, *Identification of Candidate Substrates of SIK2 in Vitro*, M.S. Thesis, Boğaziçi University.

Lamothe, B., M. Yamada, U. Schaeper, W. Birchmeier, I. Lax, and J. Schlessinger, 2004, "The Docking Protein Gab1 is an Essential Component of an Indirect Mechanism for Fibroblast Growth Factor Stimulation of the Phosphatidylinositol 3-Kinase/Akt Antiapoptotic Pathway", *Molecular Cell Biology,* Vol. 24, No. 13, pp. 5657-5666.

Lanjuin, A., and P. Sengupta, 2002, "Regulation of Chemosensory Receptor Expression and Sensory Signaling by the KIN-29 Ser/Thr Kinase", *Neuron,* Vol. 33, No. 3, pp. 369-381.

Lawrence, J. M., S. Singhal, B. Bhatia, D. J. Keegan, T. A. Reh, P. J. Luthert, P. T. Khaw, and G. A. Limb, 2007, "MIO-M1 Cells and Similar Müller Glial Cell Lines Derived from Adult Human Retina Exhibit Neural Stem Cell Characteristics", *Stem Cells,* Vol. 25, No. 8, pp. 2033-2043.

Lax, I., A. Wong, B. Lamothe, A. Lee, A. Frost, J. Hawes, and J. Schlessinger, 2002, "The Docking Protein FRS2alpha Controls a MAP Kinase-Mediated Negative Feedback Mechanism for Signaling by FGF Receptors", *Molecular Cell,* Vol. 10, No. 4, pp. 709-719.

Layton, C. J., S. Becker, and N. N. Osborne, 2006, "The Effect of Insulin And Glucose Levels on Retinal Glial Cell Activation and Pigment Epithelium-Derived Fibroblast Growth Factor-2", *Molecular Vision,* Vol. 12, No., pp. 43-54.

Lehr, S., J. Kotzka, H. Avci, A. Sickmann, H. E. Meyer, A. Herkner, and D. Muller-Wieland, 2004, "Identification of Major ERK-Related Phosphorylation Sites in Gab1", *Biochemistry,* Vol. 43, No. 38, pp. 12133-12140.

Lehr, S., J. Kotzka, A. Herkner, A. Sikmann, H. E. Meyer, W. Krone, and D. Muller-Wieland, 2000, "Identification of Major Tyrosine Phosphorylation Sites in the Human Insulin Receptor Substrate Gab-1 by Insulin Receptor Kinase *in Vitro*", *Biochemistry,* Vol. 39, No. 35, pp. 10898-10907.

Lewis, G. P., and S. K. Fisher, 2000, "Müller Cell Outgrowth After Retinal Detachment: Association with Cone Photoreceptors", *Investigative Ophthalmology and Visual Science,* Vol. 41, No. 6, pp. 1542-1545.

Li, J., K. DeFea, and R. A. Roth, 1999, "Modulation of Insulin Receptor Substrate-1 Tyrosine Phosphorylation by an Akt/Phosphatidylinositol 3-Kinase Pathway", *Journal of Biological Chemistry,* Vol. 274, No. 14, pp. 9351-9356.

Li, Q., and D. G. Puro, 2002, "Diabetes-Induced Dysfunction of the Glutamate Transporter in Retinal Müller Cells", *Investigative Ophthalmology and Visual Science,* Vol. 43, No. 9, pp. 3109-3116.

Lieth, E., A. J. Barber, B. Xu, C. Dice, M. J. Ratz, D. Tanase, and J. M. Strother, 1998, "Glial Reactivity and Impaired Glutamate Metabolism in Short-Term Experimental Diabetic Retinopathy", *Diabetes,* Vol. 47, No. 5, pp. 815-820.

Limb, G. A., T. E. Salt, P. M. Munro, S. E. Moss, and P. T. Khaw, 2002, "*In Vitro* Characterization of a Spontaneously Immortalized Human Muller Cell Line (MIO-M1)", *Investigative Ophthalmology and Visual Science,* Vol. 43, No. 3, pp. 864-869.

Liu, Y., and L. R. Rohrschneider, 2002, "The Gift of Gab", *FEBS Letters,* Vol. 515, No. 1-3, pp. 1-7.

Lizcano, J. M., O. Goransson, R. Toth, M. Deak, N. A. Morrice, J. Boudeau, S. A. Hawley, L. Udd, T. P. Makela, D. G. Hardie, and D. R. Alessi, 2004, "LKB1 is a Master Kinase that Activates 13 Kinases of the AMPK Subfamily, Including MARK/PAR-1", *EMBO Journal,* Vol. 23, No. 4, pp. 833-843.

Lock, L. S., I. Royal, M. A. Naujokas, and M. Park, 2000, "Identification of an Atypical Grb2 Carboxyl-Terminal Sh3 Domain Binding Site in Gab Docking Proteins Reveals Grb2-Dependent and -Independent Recruitment of Gab1 to Receptor

Tyrosine Kinases", *Journal of Biological Chemistry,* Vol. 275, No. 40, pp. 31536-31545.

Luttrell, L. M., B. E. Hawes, K. Touhara, T. van Biesen, W. J. Koch, and R. J. Lefkowitz, 1995, "Effect of Cellular Expression of Pleckstrin Homology Domains on Gi-Coupled Receptor Signaling", *Journal of Biological Chemistry,* Vol. 270, No. 22, pp. 12984-12989.

Maffucci, T., C. Raimondi, S. Abu-Hayyeh, V. Dominguez, G. Sala, I. Zachary, and M. Falasca, 2009, "A Phosphoinositide 3-Kinase/Phospholipase Cgamma1 Pathway Regulates Fibroblast Growth Factor-Induced Capillary Tube Formation", *Public Library of Science One,* Vol. 4, No. 12, pp. 8285.

Maroun, C. R., M. Holgado-Madruga, I. Royal, M. A. Naujokas, T. M. Fournier, A. J. Wong, and M. Park, 1999, "The Gab1 PH Domain is Required for Localization of Gab1 at Sites of Cell-Cell Contact and Epithelial Morphogenesis Downstream from the Met Receptor Tyrosine Kinase", *Molecular Cell Biology,* Vol. 19, No. 3, pp. 1784-1799.

Marshall, C. J., 1994, "MAP Kinase Kinase Kinase, MAP Kinase Kinase and MAP Kinase", *Current Opinion in Genetics and Development,* Vol. 4, No. 1, pp. 82-89.

Mason, I., 2007, "Initiation to End Point: The Multiple Roles of Fibroblast Growth Factors in Neural Development", *Nature Reviews Neuroscience,* Vol. 8, No. 8, pp. 583-596.

Maw, M. A., B. Kennedy, A. Knight, R. Bridges, K. E. Roth, E. J. Mani, J. K. Mukkadan, D. Nancarrow, J. W. Crabb, and M. J. Denton, 1997, "Mutation of the Gene Encoding Cellular Retinaldehyde-Binding Protein in Autosomal Recessive Retinitis Pigmentosa", *Nature Genetics,* Vol. 17, No. 2, pp. 198-200.

McCabe, K. L., E. C. Gunther, and T. A. Reh, 1999, "The Development of the Pattern of Retinal Ganglion Cells in the Chick Retina: Mechanisms that Control Differentiation", *Development,* Vol. 126, No. 24, pp. 5713-5724.

Meyer-Franke, A., M. R. Kaplan, F. W. Pfrieger, and B. A. Barres, 1995, "Characterization of the Signaling Interactions that Promote the Survival and Growth of Developing Retinal Ganglion Cells in Culture", *Neuron,* Vol. 15, No. 4, pp. 805-819.

Miyake, A., M. Konishi, F. H. Martin, N. A. Hernday, K. Ozaki, S. Yamamoto, T. Mikami, T. Arakawa, and N. Itoh, 1998, "Structure and Expression of a Novel Member, FGF-16, on the Fibroblast Growth Factor Family", *Biochemical and Biophysical Research Communications,* Vol. 243, No. 1, pp. 148-152.

Mohammadi, M., A. M. Honegger, D. Rotin, R. Fischer, F. Bellot, W. Li, C. A. Dionne, M. Jaye, M. Rubinstein, and J. Schlessinger, 1991, "A Tyrosine-Phosphorylated Carboxy-Terminal Peptide of the Fibroblast Growth Factor Receptor (Flg) is a Binding Site for the SH2 Domain of Phospholipase C-Gamma 1", *Molecular Cell Biology,* Vol. 11, No. 10, pp. 5068-5078.

Montagner, A., A. Yart, M. Dance, B. Perret, J. P. Salles, and P. Raynal, 2005, "A Novel Role for Gab1 and Shp2 in Epidermal Growth Factor-Induced Ras Activation", *Journal of Biological Chemistry,* Vol. 280, No. 7, pp. 5350-5360.

Mood, K., C. Saucier, Y. S. Bong, H. S. Lee, M. Park, and I. O. Daar, 2006, "Gab1 is Required for Cell Cycle Transition, Cell Proliferation, and Transformation Induced by an Oncogenic Met Receptor", *Molecular Biology of the Cell,* Vol. 17, No. 9, pp. 3717-3728.

Muraoka, M., A. Fukushima, S. Viengchareun, M. Lombes, F. Kishi, A. Miyauchi, M. Kanematsu, J. Doi, J. Kajimura, R. Nakai, T. Uebi, M. Okamoto, and H. Takemori, 2009, "Involvement of SIK2/TORC2 Signaling Cascade in the Regulation of Insulin-Induced Pgc-1alpha and Ucp-1 Gene Expression in Brown Adipocytes",

American Journal of Physiology Endocrinology and Metabolism, Vol. 296, No. 6, pp. E1430-1439.

Myers, M. G., Jr., R. Mendez, P. Shi, J. H. Pierce, R. Rhoads, and M. F. White, 1998, "The COOH-Terminal Tyrosine Phosphorylation Sites on IRS-1 Bind Shp-2 and Negatively Regulate Insulin Signaling", *Journal of Biological Chemistry,* Vol. 273, No. 41, pp. 26908-26914.

Nagel, S., E. Leich, H. Quentmeier, C. Meyer, M. Kaufmann, M. Zaborski, A. Rosenwald, H. G. Drexler, and R. A. Macleod, 2010, "Amplification at 11q23 Targets Protein Kinase SIK2 in Diffuse Large B-Cell Lymphoma", *Leukemia and Lymphoma,* Vol. 51, No. 5, pp. 881-891.

Nakamura, M., A. J. Barber, D. A. Antonetti, K. F. LaNoue, K. A. Robinson, M. G. Buse, and T. W. Gardner, 2001, "Excessive Hexosamines Block the Neuroprotective Effect of Insulin And Induce Apoptosis in Retinal Neurons", *Journal of Biological Chemistry,* Vol. 276, No. 47, pp. 43748-43755.

Neophytou, C., A. B. Vernallis, A. Smith, and M. C. Raff, 1997, "Müller-Cell-Derived Leukaemia Inhibitory Factor Arrests Rod Photoreceptor Differentiation at a Postmitotic Pre-Rod Stage of Development", *Development,* Vol. 124, No. 12, pp. 2345-2354.

Okamoto, M., H. Takemori, and Y. Katoh, 2004, "Salt-Inducible Kinase in Steroidogenesis and Adipogenesis", *Trends in Endocrinology and Metabolism,* Vol. 15, No. 1, pp. 21-26.

Oku, H., T. Ikeda, Y. Honma, C. Sotozono, K. Nishida, Y. Nakamura, T. Kida, and S. Kinoshita, 2002, "Gene Expression of Neurotrophins and Their High-Affinity Trk Receptors in Cultured Human Müller Cells", *Ophthalmic Research,* Vol. 34, No. 1, pp. 38-42.

Ola, M. S., K. Hosoya, and K. F. Lanoue, 2011, "Influence of İnsulin on Glutamine Synthetase in the Müller Glial Cells of Retina", *Metabolic Brain Disease,* Vol. 26, No. 3, pp. 195-202.

O'Neill, T. J., A. Craparo, and T. A. Gustafson, 1994, "Characterization of an İnteraction Between Insulin Receptor Substrate 1 and The Insulin Receptor by Using the Two-Hybrid System", *Molecular Cell Biology,* Vol. 14, No. 10, pp. 6433-6442.

Ong, S. H., Y. R. Hadari, N. Gotoh, G. R. Guy, J. Schlessinger, and I. Lax, 2001, "Stimulation of Phosphatidylinositol 3-Kinase by Fibroblast Growth Factor Receptors is Mediated by Coordinated Recruitment of Multiple Docking Proteins", *Proceedings National Academy of Science U S A,* Vol. 98, No. 11, pp. 6074-6079.

Ong, S. H., Y. P. Lim, B. C. Low, and G. R. Guy, 1997, "SHP2 Associates Directly with Tyrosine Phosphorylated P90 (Snt) Protein in FGF-Stimulated Cells", *Biochemical and Biophysical Research Communications,* Vol. 238, No. 1, pp. 261-266.

Ornitz, D. M., 2000, "FGFs, Heparan Sulfate and FGFRs: Complex Interactions Essential for Development", *Bioessays,* Vol. 22, No. 2, pp. 108-112.

Ornitz, D. M., and N. Itoh, 2001, "Fibroblast Growth Factors", *Genome Biology,* Vol. 2, No. 3, pp. 300-305.

Özcan, F., 2003, *Identification of Putative Serine/Threoninw Kinase Implicated in FGF Signal Transduction and Its Compatibility With an FGF Pathway Simulation Model*, Ph.D. Thesis, Boğaziçi University.

Özmen, Y., 2006, *SIK2 Expression in Retinal Cells And Its Possible İnvolvement along with PKA in FGF9 Signal Transduction*, Ph.D. Thesis, Boğaziçi University.

Pannicke, T., I. Iandiev, A. Wurm, O. Uckermann, F. vom Hagen, A. Reichenbach, P. Wiedemann, H. P. Hammes, and A. Bringmann, 2006, "Diabetes Alters Osmotic

Swelling Characteristics and Membrane Conductance of Glial Cells in Rat Retina", *Diabetes,* Vol. 55, No. 3, pp. 633-639.

Pawson, T., 1995, "Protein Modules and Signalling Networks", *Nature,* Vol. 373, No. 6515, pp. 573-580.

Peterson, W. M., Q. Wang, R. Tzekova, and S. J. Wiegand, 2000, "Ciliary Neurotrophic Factor and Stress Stimuli Activate the Jak-Stat Pathway in Retinal Neurons and Glia", *Journal of Neuroscience,* Vol. 20, No. 11, pp. 4081-4090.

Pittack, C., G. B. Grunwald, and T. A. Reh, 1997, "Fibroblast Growth Factors Are Necessary for Neural Retina But Not Pigmented Epithelium Differentiation in Chick Embryos", *Development,* Vol. 124, No. 4, pp. 805-816.

Plotnikov, A. N., J. Schlessinger, S. R. Hubbard, and M. Mohammadi, 1999, "Structural Basis for FGF Receptor Dimerization and Activation", *Cell,* Vol. 98, No. 5, pp. 641-650.

Poitry-Yamate, C. L., S. Poitry, and M. Tsacopoulos, 1995, "Lactate Released by Müller Glial Cells is Metabolized by Photoreceptors from Mammalian Retina", *Journal of Neuroscience,* Vol. 15, No. 7 Pt 2, pp. 5179-5191.

Pouyssegur, J., and P. Lenormand, 2003, "Fidelity and Spatio-Temporal Control in MAP Kinase (ERKs) Signalling", *European Journal of Biochemistry,* Vol. 270, No. 16, pp. 3291-3299.

Pouyssegur, J., V. Volmat, and P. Lenormand, 2002, "Fidelity and Spatio-Temporal Control in MAP Kinase (ERKs) Signalling", *Biochemical Pharmacology,* Vol. 64, No. 5-6, pp. 755-763.

Pow, D. V., and D. K. Crook, 1995, "Immunocytochemical Evidence for the Presence of High Levels of Reduced Glutathione in Radial Glial Cells and Horizontal Cells in the Rabbit Retina", *Neuroscience Letters,* Vol. 193, No. 1, pp. 25-28.

Powell, P. P., and M. Klagsbrun, 1991, "Three Forms of Rat Basic Fibroblast Growth Factor Are Made from a Single mRNA and Localize to the Nucleus", *Journal of Cell Physiology,* Vol. 148, No. 2, pp. 202-210.

Preger, E., I. Ziv, A. Shabtay, I. Sher, M. Tsang, I. B. Dawid, Y. Altuvia, and D. Ron, 2004, "Alternative Splicing Generates an Isoform of the Human Sef Gene with Altered Subcellular Localization and Specificity", *Proceedings National Academy of Science U S A,* Vol. 101, No. 5, pp. 1229-1234.

Qiao, L. Y., R. Zhande, T. L. Jetton, G. Zhou, and X. J. Sun, 2002, "*In Vivo* Phosphorylation of Insulin Receptor Substrate 1 at Serine 789 by a Novel Serine Kinase in Insulin-Resistant Rodents", *Journal of Biological Chemistry,* Vol. 277, No. 29, pp. 26530-26539.

Rajala, R. V., B. Wiskur, M. Tanito, M. Callegan, and A. Rajala, 2009, "Diabetes Reduces Autophosphorylation of Retinal Insulin Receptor and Increases Protein-Tyrosine Phosphatase-1b Activity", *Investigative Ophthalmology and Visual Science,* Vol. 50, No. 3, pp. 1033-1040.

Rakhit, S., S. Pyne, and N. J. Pyne, 2000, "The Platelet-Derived Growth Factor Receptor Stimulation of P42/P44 Mitogen-Activated Protein Kinase in Airway Smooth Muscle Involves a G-Protein-Mediated Tyrosine Phosphorylation of Gab1", *Molecular Pharmacology,* Vol. 58, No. 2, pp. 413-420.

Ramakers, C., J. M. Ruijter, R. H. Deprez, and A. F. Moorman, 2003, "Assumption-Free Analysis of Quantitative Real-Time Polymerase Chain Reaction (PCR) Data" *Neuroscience Letters,* Vol. 339, No. 1, pp. 62-66.

Reichelt, W., J. Stabel-Burow, T. Pannicke, H. Weichert, and U. Heinemann, 1997, "The Glutathione Level of Retinal Müller Glial Cells is Dependent on the High-Affinity Sodium-Dependent Uptake of Glutamate", *Neuroscience,* Vol. 77, No. 4, pp. 1213-1224.

Reifers, F., H. Bohli, E. C. Walsh, P. H. Crossley, D. Y. Stainier, and M. Brand, 1998, "Fgf8 is Mutated in Zebrafish Acerebellar (ace) Mutants and is Required for Maintenance of Midbrain-Hindbrain Boundary Development and Somitogenesis", *Development,* Vol. 125, No. 13, pp. 2381-2395.

Reiter, C. E., and T. W. Gardner, 2003, "Functions of Insulin and Insulin Receptor Signaling in Retina: Possible Implications for Diabetic Retinopathy", *Progress in Retinal Eye Research,* Vol. 22, No. 4, pp. 545-562.

Reiter, C. E., L. Sandirasegarane, E. B. Wolpert, M. Klinger, I. A. Simpson, A. J. Barber, D. A. Antonetti, M. Kester, and T. W. Gardner, 2003, "Characterization of Insulin Signaling in Rat Retina *in Vivo* and *Ex Vivo*", *American Journal of Physiology Endocrinology and Metabolism,* Vol. 285, No. 4, pp. 763-774.

Reiter, C. E., X. Wu, L. Sandirasegarane, M. Nakamura, K. A. Gilbert, R. S. Singh, P. E. Fort, D. A. Antonetti, and T. W. Gardner, 2006, "Diabetes Reduces Basal Retinal Insulin Receptor Signaling: Reversal with Systemic and Local Insulin", *Diabetes,* Vol. 55, No. 4, pp. 1148-1156.

Ricort, J. M., J. F. Tanti, E. Van Obberghen, and Y. Le Marchand-Brustel, 1995, "Alterations in Insulin Signalling Pathway Induced by Prolonged Insulin Treatment of 3T3-L1 Adipocytes", *Diabetologia,* Vol. 38, No. 10, pp. 1148-1156.

Rocchi, S., S. Tartare-Deckert, J. Murdaca, M. Holgado-Madruga, A. J. Wong, and E. Van Obberghen, 1998, "Determination of Gab1 (Grb2-Associated Binder-1) Interaction with Insulin Receptor-Signaling Molecules", *Molecular Endocrinology,* Vol. 12, No. 7, pp. 914-923.

Rodriguez-Viciana, P., P. H. Warne, R. Dhand, B. Vanhaesebroeck, I. Gout, M. J. Fry, M. D. Waterfield, and J. Downward, 1994, "Phosphatidylinositol-3-OH Kinase as a Direct Target of Ras", *Nature,* Vol. 370, No. 6490, pp. 527-532.

Ronchetti, D., A. Greco, S. Compasso, G. Colombo, P. Dell'Era, T. Otsuki, L. Lombardi, and A. Neri, 2001, "Deregulated FGFR3 Mutants in Multiple Myeloma Cell Lines with t(4;14): Comparative Analysis of Y373C, K650E and the Novel G384D Mutations", *Oncogene,* Vol. 20, No. 27, pp. 3553-3562.

Rosenthal, A. R., and B. Appleton, 1975, "Histochemical Localization of Intraocular Copper Foreign Bodies", *American Journal of Ophthalmology,* Vol. 79, No. 4, pp. 613-625.

Roth, S., 1997, "Role of Nitric Oxide in Retinal Cell Death", *Clinical Neuroscience,* Vol. 4, No. 5, pp. 216-223.

Ruiz, J. C., F. L. Conlon, and E. J. Robertson, 1994, "Identification of Novel Protein Kinases Expressed in the Myocardium of the Developing Mouse Heart", *Mechanisms of Development,* Vol. 48, No. 3, pp. 153-164.

Sachs, M., H. Brohmann, D. Zechner, T. Muller, J. Hulsken, I. Walther, U. Schaeper, C. Birchmeier, and W. Birchmeier, 2000, "Essential Role of Gab1 for Signaling by the c-Met Receptor *in Vivo*", *Journal Cell Biology,* Vol. 150, No. 6, pp. 1375-1384.

Saltiel, A. R., and C. R. Kahn, 2001, "Insulin Signalling and the Regulation of Glucose and Lipid Metabolism", *Nature,* Vol. 414, No. 6865, pp. 799-806.

Sano, H., S. Kane, E. Sano, C. P. Miinea, J. M. Asara, W. S. Lane, C. W. Garner, and G. E. Lienhard, 2003, "Insulin-Stimulated Phosphorylation of a Rab GTPase-Activating Protein Regulates GLUT4 Translocation", *Journal of Biological Chemistry,* Vol. 278, No. 17, pp. 14599-14602.

Sarthy, V. P., S. J. Brodjian, K. Dutt, B. N. Kennedy, R. P. French, and J. W. Crabb, 1998, "Establishment and Characterization of a Retinal Müller Cell Line", *Investigative Ophthalmology and Visual Science,* Vol. 39, No. 1, pp. 212-216.

Sasaki, T., H. Takemori, Y. Yagita, Y. Terasaki, T. Uebi, N. Horike, H. Takagi, T. Susumu, H. Teraoka, K. Kusano, O. Hatano, N. Oyama, Y. Sugiyama, S. Sakoda, and K. Kitagawa, 2011, "SIK2 is a Key Regulator for Neuronal Survival after Ischemia via TORC1-CREB", *Neuron,* Vol. 69, No. 1, pp. 106-119.

Schaeper, U., N. H. Gehring, K. P. Fuchs, M. Sachs, B. Kempkes, and W. Birchmeier, 2000, "Coupling of Gab1 to c-Met, Grb2, and Shp2 Mediates Biological Responses", *Journal of Cell Biology,* Vol. 149, No. 7, pp. 1419-1432.

Schlessinger, J., 2000, "Cell Signaling by Receptor Tyrosine Kinases", *Cell,* Vol. 103, No. 2, pp. 211-225.

Schutte, M., and P. Werner, 1998, "Redistribution of Glutathione in the Ischemic Rat Retina", *Neuroscience Letters,* Vol. 246, No. 1, pp. 53-56.

Screaton, R. A., M. D. Conkright, Y. Katoh, J. L. Best, G. Canettieri, S. Jeffries, E. Guzman, S. Niessen, J. R. Yates, 3rd, H. Takemori, M. Okamoto, and M. Montminy, 2004, "The CREB Coactivator TORC2 Functions as a Calcium- and cAMP-Sensitive Coincidence Detector", *Cell,* Vol. 119, No. 1, pp. 61-74.

Seki, M., T. Tanaka, Y. Sakai, T. Fukuchi, H. Abe, H. Nawa, and N. Takei, 2005, "Müller Cells as a Source of Brain-Derived Neurotrophic Factor in the Retina: Noradrenaline Upregulates brain-Derived Neurotrophic Factor Levels in Cultured Rat Müller Cells", *Neurochemical Research,* Vol. 30, No. 9, pp. 1163-1170.

Slack, J., 1994, "Role of Fibroblast Growth Factors as Inducing Agents in Early Embryonic Development", *Molecular Reproduction and Development,* Vol. 39, No. 1, pp. 118-124; discussion 124-115.

Smallwood, P. M., I. Munoz-Sanjuan, P. Tong, J. P. Macke, S. H. Hendry, D. J. Gilbert, N. G. Copeland, N. A. Jenkins, and J. Nathans, 1996, "Fibroblast Growth Factor (Fgf) Homologous Factors: New Members of the FGF Family Implicated in Nervous

System Development", *Proceedings National Academy of Science U S A,* Vol. 93, No. 18, pp. 9850-9857.

Sugiyama, T., K. Katsumura, K. Nakamura, M. Kobayashi, M. Muramatsu, M. Maruichi, H. Oku, S. Takai, M. Miyazaki, and T. Ikeda, 2006, "Effects of Chymase on the Macular Region in Monkeys and Porcine Müller Cells: Probable Involvement of Chymase in the Onset of Idiopathic Macular Holes", *Ophthalmic Research,* Vol. 38, No. 4, pp. 201-208.

Sun, X. J., D. L. Crimmins, M. G. Myers, Jr., M. Miralpeix, and M. F. White, 1993, "Pleiotropic Insulin Signals aAre Engaged by Multisite Phosphorylation of IRS-1", *Molecular Cell Biology,* Vol. 13, No. 12, pp. 7418-7428.

Sun, X. J., M. Miralpeix, M. G. Myers, Jr., E. M. Glasheen, J. M. Backer, C. R. Kahn, and M. F. White, 1992, "Expression and Function of IRS-1 in Insulin Signal Transmission", *Journal of Biological Chemistry,* Vol. 267, No. 31, pp. 22662-22672.

Sun, X. J., P. Rothenberg, C. R. Kahn, J. M. Backer, E. Araki, P. A. Wilden, D. A. Cahill, B. J. Goldstein, and M. F. White, 1991, "Structure of the Insulin Receptor Substrate IRS-1 Defines a Unique Signal Transduction Protein", *Nature,* Vol. 352, No. 6330, pp. 73-77.

Takeda, M., A. Takamiya, A. Yoshida, and H. Kiyama, 2002, "Extracellular Signal-Regulated Kinase Activation Predominantly in Müller Cells of Retina with Endotoxin-Induced Uveitis", *Investigative Ophthalmology and Visual Science,* Vol. 43, No. 4, pp. 907-911.

Tanti, J. F., T. Gremeaux, E. Van Obberghen, and Y. Le Marchand-Brustel, 1991, "Effects of Okadaic Acid, an Inhibitor of Protein Phosphatases-1 and -2a, on Glucose Transport and Metabolism in Skeletal Muscle", *Journal of Biological Chemistry,* Vol. 266, No. 4, pp. 2099-2103.

Tezel, G., and M. B. Wax, 2003, "Glial Modulation of Retinal Ganglion Cell Death in Glaucoma", *Journal of Glaucoma,* Vol. 12, No. 1, pp. 63-68.

Tran, H., A. Brunet, E. C. Griffith, and M. E. Greenberg, 2003, "The Many Forks in FOXO's Road", *Science Signaling: The Signal Transduction Knowledge Environment,* Vol. 2003, No. 172, pp. 3-5.

Tsang, M., and I. B. Dawid, 2004, "Promotion and Attenuation of FGF Signaling Through the Ras-MAPK Pathway", *Science Signaling: The Signal Transduction Knowledge Environment,* Vol. 2004, No. 228, pp. 17-20.

Tschopp, O., Z. Z. Yang, D. Brodbeck, B. A. Dummler, M. Hemmings-Mieszczak, T. Watanabe, T. Michaelis, J. Frahm, and B. A. Hemmings, 2005, "Essential Role of Protein Kinase B Gamma (PKB Gamma/Akt3) in Postnatal Brain Development But Not in Glucose Homeostasis", *Development,* Vol. 132, No. 13, pp. 2943-2954.

Ueki, K., C. M. Yballe, S. M. Brachmann, D. Vicent, J. M. Watt, C. R. Kahn, and L. C. Cantley, 2002, "Increased Insulin Sensitivity in Mice Lacking P85beta Subunit of Phosphoinositide 3-Kinase", *Proceedings National Academy of Science U S A,* Vol. 99, No. 1, pp. 419-424.

Uysal, A., 2005, *SMP is a Rat Orthologue of Salt-Inducible Kinase 2*, M.S. Thesis, Boğaziçi University.

Vogel-Hopker, A., T. Momose, H. Rohrer, K. Yasuda, L. Ishihara, and D. H. Rapaport, 2000, "Multiple Functions of Fibroblast Growth Factor-8 (Fgf-8) in Chick Eye Development", *Mechanisms of Development,* Vol. 94, No. 1-2, pp. 25-36.

Wahlin, K. J., P. A. Campochiaro, D. J. Zack, and R. Adler, 2000, "Neurotrophic Factors Cause Activation of Intracellular Signaling Pathways in Müller Cells and Other Cells of the Inner Retina, But Not Photoreceptors", *Investigative Ophthalmology and Visual Science,* Vol. 41, No. 3, pp. 927-936.

Walshe, J., and I. Mason, 2003, "Fgf Signalling is Required for Formation of Cartilage in the Head", *Developmental Biology,* Vol. 264, No. 2, pp. 522-536.

Wang, S., W. M. Yu, W. Zhang, K. R. McCrae, B. G. Neel, and C. K. Qu, 2009, "Noonan Syndrome/Leukemia-Associated Gain-Of-Function Mutations in Shp-2 Phosphatase (PTPN11) Enhance Cell Migration and Angiogenesis", *Journal of Biological Chemistry,* Vol. 284, No. 2, pp. 913-920.

Wang, Z., H. Takemori, S. K. Halder, Y. Nonaka, and M. Okamoto, 1999, "Cloning of a Novel Kinase (SIK) of the SNF1/AMPK Family from High Salt Diet-Treated Rat Adrenal", *FEBS Letters,* Vol. 453, No. 1-2, pp. 135-139.

Wei, M., L. Ong, M. T. Smith, F. B. Ross, K. Schmid, A. J. Hoey, D. Burstow, and L. Brown, 2003, "The Streptozotocin-Diabetic Rat as a Model of the Chronic Complications of Human Diabetes", *Heart, Lung and Circulation,* Vol. 12, No. 1, pp. 44-50.

White, M. F., R. Maron, and C. R. Kahn, 1985, "Insulin Rapidly Stimulates Tyrosine Phosphorylation of a Mr-185,000 Protein in Intact Cells", *Nature,* Vol. 318, No. 6042, pp. 183-186.

Winkler, B. S., M. J. Arnold, M. A. Brassell, and D. G. Puro, 2000, "Energy Metabolism in Human Retinal Müller Cells", *Investigative Ophthalmology and Visual Science,* Vol. 41, No. 10, pp. 3183-3190.

Wong, A., B. Lamothe, A. Lee, J. Schlessinger, and I. Lax, 2002, "FRS2 Alpha Attenuates FGF Receptor Signaling by Grb2-Mediated Recruitment of the Ubiquitin Ligase Cbl", *Proceedings National Academy of Science U S A,* Vol. 99, No. 10, pp. 6684-6689.

Xi, X., L. Gao, D. A. Hatala, D. G. Smith, M. C. Codispoti, B. Gong, T. S. Kern, and J. Z. Zhang, 2005, "Chronically Elevated Glucose-Induced Apoptosis is Mediated by

Inactivation of Akt in Cultured Müller Cells", *Biochemical and Biophysical Research Communications,* Vol. 326, No. 3, pp. 548-553.

Xie, M. H., I. Holcomb, B. Deuel, P. Dowd, A. Huang, A. Vagts, J. Foster, J. Liang, J. Brush, Q. Gu, K. Hillan, A. Goddard, and A. L. Gurney, 1999, "FGF-19, a Novel Fibroblast Growth Factor with Unique Specificity for FGFR4", *Cytokine,* Vol. 11, No. 10, pp. 729-735.

Yamasaki, S., K. Nishida, Y. Yoshida, M. Itoh, M. Hibi, and T. Hirano, 2003, "Gab1 is Required for EGF Receptor Signaling and the Transformation by Activated ErbB2", *Oncogene,* Vol. 22, No. 10, pp. 1546-1556.

Yang, X. J., 2004, "Roles of Cell-Extrinsic Growth Factors in Vertebrate Eye Pattern Formation and Retinogenesis", *Seminars in Cell and Developmental Biology,* Vol. 15, No. 1, pp. 91-103.

Yasuhara, T., T. Shingo, K. Kobayashi, A. Takeuchi, A. Yano, K. Muraoka, T. Matsui, Y. Miyoshi, H. Hamada, and I. Date, 2004, "Neuroprotective Effects of Vascular Endothelial Growth Factor (VEGF) upon Dopaminergic Neurons in a Rat Model of Parkinson's Disease", *European Journal of Neuroscience,* Vol. 19, No. 6, pp. 1494-1504.

Yeh, W. C., B. E. Bierer, and S. L. McKnight, 1995, "Rapamycin Inhibits Clonal Expansion and Adipogenic Differentiation of 3T3-L1 Cells", *Proceedings National Academy of Science U S A,* Vol. 92, No. 24, pp. 11086-11090.

Yoshida-Moriguchi, T., L. Yu, S. H. Stalnaker, S. Davis, S. Kunz, M. Madson, M. B. Oldstone, H. Schachter, L. Wells, and K. P. Campbell, 2010, "O-Mannosyl Phosphorylation of Alpha-Dystroglycan is Required for Laminin Binding", *Science,* Vol. 327, No. 5961, pp. 88-92.

Yılmaz-Sert, Y., 2011, *SIK2 Involvement in Downregulation of FGF Signaling Through Gab1 ad Raf-1*, M.S. Thesis, Boğaziçi University.

Yu, C., Y. Chen, G. W. Cline, D. Zhang, H. Zong, Y. Wang, R. Bergeron, J. K. Kim, S. W. Cushman, G. J. Cooney, B. Atcheson, M. F. White, E. W. Kraegen, and G. I. Shulman, 2002, "Mechanism by which Fatty Acids Inhibit Insulin Activation of Insulin Receptor Substrate-1 (IRS-1)-Associated Phosphatidylinositol 3-Kinase Activity in Muscle", *Journal of Biological Chemistry,* Vol. 277, No. 52, pp. 50230-50236.

Zhang, S. Q., W. G. Tsiaras, T. Araki, G. Wen, L. Minichiello, R. Klein, and B. G. Neel, 2002, "Receptor-Specific Regulation of Phosphatidylinositol 3'-Kinase Activation by the Protein Tyrosine Phosphatase Shp2", *Molecular Cell Biology,* Vol. 22, No. 12, pp. 4062-4072.

Zhu, X., H. Komiya, A. Chirino, S. Faham, G. M. Fox, T. Arakawa, B. T. Hsu, and D. C. Rees, 1991, "Three-Dimensional Structures of Acidic and Basic Fibroblast Growth Factors", *Science,* Vol. 251, No. 4989, pp. 90-93.

Zick, Y., 2005, "Ser/Thr Phosphorylation of IRS Proteins: A Molecular Basis for Insulin Resistance", *Science Signaling: The Signal Transduction Knowledge Environment,* Vol. 2005, No. 268, pp. 4.